Connections to Cognition: Early White Matter Development and Outcomes in Children Born Very Preterm

by

Julia Mary Young

A thesis submitted in conformity with the requirements
for the degree of Doctor of Philosophy

Department of Psychology
University of Toronto

Connections to Cognition: Early White Matter Development and Outcomes in Children Born Very Preterm

Julia Mary Young

Doctor of Philosophy

Department of Psychology
University of Toronto

2019

Abstract

Children born very preterm (VPT) at <32 weeks' gestational age are vulnerable to disrupted brain maturation and compromised cognitive abilities. The present thesis investigated the first six years of life in children born VPT, which involves dynamic brain growth and developmental milestones, a foundational period for later cognitive abilities. Using diffusion neuroimaging and cognitive measures of outcome, the first objective was to characterize longitudinal white matter maturation over the first four years of life in the children born VPT and explore associations between white matter changes during the preterm period with four-year outcomes (Study1). Subsequent objectives were to compare white matter microstructural properties at four and six years of age and investigate their links with outcomes (Study 2 and Study 3). Whole brain white matter was examined with diffusion tensor imaging metrics including fractional anisotropy (FA), mean diffusivity (MD), radial diffusivity (RD), and axial diffusivity (AD) across studies as well as neurite orientation dispersion and density imaging metrics including neurite orientation dispersion index (ODI) and neurite density (ND) in the third study. Study 1 characterized growth trajectories of individual white matter tracts, demonstrating the greatest age-related changes in the first two years of life. Slower MD and RD rates of change within the external and internal capsule during the preterm period were associated with lower IQ and language scores. Study 2

and Study 3 demonstrated reduced FA within major white matter tracts in the children born VPT compared to term-born children. In addition, Study 2 revealed reduced measures of white matter connectivity in the children born VPT within lateral frontal, middle and superior temporal, and lateral occipital regions. Study 3 further revealed increased ODI within the corpus callosum and corona radiata and positive associations between increasing FA and ND with higher IQ in the children born VPT. Together, these studies identified white matter maturational changes and microstructural differences during the first six years of life in children born VPT. Divergences from typical white matter development and lower cognitive outcomes were apparent, and thus an integral focus for future research and interventions.

Acknowledgments

I would like to thank my supervisor, Dr. Margot Taylor, for believing in me and guiding me through this life changing journey over the past six years. I appreciate your unwavering support and the time you have dedicated towards being my supervisor. It has been an absolute privilege to be a part of your lab and I have taken away more from my experience at SickKids Hospital than I could have ever asked for. Thank you to my supervisory committee member Dr. John Sled for your invaluable guidance, critical thinking, and reassurance. I would also like to thank Dr. Mary Lou Smith for your support and timely constructive feedback throughout the years. I would not have been able to complete this work without you!

Thank you to all of the incredible friends who I have been fortunate to meet within the MJT lab and grad school. In particular, thank you Ben Morgan for all of your advice and being the most dependable, patient, kind and important person in my life during this time. I don't think my computer, or I could have survived graduate school without you. Drs. Rachel Leung and Vanessa Vogan – thank you for your irreplaceable friendship that has been filled with laughs, tears, and travel adventures. You have both been an inspiration to me. Sarah Lin - thank you for being my closest companion during such a memorable part of my life. Thanks to Susan for your friendship, humour, words of wisdom, outdoor adventures, and holiday cakes. Special thanks to Dr. George Ibrahim, Sarah Mossad, Wayne Lee, Marlee Vandewouw, Alex Daros, Lauryn Conway, Amanda Robertson, Simeon Wong, Veronika Yuk, Julie Sato and many more whom I have shared this experience with as a part of CLEX, MJT lab, and graduate school.

Thank you to all of my clinical supervisors for their patience, important lessons, and encouragement throughout my clinical neuropsychology training. Immense thanks and gratitude to my practicum supervisors, Dr. Robyn Westmacott and Dr. Kim Edelstein. To my internship

supervisors, Dr. Mary Pat McAndrews, Dr. David Gold, Dr. Melanie Cohn, and Dr. Marta Statucka - I am so grateful for your incredible training. Thank you, Dr. Amy Wilkinson for your friendship, example as a fellow CLEX student, and clinical guidance.

Finally, I would like to thank my family who have encouraged and supported me throughout my PhD. Thank you to my parents who have been cheering me on since the beginning of graduate school and generously providing much needed plane tickets back home to San Diego several times a year. Thanks to my grandparents who I have been so lucky to spend more time with in London and who were the first to spark my intellectual curiosity. I will be forever grateful for all of the food I was given to take back to Toronto. Thanks Jessica for taking the time to travel to Canada and being my closest confidant. Last but not least, thanks to Benji the cat for being my best therapy and fur friend throughout my PhD.

Table of Contents

List of Tables

List of Figures

List of Appendices

Chapter 1
Introduction

1 Introduction

1.1 Preterm Birth

Premature birth, which compromises neurodevelopment and cognitive abilities throughout the lifespan, is a serious public health concern. Prematurity is the leading cause of perinatal mortality and morbidity, accounting for 75% of perinatal mortality and more than half of the long-term morbidity (McCormick, 1985). It remains a risk factor that negatively impacts brain development and functional outcomes, setting those born premature at risk for distinct developmental disadvantages. There is an important need to elucidate the impacts of prematurity on neurodevelopment during early childhood to help improve medical care and advocate for early interventions to optimize cognitive abilities.

The classification of prematurity was defined by the World Health Organization in 1976, as any birth under 37 weeks' gestational age (WHO, 1977). Three subgroups of prematurity are delineated by gestational age: late preterm birth (32-37 weeks of gestation), very preterm birth (28-32 weeks of gestation), and extremely preterm birth (less than 28 weeks of gestation) (WHO, 1977). On a worldwide level, 14.9 million babies were estimated to be born premature in 2010 (Blencowe et al., 2012). Regions with the highest rates of preterm birth include Southern Asia and Sub-Sarahan Africa of low-income countries and the United States of America of high-income countries (Blencowe et al., 2012; Simmons, Rubens, Darmstadt, & Gravett, 2010). In the United States, the rate of preterm birth was 9.62% in 2015, which consisted primarily of late preterm birth (Purisch & Gyamfi-Bannerman, 2017). In Canada, data from 2014 indicated that in-hospital preterm birth was at 8.1%, an increase from prior years due to rises in obstetric intervention, maternal age, and multiple births (Public Health Agency of Canada, 2008, 2017).

Recent advances in medical care since the 1990s have improved the survival of preterm infants. These include interventions such as the administration of antenatal corticosteroids, assisted ventilation, and surfactant (Saigal & Doyle, 2008). In high-income countries, 90% of preterm babies born less than 28 weeks gestational age are able to survive (Blencowe et al., 2012). However, in low-income countries, only 10% of these babies will survive, highlighting the importance of these medical interventions (Blencowe et al., 2012). Yet as mortality has decreased for these infants in developed countries, short and long-term morbidities have amplified. There are now higher incidences of neonatal complications, time spent within the

neonatal intensive care unit, costs of medical care, and long-term neurodevelopmental impairments (Mento & Nosarti, 2015). Furthermore, each increasing week of prematurity poses greater risks for later morbidities (Purisch & Gyamfi-Bannerman, 2017).

The subgroup of children with preterm birth at less than 32 weeks gestational age, very preterm birth, will be the focus of the present thesis. This group of preterm infants comprises 10.4% of all preterm births, accounting for about 1.6 million babies worldwide (Blencowe et al., 2012). Infants born in the very preterm period have been shown to be more vulnerable than infants in the late preterm period in terms of their medical courses, risk for brain injury, altered brain development, and neuropsychological outcomes.

1.1.1 Perinatal clinical factors

The specific mechanisms of prematurity are not well understood. Preterm birth is due to a variety of reasons, such as spontaneous labour with intact membranes, premature rupture of membranes, and labour induction (Goldenberg, Culhane, Iams, & Romero, 2008). Spontaneous preterm births (a combination of spontaneous labour with intact membranes and premature rupture of membranes) can be due to numerous maternal risk factors and pathological mechanisms during pregnancy (Romero, Dey, & Fisher, 2015). For example, maternal risk factors may include maternal age (younger or older), short intervals between pregnancies, low BMI, multiple pregnancies, parity (number of previous births), diabetes, hypertension, stress, obesity or other pre-existing conditions (McDonald, Han, Mulla, & Beyene, 2010; Simmons et al., 2010). A family history of preterm birth due to genetic predispositions is also large risk factor (Muglia & Katz, 2010). Pathological mechanisms during pregnancy may include intra-amniotic infection (chorioamnionitis), decidual haemorrhage, decidual senescence, maternal-fetal intolerance, decline in progesterone, and maternal stress, among others (Romero et al., 2015). A “multi-hit” model has been proposed, hypothesizing that cumulative effects of perinatal inflammation such as chorioamnionitis, necrotizing enterocolitis, meningitis, and fungal infections among others, increases the likelihood of preterm brain injury such as white matter injury and ventriculomegaly (Korzeniewski et al., 2014).

Following preterm birth, infants are susceptible to a host of complications in the short- and long-term. As a result, the population of children following very preterm birth are quite heterogeneous and diverse in their medical courses, which can affect later neurodevelopment. Medical

complications while receiving care in the hospital can occur, such as respiratory distress, sepsis, and brain injury (Allen, 2002). Other complications may include cerebral palsy, retinopathy of prematurity, and neurodevelopmental impairment that can span multiple cognitive domains (Saigal & Doyle, 2008). During the prolonged hospital stays, neonates born very preterm are also subjected to multiple painful procedures and nutritional assistance that can implicate brain development and outcomes (Duerden et al., 2018; Schneider et al., 2017, 2018).

Understanding the relation between perinatal clinical factors and later neurodevelopment is an important area of research that involves many complex variables. A prospective study found that exposure to antenatal corticosteroids, female sex, singleton birth, and higher birth weight were associated with reduced risk of death and neurodevelopmental impairment (Tyson, Parikh, Langer, Green, & Higgins, 2008). Severe retinopathy of prematurity and postnatal infections were identified to be associated with abnormal white matter development as well as poorer developmental outcomes (Glass et al., 2017, 2018). In addition, early postnatal growth and parental education, amongst a variety of factors, were identified to influence executive function ability in childhood (Aarnoudse-Moens, Duivenvoorden, Weisglas-Kuperus, Van Goudoever, & Oosterlaan, 2012).

A prospective Canadian cohort study across twenty-eight Canadian institutions identified gestational age, sex, illness severity, bronchopulmonary dysplasia, necrotizing enterocolitis, late-onset sepsis, retinopathy of prematurity, and abnormal neuroimaging to be associated with neurodevelopmental impairments at 21 months of age (Synnes et al., 2017). In addition, they found that 83.5% of surviving infants did not have significant neurodevelopmental impairments, however 46% had less severe impairments (Synnes et al., 2017). In another Canadian cohort, data-driven multivariate methods identified intrauterine growth restriction, male sex, absence of antenatal corticosteroids, and persistent identification of white matter injury at term-equivalent age to be associated with adverse cognitive and language skills as well as more problems with behavioural symptoms and executive function at two and four years of age (Young et al., 2016).

1.1.2 Social factors

The incidence of preterm birth is also influenced by socioecomonic, psychosocial, and sociocultural factors. Socioeconomic status comprises factors such as parental education, occupation, and income level (McLoyd, 1998). A positive association has been found between

the prevalence of preterm birth and socioeconomic status, where factors such as poverty, limited maternal education, single mothers, and inadequate prenatal care increase the risk of preterm birth (Kramer et al., 2001; Muglia & Katz, 2010). In addition, factors such as anxiety, depression, stress, substance use and race have been associated with the prevalence of preterm birth (Kramer et al., 2001; Staneva, Bogossian, Pritchard, & Wittkowski, 2015). In the United States, preterm birth rates were found to be 48% higher in black women compared to other races due to both socioeconomic and genetic reasons (Purisch & Gyamfi-Bannerman, 2017).

Health and developmental outcomes of preterm children are also influenced by socioeconomic and psychosocial factors. In a universal health care model such as France, children born preterm who lived in areas of socioeconomic deprivation were more likely to be rehospitalized within the first year of life, indicating more medical issues (Laugier et al., 2017). With respect to developmental outcomes, low socioeconomic status negatively impacts language function in toddlers born preterm (Wild, Betancourt, Brodsky, & Hurt, 2013). Behavioural problems in children born preterm at five and six years of age are associated with low maternal education and inadqeuate income (de Laat, Essink-Bot, van Wassenaer-Leemhuis, & Vrijkotte, 2016). Furthermore, a review study argued that the impact of perinatal risk factors on development decreases with time, while the impact of environmental factors increases with time (Linsell, Malouf, Morris, Kurinczuk, & Marlow, 2015). Children born preterm who were younger than five years of age, male sex, nonwhite race, lower birth weight, and had lower parental education predicted global cognitive impairments at five years of age; however, in older children, the influence of parental education was the primary influence on cognitive abilities (Linsell et al., 2015).

1.2 Neuropsychological Outcomes

In healthy children, fundamental aspects of cognition are actively developing during the first six years of life in conjunction with brain development. These include visual-motor integration skills, intelligence, and language. Visual-motor function is one of the first cognitive skills to be developed and undergoes ongoing refinement across early childhood. Independently, both visual and motor skills undergo changes. For instance, while a child at three years of age may be able to only focus only on the overall features of an object or image, a child at four to five years of age can begin to focus on the individual parts and features of visual stimuli (Beery, Buktenica, &

Beery, 2010). Then, by six years of age, children are able to focus upon details. With motor development, gross motor skills are acquired first and then followed by fine motor skills and finger control, with development of the cerebellum and motor pathways (Beery, Buktenica, & Beery, 2010). Visual motor integration is the ability to coordinate visual perception and fine motor skills concurrently, using visual cues to guide motor behavior (Beery, Buktenica, & Beery, 2010). This coordination of both visual and motor skills is an integral step in the development of sensory integration.

Measures of intelligence evaluate the collective functioning of numerous cognitive skills such as verbal reasoning, visual spatial reasoning, working memory, and processing speed (Anderson, 2014). At three years of age, children are able to make simple causal inferences, yet they still make errors with multiple causal inferences (Wechsler, 2002). Language development also undergoes rapid changes within the first six years of life, where children quickly acquire receptive and expressive language skills (Cusson, 2003). By three years of age, children can begin to communicate in complex sentences (Cusson, 2003). At 4 years of age, children's language skills, motor skills, and abstract reasoning vary with differences in social maturity and environmental experiences warranting broad assessments of cognitive ability (Wechsler, 2002). By 6 years of age, children's reasoning skills become more refined, and their vocabulary continues to expand to several thousand words with the ability to use complete sentence structures (Cusson, 2003; Wechsler, 2002).

1.2.1 Motor and visual-motor abilities

Motor skills are one of the first developmental milestones to emerge during early childhood. By two years of age, children are expected to have relatively developed gross and fine motor skills such as walking, grasping and gripping of objects (Capute, Shapiro, Palmer, Ross, & Wachtel, 1985; Piper, Byrne, Darrah, & Watt, 1989). Major neurological and sensory disabilities can be identified by this age based, in part, on motor abilities (Marlow, 2004). Children born very preterm have elevated incidences of delayed motor skills and susceptibility to developing major motor disabilities such as cerebral palsy, particularly as gestational age decreases. Prevalence of cerebral palsy is linked to the presence of early brain injury such as damage to the periventricular regions and internal capsule (Bracewell & Marlow, 2002). Incidence rates of cerebral palsy have been previously reported to occur from 8-18% in very low birthweight (VLBW) and very

preterm cohorts (Bracewell & Marlow, 2002; Marlow, 2004; Woodward et al., 2009). A more recent cohort study conducted by Pierrat and colleagues (2017) assessed neurodevelopmental outcomes of children born very preterm at two years of age in a French population study and reported increasing rates of overall survival as well as survival without severe or moderate motor and sensory disabilities. They also reported lower rates of cerebral palsy with an incidence rate of 1–7% that was linearly associated gestational ages from 34 to 24 weeks.

Impairments are found in gross and fine motor abilities as well as visual-motor abilities in children born very preterm compared to term-born children (Anderson, 2014). A meta-analysis analysing studies that included measures of fine and gross motor ability from birth to adolescence found that on average, very preterm and VLBW children were 0.57 to 0.88 standard deviations behind term-born children (de Kieviet, Piek, Aarnoudse-Moens, & Oosterlaan, 2009). One study assessing children born very preterm at seven and eight years of age found that in comparison to term-born children, the children born very preterm scored significantly lower with higher incidence of mild motor impairments across tests of visual motor integration, fine and gross motor abilities (Foulder-Hughes & Cooke, 2003).

Two ongoing hypotheses connect motor and cognitive development in children born very preterm. The first is an embodied cognition approach, which hypothesizes that earlier developing motor skills encourage children's interactions with their environment, and as a result, influence their cognitive development (Oudgenoeg-Paz, Mulder, Jongmans, van der Ham, & Van der Stigchel, 2017). The second hypothesis is that there is a co-occurrence of abilities across multiple cognitive domains, and in children born very preterm, deficits in multiple domains are caused by brain injury and inherent alterations in brain maturation (Oudgenoeg-Paz et al., 2017). Longitudinal studies assessing both motor and cognitive abilities in VLBW and/or children born very preterm have supported both hypotheses, and indicate a presence of deficits in early motor skills in conjunction with deficits in later cognitive abilities (Howe, Sheu, Hsu, Wang, & Wang, 2016; Piek, Dawson, Smith, & Gasson, 2008; Van Baar, Ultee, Gunning, Soepatmi, & De Leeuw, 2006).

1.2.2 Intelligence

In early childhood and during school-age, children born very preterm are at risk for poorer acquisition of cognitive skills compared to full-term children. Measures of intelligence are a

composite of multiple cognitive skills such as verbal reasoning, non-verbal reasoning, working memory, and processing speed (Anderson, 2014). Assessing children born very preterm during early childhood is important for determining potential weaknesses and implementing support before the children enter school age. A meta-analysis investigating the predictive ability of early assessments conducted between one and three years of age in preterm or very low birth weight (<1500g) children identified accurate predictions for the absence of school-age deficits, while predictions were not sensitive towards identifying those who do develop cognitive difficulties at school-age (Wong, Santhakumaran, Cowan, & Modi, 2016).

A cross-sectional study assessing multiple aspects of neurodevelopment including intelligence, language, motor ability and behaviour in four-year-old children born very preterm found that 46% of the children demonstrated cognitive delays (Woodward et al., 2009). Moreover, of those with one impairment, almost half exhibited difficulties in multiple domains (Woodward et al., 2009). At five years of age, children born very preterm continued to score lower than full-term children on cognitive testing by about one standard deviation (Wolke & Meyer, 1999). Lower cognitive performance was also found to be associated with increased behavioural problems (Delobel-Ayoub et al., 2009a). A meta-analysis evaluating cognition in preterm children, including other gestational ages (<37 weeks), also found that the preterm children at five years of age have lower cognitive scores with about a 10-point mean or 0.7 SD difference in contrast to term-born children (Bhutta, Cleves, Casey, Cradock, & Anand, 2002). In addition, children with low birth weight assessed at five and a half years of age demonstrated greater variability within their scores compared to term-born children (Böhm, Katz-Salamon, Smedler, Ann-Charlotte; Lagercrantz, & Forssberg, 2002).

Few longitudinal studies have described the trajectories of cognitive abilities in children and adolescents born very preterm. One such study included both children born very preterm and full-term beginning from four years of age and then subsequently at six, nine and twelve years of age (Mangin, Horwood, & Woodward, 2017). They found that the cognitive trajectories based upon estimates of intelligence were stable, yet the children born very preterm had a lower mean intelligence scores compared to the full-term children, with about a consistent 10-point difference between groups, as well as greater intra- and inter- individual variability (Mangin et al., 2017). Furthermore, adolescents born very preterm assessed at fifteen and nineteen years of age demonstrated similar discrepancies of intelligence measures compared to term-born

individuals (Allin et al., 2008). Taken together, the literature suggests that cognitive deficits are detected reliably at four years of age and continue throughout late childhood, adolescence, and early adulthood.

1.2.3 Language skills

Language abilities dramatically increase within the first years of life and are essential for later cognitive, academic and social competence. Children born very preterm are at risk for delayed language skills from when they first begin to acquire language. In early childhood, a linear relationship has been shown between progressive decreases in gestational age and reduced acquisition of language skills in both simple language (receptive and expressive vocabulary) and complex language (meaning of concepts) independent of socio-economic status (Foster-Cohen, Edgin, Champion, & Woodward, 2007; Gayraud & Kern, 2007). Follow-up at multiple time points through to two years of age indicated that expressive and receptive language were delayed in preterm children and exacerbated by clinical factors such as length of hospital stay, birth weight, Apgar scores, and infant irritability (Cusson, 2003). Studies in middle childhood, indicate that children born very preterm demonstrate fewer language skills in pre-reading ability and speech articulation (Reidy et al., 2013; Wolke & Meyer, 1999). Furthermore, white matter injury at birth was found to mediate deficits in phonological awareness and partially mediate deficits in semantics, grammar, and discourse in children born very preterm at seven years of age (Reidy et al., 2013).

Longitudinal studies beginning from early childhood to adolescence have characterized the stability of language deficits in children born very preterm. Lower language performance was found to be consistent beginning from five months of age to eight years of age in children born very preterm, with more stability in the first four years of life (Putnick, Bornstein, Eryigit-Madzwamuse, & Wolke, 2017). Another study examining preterm-born children between three and twelve years of age found that while delays in simple language caught up with same-aged peers by twelve years of age, deficits in complex language skills became more pronounced over time (van Noort-van der Spek, Franken, & Weisglas-Kuperus, 2012). This suggests that poor language performance early in life is predictive of later abilities in language.

1.3 Structural Neuroimaging

Technological advances in Magnetic Resonance Imaging (MRI) has allowed researchers to greatly increase the non-invasive study of brain development. MRI is primarily used clinically and provides much better resolution than cranial ultrasound imaging. In the past few decades, MRI has been applied to clinical and basic research towards understanding brain development in typically developing and clinical populations. The application of structural neuroimaging in children born preterm has provided more detailed information on early brain injury and has contributed considerable evidence on how their brains are developing differently compared to term-born children. A structural neuroimaging sequence, diffusion weighted imaging, is sensitive for the study of white matter within the brain and is the primary imaging modality used within the present thesis.

1.3.1 Diffusion weighted imaging

Diffusion weighted imaging emerged in the mid-1980s to measure diffusion coefficients in different types of tissues (Beaulieu, 2002). This MRI sequence is designed to detect the amount of water diffusion in vivo and is useful for studying properties of white matter within the brain. Diffusion weighted imaging uses a pulsed magnetic field gradient applied at different rates to measure water diffusion based on the amount of signal loss in a given spatial area (Qiu, Mori, & Miller, 2015). The signal loss depends on three factors such as the distribution of proton displacements along a gradient during the diffusion time, gradient strength, and gradient duration (Qiu et al., 2015). In combination, these three factors comprise a b-value and relate to the rates of diffusion (Jones, Knösche, & Turner, 2013). Higher b-values are more sensitive to the orientation of fibres but can reduce the signal-to-noise ratio (Jones et al., 2013). Most diffusion-weighted MRI studies to date use one b-value, a "single shell", that is sampled over multiple axes (number of directions) to measure the dephasing of water molecules within a voxel (Jones et al., 2013).

This signal loss is sensitive to how mobile water is within tissue and microstructural components such as cell membranes, myelin sheaths, microtubules, and neurofilaments that hinder or restrict diffusing molecules (Jones et al., 2013). In the instance where water molecules freely diffuse, diffusion occurs in all directions that can be visualised as a sphere and is considered isotropic. However, if water molecules do not diffuse freely and are restricted by tube-like structures along

a primary direction such as within white matter axons, diffusion is considered anisotropic. Diffusion can be visualized as an ellipsoid (see Figure 1) and quantified in multiple directions (Qiu et al., 2015).

The diffusion weighted MRI sequence was first applied to study the human brain in 1987 (Thomsen, 1987). This study identified diffusion imaging as useful in clinical populations as differences in diffusion were found between grey and white matter as well as regional variations within white matter (Thomsen, 1987). Diffusion in white matter was first hypothesized to be anisotropic due to myelination and the orientation of myelin sheaths (Thomsen, 1987). This hypothesis was confirmed based on findings from diffusion data in a cat brain, which demonstrated anisotropic diffusion within white matter and the spinal cord, yet no clear evidence of anisotropic diffusion in cortical or subcortical grey matter (Moseley et al., 1990).

1.3.2 White matter microstructure

A diffusion tensor can be fit to the diffusion weighted images to measure the extent of diffusion in all directions of 3-dimensional space within a voxel (Qiu et al., 2015). There are three eigenvalues that represent the magnitude of diffusion along the principle axis (λ_1) and two perpendicular axes (λ_2, λ_3) as shown in .

Figure 1. The diffusion ellipsoid

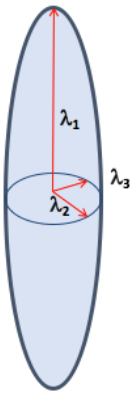

The principle eigenvalue (λ_1) is the axial diffusivity (AD), which is the main fibre orientation. Radial diffusivity (RD) comprises water mobility along the average of the two perpendicular

eigenvalues (λ_2, λ_3) from the principle eigenvalue, which is sensitive to myelination (Song et al., 2005). Mean diffusivity (MD), also known as apparent diffusion coefficient (ADC), is the average of all three eigenvalues (λ_1, λ_2, λ_3) and provides a measure of the average rate of diffusion within a voxel (Soares, Marques, Alves, & Sousa, 2013).

Fractional anisotropy (FA) quantifies the degree that water diffusion is restricted in one direction relative to the other directions (Qiu et al., 2015). In other words, it is a non-directional, normalized measure of the fraction of the tensor's magnitude based on anisotropic diffusion (Soares et al., 2013). The anisotropic diffusion ranges between 0 and 1, where 0 represents isotropic diffusion and 1 represents anisotropic diffusion (Soares et al., 2013). The equation for FA represents the ratio of standard deviation and root mean square of the eigenvalues:

$$FA = \sqrt{\frac{3}{2}} \sqrt{\frac{(\lambda_1 - MD)^2 + (\lambda_2 - MD)^2 + (\lambda_3 - MD)^2}{{\lambda_1}^2 + {\lambda_2}^2 + {\lambda_3}^2}}$$

The interpretation of FA in its meaning for white matter microstructure is non-specific. FA can be influenced by multiple factors within a voxel such as orientation dispersion, myelination, axon density, membrane permeability, partial volume effects, axon size and the number of axons (Jones et al., 2013). Trends in the diffusivity measures (AD, MD, RD) and FA are apparent during early brain development such that diffusivity decreases while FA increases over time (Qiu et al., 2015).

When multiple b-values, or "multi-shell" diffusion data are acquired, the additional information from the b-values can assist in delineating the non-specific nature of FA. A technique such as neurite orientation dispersion and density imaging (NODDI), can provide two additional measures to describe the nature of axons and dendrites (neurites) within white matter (Zhang, Schneider, Wheeler-Kingshott, & Alexander, 2012). The NODDI model differentiates three different tissue types: intra-cellular, extra-cellular, and CSF compartments which are important for measuring neurite morphology (Zhang et al., 2012). The intra-cellular compartment describes the space bounded by the membranes of neurites while the extra-cellular compartments describe the space around neurites including glial cells and cell bodies (Zhang et al., 2012).The measure of orientation dispersion index characterises the angular variation of neurite orientations, quantifying the bending and fanning of axons (Zhang et al., 2012). The measure of neurite

density is the density of axons in white matter or the intra-cellular volume fraction that quantifies the number of axons and space between axons (Zhang et al., 2012). FA is more influenced by orientation dispersion index, and is negatively correlated with orientation dispersion index (Chang et al., 2015). In contrast, FA is more weakly influenced by neurite density, and is positively correlated with neurite density (Chang et al., 2015).

When analyzing the DTI and NODDI metrics to detect group differences (e.g. children born very preterm versus full-term-born children) or within group associations (e.g. correlations between children born very preterm and outcome measures such as IQ), several approaches are possible including a region of interest (ROI) approach and voxel-wise approach such as tract based spatial statistics (TBSS) (Soares et al., 2013). Other methods may include histogram analyses or voxel-based analysis (VBA). An ROI approach uses a predetermined region or established atlases such as the JHU white matter atlas that are applied to co-registered diffusion data across individuals to extract individual DTI metrics within those regions and then subjected to statistical analyses (Oishi et al., 2011). TBSS is an alternative voxel-based approach that uses the skeletonization of FA images to represent the centre of whole brain white matter. Group statistics are then performed on the whole brain FA skeleton, which has the advantage of not requiring an *a priori* region defined, such as an ROI approach (Smith et al., 2006). It also has the ability to perform analyses on fewer voxels compared to a whole brain VBA approach (Smith et al., 2006). It is important to note that the accuracy of each of these methods is dependent on the co-registration between subjects.

1.3.3 White matter connectivity

Another approach to studying white matter is from a connectivity perspective. Obtaining measures of connectivity is typically performed using tractography, which reconstructs connections between regions based on local estimates of fibre orientation (Jones et al., 2013). The estimates of fibre orientation can either be calculated from the diffusion orientation density function (dODF) or the fibre orientation density function (fODF). The dODF measures the number of particles that have diffused along an axis between two points, which should peak on the long axis of the fibres (Jones et al., 2013). The fODF represents that number of fibres oriented along an axis (Jones et al., 2013). With deterministic tractography, tracts are estimated by counting the number of times a streamline can be created between the two regions (Jones et

al., 2013). Tracts will begin in one or more voxels and use the same local fibre orientation information derived from the orientation density function. The decision of whether a tract should be continued through voxels depends on set parameters such as fibre stiffness or maximum curvature (Jones et al., 2013).

Connectivity within the brain is complex and network analyses can be applied to understand its topological characteristics. The organization of brain networks is understood to be a balance between minimal wiring costs and maximum adaptive value constrained by physical properties such as its volume (Bullmore & Sporns, 2012). Graph theoretical measures capture properties of network topologies by applying the concept of a graph to brain structures. This is achieved by describing grey matter regions determined by a chosen brain atlas as the graph's nodes and axonal projections derived from streamlines generated from tractography methods as the graph's edges (Bullmore & Sporns, 2009). Brain regions that are more spatially close to one another are more likely to be connected to each other, whereas regions that are farther apart are less likely to be connected (Bullmore & Sporns, 2009). Longer tracts as well as hub regions are more vulnerable to disease models (Bullmore & Sporns, 2012).

Specific graph theoretical measures can address many different questions regarding the nature of connectivity and subjected to group-level statistics. A fundamental graph measure is degree, which represents the number of connections to a given node or the number of neighbours to a node (Rubinov & Sporns, 2010). The weighted variant of degree is known as strength, which is the sum of all neighbouring connections and their weights (the number of streamlines between two nodes) (Rubinov & Sporns, 2010). With respect to development, the balance between segregating and integrating networks is relevant to brain maturation. Segregation occurs where there are highly clustered connections that favour the segregation of information in relation to functional processes (e.g. motor function). Graph measures that describe segregation include local efficiency and clustering coefficient. Local efficiency is the average of the inverse minimum path length of each node (Achard & Bullmore, 2007). Clustering coefficient is the proportion of the node's neighbours that are also neighbours to each other (Rubinov & Sporns, 2010). In contrast, integration occurs by aggregating information from spatially distributed brain regions and is based on paths that reflect possible routes of information (Rubinov & Sporns, 2010). Thus, integration favours different functional abilities such as intelligence and executive function (Bullmore & Sporns, 2012). One graph measure of integration is global efficiency,

which characterises the average inverse shortest path length, representing more complex networks with mean short path lengths (Achard & Bullmore, 2007).

1.4 Perinatal brain injury

1.4.1 White matter injury

Children born very preterm are at risk for acquiring early brain injury such as white matter injury. The greatest risk for developing white matter injury is from 23 to 32 weeks postmenstrual age (Back, 2017). Causes of white matter injury include hypoxia ischemia, inflammation, or infection (Volpe, 2009). Periventricular leukomalacia (PVL) is the most severe degree of white matter injury, and is characterized by focal cystic necrosis (Back, 2017). Previously, imaging studies found PVL in up to 50% of very low birth weight infants (Volpe, 2009). At present, the rate of PVL has decreased significantly in very preterm infants due to improved medical care and less severe, non-cystic white matter injury has become more prevalent, such as diffuse and small punctate lesions (Back, 2017; Volpe, 2013).

Structural MRI sequences such as T1-weighted images obtained in the neonatal period can identify white matter injury following very preterm birth. Detecting white matter injury at an early age before term-equivalent age has been shown to be the most representative of the actual extent and presence of white matter injury in these children, as the injury can resolve with time (Guo et al., 2017). White matter injury poses a serious threat to vulnerable cell populations such as the pre-oligodendrocytes that are responsible for the pre-myelination of axons as well as the early subplate neurons that peak in size at 24 weeks post menstrual age (Ferriero & Miller, 2010). Diffuse white matter injury, in particular, selectively degenerates the pre-oligodendrocytes within the necrotic foci, although axons are mostly spared (Back, 2017). Over the course of development, downstream effects of white matter injury results in reduced myelination, cortical and subcortical development (Volpe, 2009).

The compound impacts of white matter injury and perinatal risk factors associated with very preterm birth can result in altered brain development and developmental outcomes. A recent study by Barnett and colleagues (2018) tested the multi-hit approach, which hypothesizes that antenatal factors may sensitize brain tissue, making it vulnerable to brain injury from secondary events. They found that at term-equivalent age, risk factors for diffuse white matter injury and

lower fractional anisotropy within the white matter were compounded by multiple factors such as lower gestational age, fetal growth restriction, increased ventilation days, parenteral nutrition, necrotizing enterocolitis, and male sex (Barnett et al., 2017).

Alterations in early brain development can be detected as early as term-equivalent age and throughout childhood. In preterm infants with punctate white matter lesions compared to those without, fractional anisotropy (FA) was found to be lower in areas such as the posterior limb of the internal capsule, cerebral and cerebellar peduncles (Bassi et al., 2011). Between preterm and term-equivalent age, the area and FA of the corpus callosum were reduced in relation to white matter injury (Malavolti et al., 2017). By seven years of age, differences in FA as well as measures of diffusivity (MD, AD, and RD) continued to be altered within the corpus callosum and cortical spinal tract of those with moderate to severe white matter abnormalities (Estep et al., 2014). In addition, severe injury such as PVL has been shown to be associated with lower thalamic volumes and FA as well as lower intelligence measures (Kersbergen et al., 2015; Zubiaurre-Elorza et al., 2012).

White matter injury at birth is associated with increased motor and cognitive deficits (Inder et al., 1999). As the severity of the brain injury increases, the likelihood of abnormal outcomes by two years of age increases (Miller et al., 2005). The location and size of the white matter lesions also influences outcomes. Guo and colleagues (2017) identified white matter lesions to be concentrated in the periventricular regions, followed by posterior and frontal regions. Greater overall volumes of white matter injury predicted poorer motor outcomes at 18 months of age, while lesions focused in the frontal areas predicted lower cognitive outcomes (Guo et al., 2017). White matter injury detected at both preterm and term-equivalent age also contributed to more parent-reported problematic internalizing behaviours, behavioural symptoms, and impaired executive functioning at four years of age (Young et al., 2016). In older cohorts, increasing extent of perinatal brain injury altered white matter tracts such as the cingulum and fornix and were related to memory function (Caldinelli et al., 2017).

1.4.2 Germinal matrix/intraventricular hemorrhage

Germinal matrix/intraventricular hemorrhage (GMH/IVH) is another prevalent insult in the very preterm brain (Volpe, 2009). As preterm infants are often quite sick after they are born, blood vessels of the highly vascular and cellular germinal matrix are prone to rupture, which can result

in hemorrhage within the germinal matrix and leaking into the lateral ventricles (Brouwer, Groenendaal, Benders, & De Vries, 2014). The extent of the GMH/IVH can be identified on cranial ultrasound and magnetic resonance imaging. Presence and grades of germinal matrix/intraventricular haemorrhage (GMH/IVH) on a scale from 0 (no haemorrhage) to 4 (periventricular venous haemorrhagic infarction (PHVI)) correspond to levels of bleeding within the germinal matrix. This correspondence is based upon the Papile scale (GMH 1 to 4) for computed tomography findings (Papile, Burstein, Burstein, & Koffler, 1978) and Volpe scale for cranial ultrasonography findings adapted to MRI findings (IVH 1 to 3, PVHI) (Volpe, 2008). More specifically, GMH1/IVH1 is haemorrhage limited to the germinal matrix, GMH2/IVH2 includes an intraventricular haemorrhagic component, GMH3/IVH3 additionally includes ventriculomegaly, and GMH4/PVHI is characterized by periventricular venous haemorrhagic infarction associated with IVH (Raybaud, Ahmad, Rastegar, Shroff, & Al Nassar, 2013).

These hemorrhages originate from the germinal matrix, which is an area where neuronal and glial cells arise. Neuronal precursor cells are present by 10-20 weeks GA (Bolisetty et al., 2014). Following the neuronal precursor cells, glial precursor cells become present, which precede the development of oligodendroglia (Bolisetty et al., 2014). Thus, hemorrhage in this area has the capacity to affect neuronal migration, glial precursor cells, and subsequent myelination (Bolisetty et al., 2014). The main neurological consequences of GMH/IVH include the destruction of the germinal matrix, white matter injury, and post-haemorrhagic ventricular dilatation (PHVD). About 30-50% of preterms with Grade III IVH or PHVI will go on to develop post-hemorrhagic ventricular dilatation (PHVD)(Murphy et al., 2002). The occurrence of PHVD is a serious consequence of haemorrhage as about 25% of preterm infants with GMH/IVH and PHVD will require neurosurgical intervention such as a reservoir, VP shunt, or lumbar puncture due to hydrocephalus and improper draining of cerebral spinal fluid (CSF) (Brouwer et al., 2014). Neurosurgical procedures are not always guaranteed to succeed on the first attempt and may require revisions (Murphy et al., 2002). Furthermore, GMH/IVH is detrimental to early brain development as well as short and long-term neurodevelopmental outcomes (Murphy et al., 2002; Pappas et al., 2018).

There is evidence that GMH/IVH particularly affects cerebellar development. A negative association was found between cerebellar volume increases across development between preterm and term-equivalent age with increasing severity of IVH (i.e. Grades 3 and 4 IVH versus grades

1 and 2 IVH) (Tam et al., 2011). No differences between the severity of ipsilateral and contralateral IVH were found with cerebellar volumes (Tam et al., 2011). Another study found that volumes of the contralateral cerebellum to the unilateral PVHI were reduced compared to volumes of the ipsilateral cerebellum (Limperopoulos, 2005). In a diffusion tensor imaging (DTI) study using tractography, preterms at term-equivalent age demonstrated reduced measures of fractional anisotropy in the superior cerebellar peduncle and motor tract as well as higher apparent diffusion coefficient in the middle cerebellar peduncle with low-grade IVH (Morita et al., 2015). Cerebellar involvement from IVH may be attributed to downstream axonal damage from the brain injury, cerebellar injury concurrent to the IVH, and toxicity of blood products in the CSF (Tam et al., 2011).

Low-grade GMH/IVH as well as more severe grades of GMH/IVH impact neurodevelopmental outcomes. A review by Mukerji and colleagues (2015) found that moderate neurodevelopmental impairments were higher in both mild and severe IVH compared to those without hemorrhage in preterm infants less than 34 weeks' gestation. In contrast, a report from the Netherlands found no differences in developmental outcomes between very preterm infants with low-grade IVH versus those without IVH (Reubsaet et al., 2017). Another study identified grade-dependent associations with outcome in infants born between 23 and 28 weeks' gestation. Those with Grade 1-II IVH had increased rate of neurosensory impairment, developmental delay, cerebral palsy, and deafness, while those with Grade III-IV IVH had even higher rates of impairment at 2 to 3 years corrected age (Bolisetty et al., 2014).

Infants that developed PHVD are also at risk of adverse neurodevelopmental outcomes. Developmental quotients and motor abilities at two years of age were linearly associated with total cerebral volumes and only motor abilities were associated with cerebellar and thalamic volumes in children with PHVD (Jary, De Carli, Ramenghi, & Whitelaw, 2012). In those infants who required intervention for PHVD and had a Grade IV haemorrhage, outcomes at 2 years of age were worse than those who only had a Grade III or IV hemorrhage (Brouwer et al., 2008). Furthermore, children who did not require interventions had better outcomes than those who did require intervention (Futagi, Suzuki, Toribe, Nakano, & Morimoto, 2005; Holwerda et al., 2016). Recent evidence has also shown that early interventions resulted in developmental outcomes that were similar to those who did not require intervention, while those who had late interventions experienced worse developmental outcomes (Leijser et al., 2018). During school-age, one study

found no differences in outcomes in preterms with PHVD requiring neurosurgical interventions compared to those who did not (Brouwer et al., 2012), however by about 10 years of age, intelligence measures, visual perception, and attention scores were lower compared to matched children without PHVD.

1.5 Structural brain development

1.5.1 The subplate zone and perinatal brain development

Structural brain development occurs in a dynamic, coordinated, and adaptive manner. Each stage of brain development is distinct and integral for its respective purpose. The first half of gestation is responsible for cortical neurogenesis within the ventricular zone beginning from 40 post conception days until mid-gestation (Rakic, 1988). Eventually, these newly formed neurons will migrate via radial glial cells through the intermediate zone to the subplate zone where they synapse prior to moving into their designated destinations within the cortical plate and becoming part of grey matter (Rakic, 1988). The second half of gestation is responsible for the formation of cerebral connections that comprise white matter, coinciding with the time of very preterm birth.

The development of cerebral connections beginning from 20 post conception weeks through the first postnatal weeks involve a transient structure, the subplate zone, which serves as a waiting zone that helps guide afferent fibres to their respective cortical areas (Kostović & Jovanov-Milosević, 2006). Based on information from histological and magnetic resonance images, Kostovic and Jovanov-Milosevic (2006) describe essential interactions between the subplate zone and developing axons during distinct stages in the second half of gestation. Beginning in the early fetal stage (20-23 post conception weeks), thalamocortical fibres extend into and synapse within the subplate during their axonal outgrowth towards the cortical plate. Simultaneously, neurons produced within the ventricular and subventricular zones migrate towards the cortical plate. In the very preterm stage (24–32 post conception weeks), thalamocortical axons reach the cortical plate at chosen sensory or other cortical regions to create synaptic contacts. Finally, during the late preterm stage (32–37 post conception weeks), the subplate zone gradually decreases to be replaced by white matter. Thus, the very preterm and late preterm stages support axonal ingrowth into the cortical plate and subsequent dendritic arborisation (Kostović & Judas, 2002).

An additional contribution of the subplate zone to the development of cerebral connections is its involvement in guiding cortico-cortical fibre interactions within the cortical layers (Kostović & Jovanov-Milosević, 2006). The subplate zone is an active contributor in cortical processing; it is also necessary for the functional maturation and plasticity of thalamocortical connections and critical for the structural reorganization of the developing cortex (Kanold & Luhmann, 2010; Kostović & Judas, 2007). In preterm infants, periventricular areas are particularly vulnerable to lesions, yet can demonstrate structural plasticity based on the waiting positions of the fibres in the subplate zone (Kostović & Jovanov-Milosević, 2006).

Postnatally, axonal connectivity dramatically increases throughout the brain and exceeds the number of connections that are present in adult-life (Innocenti & Price, 2005); this 'developmental exuberance' occurs on both macroscopic and microscopic levels. The macroscopic level is characterised by the formation of transient afferent and efferent projections between cortical regions whereas the microscopic level is characterised by the formation of structures that facilitate communication between neurons such as axonal and dendritic arborisation, synapses, and spines (Innocenti & Price, 2005). However, following this phenomenon of exuberance, successive developmental processes of synaptic pruning and cell death, primarily in glial cells, eliminate up to 50% of the produced connections and neurons in the ensuing few years of early childhood (Stiles & Jernigan, 2010). The pruning stage supresses redundant or aberrant circuits, a process which can be sensitive to environmental factors (Huttenlocher & Bonnier, 1991).

1.5.2 Grey matter development

Grey matter surface area and volume rapidly increase from 23 post conception weeks to the term-age period (Kostović & Judas, 2002). Using structural magnetic resonance imaging, cortical surface area and cerebral volume were demonstrated to undergo an exponential increase according to a scaling law between 23 weeks' gestational age until term-corrected age (Kapellou et al., 2006). In addition, deep grey matter, comprising the thalamus, caudate, globus pallidus, and putamen demonstrated about a five-fold increase in volume between 25 and 47 post conception weeks in very preterm neonates (Young et al., 2015). Moreover, the growth rate of the caudate and globus pallidus during the preterm period was linearly associated with long-term outcomes of visual-motor and language abilities (Young et al., 2015). When contrasting term-

born infants to those born very preterm, the infants born very preterm already displayed reduced cortical grey matter, deep grey matter, and cerebellar volumes by term-equivalent age, which have been shown to relate to later neurodevelopmental impairments at one and two years of age (Inder, Warfield, Wang, Hüppi, & Volpe, 2005; Lind et al., 2011).

Brain volume increases by 101% in the first year of life and 15% in the second year, primarily due to grey matter development (Knickmeyer et al., 2008). Between term-equivalent age and seven years of age, children born very preterm exhibited less growth in absolute cortical and subcortical grey and white matter volumes compared to term-born children (Monson et al., 2016). The discrepancies in brain volumes were sustained at both time points, indicating that brain maturation in children born very preterm did not catch up to full-term children across early and middle childhood (Monson et al., 2016). Other studies have also displayed this reduced pattern of volumes within subregions of the frontal, temporal, and parietal lobes as well as the cerebellum, basal ganglia, hippocampus, and amygdala (Kesler et al., 2004; Peterson et al., 2000). In contrast, children born very preterm display increased cortical thickness in frontal, temporal, and parietal regions, suggesting that they have a more protracted developmental process of cortical thinning and synaptic pruning (Mürner-Lavanchy et al., 2014). Differences in grey matter volumes and cortical thickness persist into adolescence and early adulthood, signifying long-term altered grey matter developmental trajectories (Karolis et al., 2017; Ment et al., 2009; Nagy et al., 2009; Nam et al., 2015).

1.5.3 White matter development

White matter matures relatively slowly compared to grey matter (Qiu et al., 2015), but also makes significant gains during infancy and early childhood. White matter increases from 50 cm^3 to 170 cm^3 between 29 and 44 post conception weeks, and then subsequently increases by 11% the first year and 19% the second year of childhood (Knickmeyer et al., 2008; Kuklisova-Murgasova et al., 2011). Three main stages of white matter development include fibre organization, membrane proliferation/pre-myelination, and fibre myelination (Dubois et al., 2008). The last maturational process of white matter development is myelination, which begins in the second trimester of pregnancy and continues through adolescence and into adulthood (Qiu et al., 2015).

Myelination increases the conduction speed of the nerve impulses and improves the functional efficiency of communication among brain regions (van der Knaap et al., 1991). Proliferation of oligodendrocyte glial cells are responsible for myelinating axons; one oligodendrocyte will simultaneously myelinate multiple axons (Dubois et al., 2014; Dubois et al., 2008). Oligodendrocytes have different phases of maturation that correspond to stages of white matter myelination. For instance, oligodendrocyte progenitor cells and pre-oligodendrocytes are present during the membrane proliferation and pre-myelination stage, while immature and mature oligodendrocytes are present during the fibre myelination stage (Back, 2017; Dubois et al., 2008). Immature oligodendrocytes comprise 30-40% of the oligodendroglia in the preterm period (Dubois et al., 2014).

Each stage of myelination influences water diffusion intracellularly and extracellularly resulting in dynamic changes of each DTI metric (FA, MD, AD, RD) that are sensitive to the directionality of water diffusion. In the first stage of fibre organization, axons become more organized and lead to an increase in FA that can, in part, be explained by an increase in AD and decrease in RD (Dubois et al., 2008). The corpus callosum, for example, demonstrates high anisotropy of unmyelinated axons during this time due to its high organization of fibres (Dubois et al., 2008). In the second stage of membrane proliferation and pre-myelination, there is a decrease in water content and increase in density within the immature brain, resulting in a decrease in MD, AD, and RD yet increases in FA (Dubois et al., 2008; Nossin-Manor, Card, Raybaud, Taylor, & Sled, 2015). Lastly, the third stage of myelination results in a significant increase in FA and decrease in MD and RD with little change in AD as membrane permeability has decreased and the extracellular distance between membranes has also decreased (Dubois et al., 2008; Nossin-Manor et al., 2015). Crossing fibres, however, demonstrate alternate maturational trends, such that FA increases when the first fibres mature but then decreases while MD and RD increase when the second crossing fibres become mature (Dubois et al., 2014; Nossin-Manor et al., 2015).

The pattern and timing of myelination does not occur uniformly across the brain. Post-mortem data of full-term infants from birth through 33 months revealed earlier and faster rates of myelination in sensory versus motor pathways, proximal versus distal pathways, projection versus associative fibres, occipital versus parietal, and temporal versus frontal poles (Kinney, Brody, Kloman, & Gilles, 1988). Myelination also followed a caudo-rostral gradient stemming

from the centre of the brain to the periphery (Kinney et al., 1988). Some of the most rapid changes in myelin occur within the first eight months of life, which in turn, is one of the most vulnerable time periods of myelination and susceptibility to acute illness in infancy (Kinney et al., 1988). White matter regions actively myelinating during this time consist of the visual system, central corona radiata, body and splenium of the corpus callosum, cerebellar fibres, olivary tract in the spinal cord, and auditory tracts (Kinney et al., 1988). Other fibres have a more protracted pattern of myelination that spans the first two years of life, and may be more vulnerable to chronic conditions (Kinney et al., 1988). Using diffusion imaging, this increase in myelination characteristic of early brain development is reflected in exponential age-related increases in FA and decreases in diffusivity in typically developing children following birth, which slows by two years of age (Hermoye et al., 2006). Between four and nineteen years of age, neurite density based on NODDI measures exhibits an even stronger relationship with age compared to FA, MD, AD, and RD, demonstrating that neurite density is highly sensitive to age-related changes in white matter development and useful for developmental studies (Genc, Malpas, Holland, Beare, & Silk, 2017).

In children born preterm, white matter development has already been shown to be altered as early as term-equivalent age. Using a voxel-wise approach, Anjari and colleagues (2007) found lower FA in preterm infants at term-equivalent age within regions of the centrum semiovale, frontal white matter, and genu of the corpus callosum. In addition, infants who were born at 28 weeks or less had more reductions in FA within the external capsule, posterior aspect of the internal capsule, and corpus callosum (Anjari et al., 2007). Other studies have found linear associations with FA in regions within the corpus callosum, internal and external capsule, and cortical spinal tract with developmental outcomes such a motor abilities and gross cognitive scores at eighteen months and two years of age (Duerden et al., 2015; van Kooij et al., 2012). Moreover, global mean FA and apparent diffusion coefficient (ADC) values were found to associate with intelligence and social-emotional problems at five years of age, respectively (Keunen et al., 2017; Rogers et al., 2013) .

During later childhood, cross-sectional studies of very preterm children have continued to identify differences in their white matter microstructure compared to full-term children using voxel-wise methods. From seven to nine years of age, children born very preterm exhibited decreased FA in the external capsule, superior longitudinal fasciculus, uncinate fasciculus, and

inferior fronto-occipital fasciculus (Duerden, Card, Lax, Donner, & Taylor, 2013). Additional associations between fronto-striatal tracts and intelligence were identified in males (Duerden et al., 2013). Only one study to date has examined NODDI measures in seven-year-old children born very preterm, adding to our understanding of FA differences (Kelly et al., 2016). In this cohort, axon orientation dispersion index was higher in the children born very preterm compared with full-term children in the same tracts where lower FA was identified (Kelly et al., 2016). In contrast, no differences were found in axon density, although positive correlations were found in both FA and axon density with intelligence and negative correlations with behavioural measures. Moreover, while FA also correlated positively with motor and academic scores, axon orientation dispersion correlated negatively with motor scores and positively with behavioural measures (Kelly et al., 2016).

Another study by Travis and colleagues (2015) included older very preterm-born children and adolescents aged nine to seventeen years of age and identified areas of decreased FA within the bilateral uncinate fasciculus, anterior segments of the inferior frontal occipital fasciculus as well as increased FA in bilateral anterior thalamic radiations, inferior longitudinal fasciculus, and posterior segments of the right inferior frontal occipital fasciculus using a fibre tracking method. Other studies in adolescence using voxel-based morphometry and tractography methods have identified widespread decreases in FA compared to term-born adolescents in regions such as the inferior fronto-occipital fasciculus, uncinate fasciculus, splenium of the corpus callosum, internal capsule, superior longitudinal fasciculus, external capsule, and arcuate fasciculus (Constable et al., 2008; Mullen et al., 2012; Vangberg et al., 2006).

1.5.4 White matter connectivity

White matter structural connectivity changes with development and has been studied in preterm children. Within the second trimester, connectivity already evolves from a random configuration towards a more organized configuration (Cao, Huang, & He, 2017). Between 30 to 40 postmenstrual weeks, neonates demonstrated small-world modular network organization in the cortico-cortical white matter pathways (van den Heuvel et al., 2015). Small-world networks are characterised by more efficient and clustered short-range connections, suggesting that regions that are proximal are more connected to each other, as well as within hemisphere (Ratnarajah et al., 2013; Yap et al., 2011). Prematurity can also result in an imbalance between core and local

connections such that local connections are affected by gestational age whereas core connections are relatively preserved (Batalle et al., 2017). By term-equivalent age, preterm infants have altered thalamocortical connectivity compared to term-born infants, specifically between the thalamus and frontal cortex, supplementary motor regions, occipital lobe, and temporal regions (Ball, Boardman, et al., 2013). Thalamocortical connectivity at term-equivalent age is also positively related to later cognitive outcomes in preterms at two years of age (Ball et al., 2015).

In typically developing children, small-world networks and modular organization are also present following birth (Huang et al., 2015). Short-range connectivity and local clustering then decrease as a reflection of synaptic pruning (Cao et al., 2017). However, at the same time, surviving short-range connections are strengthened and long-range connections appear by 1 year of age (Cao et al., 2017). Long-range connections link communities of connections (modules) and increase the integration of brain networks across cortico-cortical connections (Cao et al., 2017). Thus, maturing connectivity is a dynamic balance between increasing global integration of connections and decreasing local segregation of connections such that there is an increase in node strength and efficiency alongside a decrease in clustering (Cao et al., 2017; Hagmann et al., 2010). Brain networks become more distributed as the long-range connections mature (Yap et al., 2011). In addition, changes during childhood development such as increasing network properties of strength, global efficiency, and local efficiency positively correlate with FA (Huang et al., 2015).

In individuals born very preterm, connectivity differences persist into childhood and early adolescence. At seven years of age, lower network densities and global efficiencies yet high local efficiencies were found in the children born very preterm in comparison to term-born children, suggesting that their whole brain structural networks show more segregation, less integration, and are less developed (Thompson et al., 2016). Moreover, poorer connectivity between networks primarily in the right hemisphere was associated with lower intelligence (Thompson et al., 2016). Another study of children six to eleven years of age with gestational ages ranging from 29 to 42 weeks, identified differences in network properties in relation to gestational age (Kim et al., 2014). Positive associations were found between higher global and local network efficiencies with longer gestational ages in medial posterior regions such as the precuneus, cuneus, and superior parietal regions, that have been found to be hub regions in structural and functional networks (Kim et al., 2014). In early adulthood, greater interconnected

subnetworks was found in preterms compared to controls, with altered connectivity particularly in basal ganglia and motor regions implicating cognitive abilities (Karolis et al., 2016).

1.6 Rationale and Hypotheses

The long-term consequences of very preterm birth are far reaching. Children born at less than 32 weeks' gestational age enter the world facing life threatening medical conditions, vulnerabilities to brain injury, disrupted brain development, and compromised developmental outcomes. Identifying early neural indicators, or biomarkers, of neurodevelopment and cognitive abilities is critical for predicting children who are at-risk for adverse outcomes, which have a high likelihood of persisting later in development when not provided treatment. In addition, identifying how the alterations in white matter development manifest in early childhood can contribute to our understanding of their brain maturation and its implications for emerging cognitive abilities, as well as the resilience and good outcomes seen in some of these children.

The present doctoral thesis addressed the hypothesis that white matter dysmaturation is at the crux of brain maldevelopment in children born very preterm. Disruptions in the underlying white matter microstructure and connectivity are paramount to the downstream developmental difficulties they experience. The neurobiological evidence of disrupted cellular structures supporting axonal outgrowth and myelination during the third trimester of pregnancy, congruent with the timing of very preterm birth, provides a compelling argument to believe that white matter development may be the most vulnerable neurodevelopmental process in these children. The literature has targeted thalamocortical networks as one of the most susceptible to very preterm birth (Ball et al., 2015; Kostovic, Kostovic-Srzentic, Benjak, Jovanovov-Milosevic, & Radoš, 2014). There is also reason to believe that white matter tracts across the whole brain are affected by very preterm birth. Animal studies of very preterm birth point to the finding that perturbed grey matter, such as improper maturation of pyramidal neurons, is a result of reduced dendritic growth, synapses and connectivity from white matter (Dean et al., 2014). Elucidating differential growth patterns of white matter as well as specific microstructural disturbances in children born very preterm will identify opportunities for amelioration and targeted treatments.

Based upon the review of the literature, it is evident that there remains a need to better understand the nature of white matter development and its consequence on outcomes during the first years of life. Studying infants and young children poses logistical challenges for

researchers, contributing to the fact that there is only a modest literature during these ages. Moreover, longitudinal studies are imperative and powerful for understanding developmental trajectories over time. In the present thesis, gaps in pivotal age groups that are currently sparse in the available literature were addressed. Data were drawn upon from a longitudinal cohort that includes neuroimaging data at multiple time points beginning from birth through 6 years of age and cognitive measures at 4 and 6 years of age. Three primary studies address the mentioned rationales:

1.6.1 Study 1: Longitudinal study of white matter development and outcomes in children born very preterm

Study 1 characterises developmental trajectories of white matter development using longitudinal information across the first four years of life. Diffusion imaging was acquired at four distinct time points in early childhood: within two weeks of birth, term-equivalent age, two years of age, and four years of age. Additional perinatal clinical information was obtained at birth, including radiological reports of brain injury. At four years of age, measures of the development of verbal and non-verbal intelligence, language ability, and visual-motor integration skills were obtained. Maturational changes within defined white matter tracts were quantified and rates of maturation were contrasted over time. The rates of change in DTI metrics of white matter tracts between birth and term-equivalent age were analysed with a multivariate model to determine associations with developmental outcomes. We hypothesized that white matter in children born very preterm would mature in a similar trajectory to what is known in term-born children. We also hypothesized that early the growth of white matter in the perinatal period would provide valuable information in predicting later outcomes.

1.6.2 Study 2: Altered white matter development in children born very preterm

Study 2 identifies cross-sectional differences in white matter microstructure and connectivity in children born very preterm in contrast to term-born children at four years of age. In both groups, diffusion imaging was obtained, and two primary analyses were performed. The first analysis utilized DTI metrics that were subjected to voxel-wise analyses along a whole brain white matter skeleton. The second analysis examined white matter connectivity differences by employing deterministic tractography and graph theoretical measures. The aim of this study was to

determine microstructural and connectivity differences in white matter of children born very preterm compared to term-born children at four years of age. Relations with perinatal brain injury and developmental outcomes were also examined with both methods. We hypothesized that children born very preterm would display less mature white matter reflected in differences in microstructure such as reduced FA, increased diffusivity, and fewer connections compared to term-born children. We also hypothesized that these differences would relate to their developmental outcomes.

1.6.3 Study 3: White matter microstructural identified using multi-shell diffusion imaging in six-year-old children born very preterm

Study 3 is a cross-sectional study from the same cohort of very preterm children at six years of age. For this study, multi-shell diffusion imaging was acquired for the children born very preterm and age-matched term-born children. This imaging sequence allowed us to obtain DTI metrics and additional information about white matter microstructure, specifically neurite orientation dispersion and density using NODDI methods. In total, six different metrics of white matter microstructure underwent voxel-wise analyses to determine group differences. They were also analysed with measures of perinatal brain injury and developmental measures. The goal of this study was to provide additional information of what microstructural properties may be contributing to differences in FA and developmental outcomes.

In summary, the present thesis thoroughly explored white matter development and its relation to cognition. The first chapter begins by evaluating growth of white matter regions from birth through four years of age and the associations with four-year developmental outcomes. In the subsequent second and third chapters, differences in whole brain white matter between children born very preterm compared to term-born children were investigated at four and six years of age as well as the relation between DTI metrics and cognitive abilities. Together, these three studies provide novel, comprehensive findings of white matter development in children born very preterm over the first six years of life. The overarching goal of the present thesis was to contribute unique information to the literature as well as provide compelling evidence towards the support of early therapeutic interventions.

Chapter 2
Longitudinal Study of White Matter Development and Outcomes in Children Born Very Preterm

Julia M. Young, Benjamin R. Morgan, Hilary E.A. Whyte, Wayne Lee, Mary Lou Smith, Charles Raybaud, Manohar M. Shroff, John G. Sled, Margot J. Taylor. (2017). Longitudinal study of white matter development and outcomes in children born very preterm. *Cerebral Cortex*, 27(8): 4094-4105.

This chapter is a reformatted version of the manuscript published in *Cerebral Cortex.*

2 Longitudinal Study of White Matter Development and Outcomes in Children Born Very Preterm

2.1 Abstract

Identifying trajectories of early white matter development is important for understanding atypical brain development and impaired functional outcomes in children born very preterm (<32 weeks gestational age (GA)). In this study, 161 diffusion images were acquired in children born very preterm (median GA: 29 weeks) shortly following birth (75), term-equivalent (39), two years (18) and four years of age (29). Diffusion tensors were computed to obtain measures of fractional anisotropy (FA), mean diffusivity (MD), axial diffusivity (AD) and radial diffusivity (RD), which were aligned and averaged. A paediatric atlas was applied to obtain diffusion metrics within twelve white matter tracts. Age-related changes ($p < 0.05$ FDR adjusted) across time points were present but plateaued between two and four years of age within the left posterior limb of the internal capsule, external capsule, posterior thalamic radiation, superior longitudinal fasciculus and superior frontal occipital fasciculus. Between preterm and term-equivalent scans, FA rates of change were slower in anterior than posterior tracts. Partial least squares analyses revealed associations between slower MD and RD rates of change within the external and internal capsule with lower IQ and language scores at four years of age. These results uniquely demonstrate early white matter development and its linkage to cognitive functions.

2.2 Introduction

Beginning early in the fetal period, brain maturation results from a dynamic interplay between pre-programmed biological and environmentally determined processes. Critical periods of brain development, particularly within the second trimester of pregnancy through to two years of age, establish foundational neuroanatomical structures that set the stage for future cognitive and behavioural functioning (Kostovic et al., 2014; Kostovic & Vasung, 2009). Cortical connectivity begins from twenty-two weeks' gestational age (GA) in the sensory motor region and is not complete until forty-seven weeks GA (Marin-Padilla, 1970); cortical myelination development starts after term age (Kostovic & Vasung, 2009). Brain development in children born very preterm (<32 weeks GA) can be impacted by the unexpected early ex-utero environment, as well as adverse circumstances, such as critical illnesses and brain injury. Cortical dysmaturation of infants born preterm is especially evident in disrupted neural connectivity (Pandit et al., 2014), as

white matter development is particularly vulnerable during periods of rapid myelination in utero and early childhood.

Individual white matter tracts undergo differential and temporal changes in early development. Essential preliminary progressions of white matter maturation include synaptogenesis, apoptosis, axonal retraction and synaptic pruning (Kostović & Jovanov-Milosević, 2006). Axons are then pre-myelinated by pre-oligodendrocytes, which are particularly sensitive to environmental changes such as preterm birth (Ferriero & Miller, 2010). Subsequently, myelination occurs in a region and function specific, asynchronous manner. Earlier and faster rates of myelination occur in sensory versus motor pathways, proximal versus distal pathways, projection versus association fibres, central versus polar regions, occipital versus posterior parietal, and temporal versus frontal poles (Kinney et al., 1988; Qiu et al., 2015). These time-dependent occurrences can be affected by very preterm birth, thus implicating white matter development in the long-term outcomes of this population.

Diffusion imaging is invaluable for quantifying early white matter development. Diffusion tensor imaging (DTI) is a method for modelling the diffusion data, allowing for the computation of diffusion metrics including fractional anisotropy (FA), axial diffusivity (AD), radial diffusivity (RD) and mean diffusivity (MD). Examining the various measures of diffusivity, such as AD and RD, are informative for understanding FA (Song et al., 2003). These measures can reflect early morphological changes in white matter and provide information of varying white matter tract properties such as water content, fibre qualities, pre-myelination and myelination stages (Dubois, Hertz-Pannier, Dehaene-Lambertz, Cointepas, & Le Bihan, 2006). Dramatic age-related increases in FA and decreases in diffusivity are seen following birth in typically developing children (Hermoye et al., 2006). This growth is exponential, where rapid change occurs within two years of life and plateaus thereafter (Dean et al., 2014; Deoni, Dean, O'Muircheartaigh, Dirks, & Jerskey, 2012; Sadeghi et al., 2013). From 29 weeks gestational age to two years of age, white matter volume increases from 50 cm^3 to 218cm^3 on average (Kuklisova-Murgasova et al., 2011).

The majority of diffusion studies in children born very preterm are cross-sectional, completed at term-equivalent age or later childhood and adolescence. Only a few longitudinal studies have investigated the preterm period (Akazawa et al., 2016; Kersbergen et al., 2014; Partridge et al.,

2004). White matter development is consistently found to be altered in children born very preterm compared to those born at full-term, such that their grey and white matter lack differentiation and myelination (Huppi et al., 1996; Li et al., 2015; Mewes et al., 2006). Prematurity contributes to widespread and long-term reductions of FA throughout the cerebrum, including the corpus callosum, internal and external capsule and frontal white matter regions (Rose et al., 2008). Reduced FA in the posterior limb of the internal capsule (PLIC) at term-equivalent age is associated with psychomotor delay and cerebral palsy at one and two years of age (De Bruïne et al., 2013; Roze et al., 2015; Shim et al., 2014). Furthermore, measures of FA in regions such as the corpus callosum, fronto-thalamic/striatal tracts and PLIC are associated with cognitive function in childhood and adolescence (Counsell et al., 2008; Duerden et al., 2013; Feldman et al., 2012; Ullman et al., 2015). Longitudinal information of white matter maturation from birth through childhood is critical to understanding the trajectories of its development and implications with outcomes.

In the present longitudinal study, our primary aim was to utilize DTI to quantify and characterize the maturation of twelve different white matter tracts at four time points beginning from very preterm birth through four years of age. We also investigated the impact of GA, sex and brain injury on the development of these tracts. Maturational differences between tracts and hemispheres were also examined. In addition, we tested the important relation between changes in DTI metrics during the preterm period with developmental outcomes at four years of age to determine the association of early white matter maturation with long-term cognitive, language and motor ability in children born very preterm.

2.3 Materials and Methods

2.3.1 Participants

As a part of a longitudinal study, 105 very preterm born neonates (median age at birth in weeks: 28.6 weeks; range 24.43-32.86 weeks; 55 males and 50 females) were recruited from the neonatal intensive care unit at the Hospital for Sick Children in Toronto. Neonates with any known chromosomal or major congenital abnormalities were not recruited into the study. All families signed an informed consent agreeing to MRI scans, access to medical records and to follow-up neuropsychological assessments. The study protocol was approved by the Hospital for Sick Children research ethics board.

2.3.2 MRI Acquisition

Each very preterm neonate underwent an MRI scan within two weeks of birth, and up to three longitudinal scans at term-equivalent, two years and four years of age. Following the first scan, five neonates passed away before term-equivalent age. Neonates (shortly after birth and term-equivalent age) were scanned while swaddled under natural sleep. At two years of age, a mild sedative of chloral-hydrate was administered by a qualified nurse to help with the scan acquisition. At four years of age, all MRI scans were acquired awake while watching a movie or during natural sleep in the evening. Refer to Table 1 for complete scan protocols.

Table 1. Scan protocols and subject demographics

MRI scan	Details	Preterm	Term	2 Year	4 Year
	MRI scanner	1.5T GE	1.5T GE	1.5T GE	3T Siemens
	Head coil	neonatal	neonatal	12 channel	12 channel
Diffusion scan	**Sequence**	SE-EPI	SE-EPI	SE-EPI	SE-EPI
	B value (mm^2 /s)/Directions	700/15	700/15	700/15	1000/60
	TR/TE/scan time (s)	15/.085/306	15/.085/306	15/.085/306	8.8/.087/400
	FOV (mm)	205x205x72	224x224x77	368x368x124	244x244x140
	Resolution (mm)	0.8x0.8x1.6	0.88x0.88x1.6	1.44x1.44x2.3	2x2x2
	Collected/Final Sample	102/75	57/39	20/18	33/29
	Gestational Age (wks) (SD)*	29.00 (1.68)	29.14 (1.32)	29.14 (1.78)	29.14 (1.46)
	Scan Age (wks) (SD)*	30.29 (1.69)	42.29 (1.95)	109.46 (6.42)	216.84 (9.97)
	Males (%)*	52	56	66	55
T1-weighted scan	**Sequence**	3D-SPGR	3D-SPGR	3D-SPGR	MPRAGE
	TR/TE/scan time (s)	.004/.023/339	.004/.023/339	.023/.004/339	2.3/.00296/300
	FOV (mm)	128x128x110	160x160x110	368x368x124	192x240x256
	Resolution (mm)	0.5x0.5x1	0.6x0.6x1	1.44x1.44x2.3	1x1x1
	Collected Sample	105	70	26	43
T2-weighted scan	**Sequence**	2D-FRFSE	2D-FRFSE	2D-FRFSE	Turbo SE
	TR/TE/scan time (s)	4/.145/256	4/.145/256	4/.145/256	9/.104/240
	FOV (mm)	128x128x92	160x160x102	288x288x137	161x230x154
	Resolution (mm)	0.5x0.5x1	0.63x0.63x1	1.1x1.1x1.5	1.2x1.2x1.2
	Collected Sample	105	70	26	43

**Final sample*

All images were inspected for gross motion artefacts and anatomical abnormalities. As the diffusion sequence is susceptible to motion and the noise of the DTI sequences often woke up the sleeping infants, many scans were not useable. Those with useable diffusion scans included 75 babies shortly following birth, 39 babies at term-equivalent age, 18 children at 2 years of age, and 29 children at 4 years of age. A flow chart with the samples at each time point are provided

in Figure A1. Attrition occurred following the initial MRI scan for a number of reasons such as inability to continue participation and loss of contact. The sedation procedure at two years of age was deterring for some families; thus, more scans were acquired at the four-year follow-up.

2.3.3 DTI Processing

The diffusion data were pre-processed, which involved the alignment of all volumes to a reference volume using FSL tools (Jenkinson, Beckmann, Behrens, Woolrich, & Smith, 2012) as well as b-vector realignment using custom scripts. Following visual inspection, volumes corrupted with motion were excluded from an individual's dataset. Up to 5 volumes of the 15-direction sequence and up to 30 volumes of the 60-direction sequence were excluded. Data from infants whose diffusion data exceeded these numbers were excluded. The RESTORE algorithm (Chang, Jones, & Pierpaoli, 2005) was subsequently applied to calculate diffusion tensors while excluding outliers on a voxel-wise basis. DTI metrics (FA, MD, AD, RD) were extracted from this model. At each time point, FA images were co-registered using MICE-build-model (https://wiki. mouseimaging.ca/display/MICePub/MICe -build-model; Lerch, Sled, & Henkelman, 2011), a software for group-wise non-linear registration of 3D images, creating an FA template for each time point. Similarly, a template using T2-weighted images for preterm and term-equivalent scans and T1-weighted images for 2- and 4-year scans were created. Nonlinear transformations were computed between adjacent time points to allow registration of the JHU-neonate-SS white matter atlas (Oishi et al., 2011) to each age group. In addition, the FA template of each time point was registered to its corresponding T1 and T2 template. Through these transformations, the JHU neonate atlas was applied to each FA template.

Tract-based spatial statistics (TBSS) tools were used to derive a white matter skeleton from the mean FA image at each time point (Smith et al., 2006). At the preterm and term time points, a threshold of FA > 0.2 was used as images at these time points have lower FA measures than the later time points. At 2 and 4 years of age, a threshold of FA > 0.25 was used. The thresholded FA skeleton was also applied to MD, AD and RD images. Average FA values within major white matter tracts of the JHU-neonate-SS white matter atlas (after applying the FA skeleton) were extracted at each time point as shown in Figure 2. Axial slices of average FA templates. DTI measures for twelve white matter tracts were extracted, including the corpus callosum (CC), anterior limb of the internal capsule (ALIC), posterior limb of the internal capsule (PLIC),

retrolenticular part of the internal capsule (RIC), anterior corona radiata (ACR), superior corona radiata (SCR), posterior corona radiata (PCR), external capsule (EC), posterior thalamic radiation (PTR), superior longitudinal fasciculus (SLF), superior fronto-occipital fasciculus (SFOF) and inferior fronto-occipital fasciculus (IFOF). In the preterm period, DTI metrics for only 9 tracts were obtained as measures in the SLF, SFOF and IFOF were not reliable enough until term-age. Developmental changes of each DTI metric across four years of life are plotted in Figure 3.

Figure 2. Axial slices of average FA templates

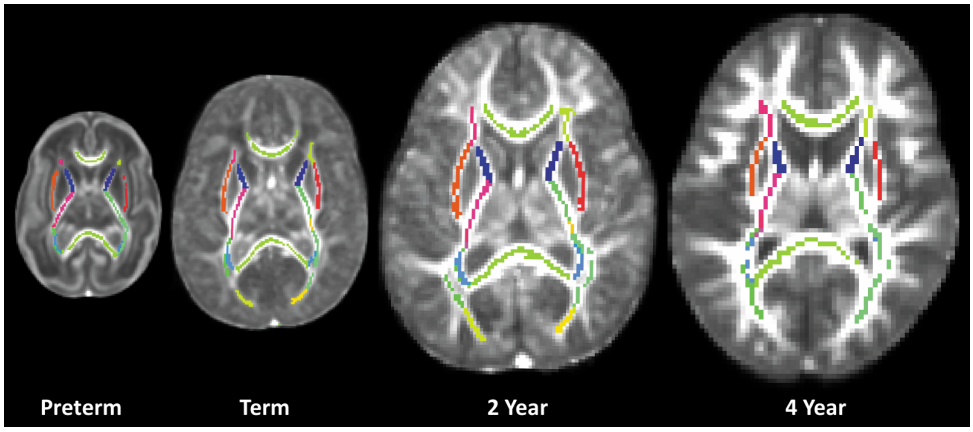

Average FA templates are shown at each sampled time point with white matter atlases overlaid. Images are scaled.

2.3.4 Assessment of Brain Injury

Two paediatric neuroradiologists (MMS and CR) evaluated the clinical images of each neonate's structural T1- and T2- weighted neuroanatomical images independently. Images were evaluated for the presence and grade of intraventricular/germinal matrix hemorrhage (IVH/GMH). In the present study, GMH1/IVH1 is defined as haemorrhage limited to the germinal matrix, GMH2/IVH2 includes an intraventricular haemorrhagic component, GMH3/IVH3 additionally includes ventriculomegaly, and GMH4/PVHI is characterized by periventricular venous haemorrhagic infarction associated with IVH (Raybaud et al., 2013). White matter injury (WMI) was graded as mild to moderate (T1 signal abnormalities in three or fewer areas), and severe (T1 signal abnormalities in >5% of hemisphere) levels of injury (Miller et al., 2003).

Figure 3. Longitudinal white matter FA plots

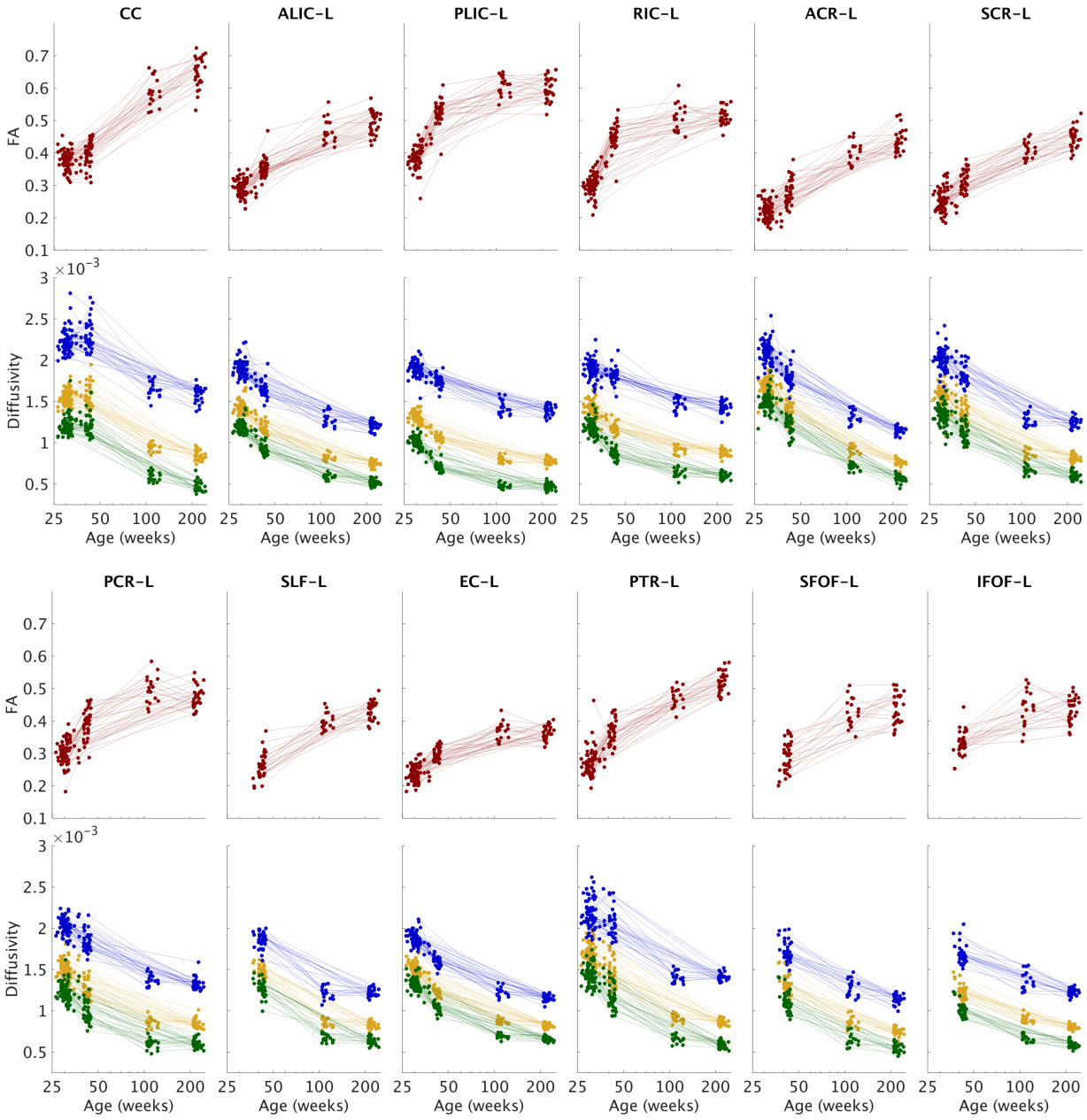

Plots depict measures of FA (red), MD (yellow), AD (blue), and RD (green) for each left-hemisphere white matter tract and individual across time. Connected points indicate longitudinal measures from the same individual at four time points: shortly following birth (median (SD) scan age: 30.29 (1.69) weeks), term-equivalent age (median (SD) scan age: 42.29 (1.95) weeks), 2 years and 4 years of age. The x-axis (age) is log-transformed.

2.3.5 Neuropsychological Assessments

Neuropsychological assessments were performed at four years of age. For each assessment, raw scores were converted into standardized scores with a population mean of 100 (50th percentile of typical development) and a standard deviation of 15. Intelligence quotients (IQ) were determined by the Wechsler Preschool and Primary Scales of Intelligence – Third Edition (WPPSI-III) (Wechsler, 2002) using Canadian norms. Three different indices of cognitive abilities were obtained: Verbal IQ (VIQ), Performance IQ (PIQ) and Full-Scale IQ (FSIQ). Overall language ability measuring receptive and expressive language yielding a core language (CL) summary score was determined by the Clinical Evaluation of Language Fundamentals – Preschool, Second Edition (CELF-Pre-2) (Semel, Wiig, & Secord, 2004). Visual-motor integration ability and supplemental tests of visual perception and motor coordination were assessed by the Beery-Buktenica Test of Visual Motor Integration (VMI) (Beery, Buktenica, & Beery, 2010).

2.4 Statistical Analyses

2.4.1 Developmental Trends

Longitudinal trajectories of FA were modeled for nine white matter tracts using non-linear mixed effects models. This approach incorporated an exponential growth function and accounted for the longitudinal structure of the data containing some incomplete data across all four time-points. Four terms were included in the exponential model such that *t* represents scan age in weeks, x_0 represents the y-intercept, x_1 represents the asymptote, and x_2 represents the growth factor of the exponential function. The model is as follows:

$$FA \sim x_0 + (x_1 - x_0)(1 - e^{-x_2 t})$$

Using this equation, the non-linear mixed effects model treated x_2 and subject as a random factor as well as x_0, x_1, and x_2 as fixed factors. Time in weeks were calculated for the time at which each tract reached 90% of the difference between FA at term-equivalent age (40 weeks) and the asymptote.

Subsequent linear mixed effects models were used to investigate the developmental changes of each DTI measure with scan age between adjacent time points for each tract, bilaterally. A total of three time windows were tested (preterm through term-equivalent age, term-equivalent

through two years of age, and two through four years of age). Measures of FA, MD, AD and RD within the left and right hemispheres across each time window were treated as dependent measures and scan age was an independent measure. The equation for this model is as follows: tract ~ scan age + subject where scan age is a continuous variable and subject is a random factor. The resulting slopes were used to compare bilateral growth in each time window. To determine the associations of GA, sex, WMI and left/right GMH with FA across time, the same analyses were performed with the inclusion of these variables in the model. The formula for this model is as follows: tract ~ scan age + GA + sex + WMI + GMH + subject. All p-values were adjusted for multiple comparisons using false discovery rate (FDR) (Benjamini & Hochberg, 1995).

The Wilcoxon signed rank test (Maritz, 1985), a non-parametric test comparing pairwise differences in mean ranks was performed to test for differences between tracts and hemispheres. Changes in FA per week within tracts were calculated only for individuals with longitudinal scans between adjacent time points. All p-values of pairwise tests also underwent FDR adjustment for multiple comparisons, with a corrected significance level of $p < 0.05$.

2.4.2 Associations with Neuropsychological Outcomes

Between preterm and term-equivalent ages, rate of change in FA, MD, AD and RD were calculated for each tract using the difference in DTI values divided by the time interval between scans. Multivariate partial least squares (PLS) analyses were used to compute associations between these slopes and neuropsychological outcomes at four years of age. Separate PLS analyses were performed for each DTI metric including data from nine white matter tracts measurable in the preterm period and three main outcome measures. The outcome measures include the composite scores of the neuropsychological assessments including full scale IQ, core language and visual motor integration scores. A total of eight analyses were performed for the left and right hemispheres separately.

A correlation matrix was then calculated between each X (DTI metrics) and Y (outcome measures) matrix, which underwent singular value decomposition to produce components explaining the maximum amount of correlation between the matrices. The amount of variance explained by each component was found by calculating the ratio of a squared singular value (eigenvalue) to the sum of all squared singular values; eigenvalues greater than one were considered significant components. Bootstrapping, sampling with replacement, was performed

5000 times to create a sampling distribution under the null hypothesis that there is no association between predictor and outcome measures. To estimate statistical reliability of the contribution of each variable to the overall pattern, a bootstrap ratio (corresponding to a z-score) was calculated (McIntosh & Mišić, 2013). Significance was determined by $|Z| > 2.58$, corresponding to $p < 0.01$.

To visualize the patterns of associations between DTI metrics and outcomes, the first components of the significant PLS analyses were plotted. Each plot depicts significant contributions of the X variables to the pattern of dependent measures. The 95% prediction intervals are also included, representing 95% of data found from 5,000 bootstraps. All statistical analyses were performed using MATLAB (MathWorks Inc., Natick MA) and R software.

2.5 Results

2.5.1 Participant Characteristics

At each time point, the mean gestational age at birth did not differ between the subsets of the very preterm cohort (75 shortly following birth, 39 at term, 18 at two years and 29 at four years) whose DTI data were included in the present study. Refer to Table 2 for the participant characteristics included at each time point.

Table 2. Participant characteristics

Details	Preterm	Term	2 Year	4 Year
Final sample, n	75	39	18	29
Males, n (%)	39 (52)	22 (56)	12 (66)	16 (55)
Gestational age, (wks)(SD)	29.00 (1.68)	29.14 (1.32)	29.14 (1.78)	29.14 (1.46)
Scan age, (wks)(SD)	30.29 (1.69)	42.29 (1.95)	109.46 (6.42)	216.84 (9.97)
Birthweight, (g) (SD)	1191.2 (276.8)	1185.1 (264.0)	1113.5 (208.3)	1169.3 (242.5)
Intrauterine growth restriction, n (%)	13 (17.3)	10 (25.6)	4 (22.2)	5 (17.2)
Sepsis (cultures positive), n (%)	23 (30.7)	10 (25.6)	4 (22.2)	9 (31.0)
Chronic lung disease, n (%)	8 (10.7)	3 (7.7)	2 (11.1)	3 (10.3)
Congenital heart defect, n (%)	13 (17.3)	7 (17.9)	4 (22.2)	4 (13.79)
Necrotizing entercolitis (stage 2-3), n (%)	6 (8.0)	2 (5.1)	1 (5.6)	3 (10.3)
White matter lesions (mild-moderate), n (%)	20 (26.7)	8 (20.5)	4 (22.2)	5 (17.2)
White matter lesions (severe), n(%)	8 (10.7)	4 (10.3)	2 (11.1)	4 (13.8)
GMH/IVH (grade 1-2) left hemisphere, n (%)	8 (10.7)	6 (15.4)	2 (11.1)	6 (20.7)
GMH/IVH (grade 1-2) right hemisphere, n (%)	12(16.0)	7 (17.9)	2 (11.1)	5 (17.2)
GMH/IVH (grade 3-4) left hemisphere, n (%)	9 (12.0)	8 (20.5)	1 (5.6)	6 (20.7)
GMH/IVH (grade 3-4) right hemisphere, n (%)	7 (9.3)	5 (12.8)	0 (0.0)	3 (10.3)

2.5.2 Developmental Trends

Longitudinal development of FA was modeled for nine white matter tracts with measures at all four time points beginning after preterm birth through four years of age using the non-linear mixed effects model and exponential growth function. These tracts included the corpus callosum, external capsule, posterior thalamic radiation, and all sub-regions of the internal capsule and corona radiata. Tracts such as the superior longitudinal fasciculus and the inferior and superior fronto-occipital fasciculus were quantified beginning at term-equivalent age due to later maturation of these tracts and the inability to reliably quantify them at the preterm time point.

Figure 4. Longitudinal FA growth curves

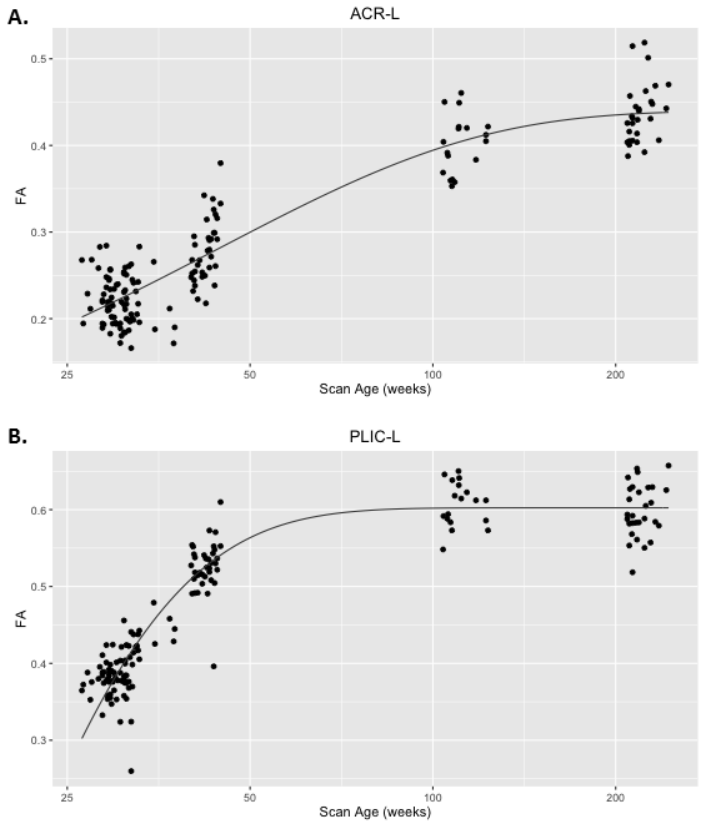

A. longitudinal growth curve of FA for all four time-points are modeled. **A.** The anterior corona radiata in the left hemisphere (ACR-L) depicts a gradual growth curve, which plateaus between two and four years of age. **B.** The posterior limb of the internal capsule in the left hemisphere (PLIC-L) depicts a contrasting growth curve, which plateaus between term-equivalent and two years of age.

In Table 3, the weeks in which each tract reached 90% of its maturation between term-equivalent and its growth peak indicates different maturational trajectories. Regions such as the posterior corona radiata and posterior limb of the internal capsule began to peak after six months of life while regions such as the anterior corona radiata, anterior limb of the internal capsule, and corpus callosum had the most protracted peak development occurring after 2 years of age as shown in Figure 4A and 4B.

Table 3. FA growth by tract

Tract	Hemisphere	90% Asymptote (weeks)	FA value of asymptote	Exponential growth rate
ACR	L	143	0.440	0.022
	R	136	0.454	0.024
ALIC	L	125	0.492	0.027
	R	147	0.550	0.022
CC	-	254	0.710	0.011
EC	L	79	0.365	0.059
	R	90	0.377	0.046
PCR	L	73	0.482	0.070
	R	79	0.469	0.059
PLIC	L	67	0.602	0.087
	R	77	0.662	0.062
PTR	L	106	0.509	0.035
	R	97	0.519	0.040
RIC	L	64	0.511	0.097
	R	75	0.550	0.066
SCR	L	105	0.439	0.035
	R	104	0.439	0.036

2.5.3 Preterm to Term-Equivalent Age

Within the first month of life, nine of twelve white matter tracts were examined again using the linear mixed effects model. Similar to the longitudinal model of all four time points the corpus callosum, external capsule, posterior thalamic radiation, and sub-regions of the internal capsule and corona radiata were examined. As shown in Figure 3, the corpus callosum and posterior limb of the internal capsule exhibited the highest FA values following birth while the external capsule and anterior corona radiata had the lowest FA values.

The majority of the tracts demonstrated bilaterally significant ($p < 0.05$ adjusted) age-related changes (increases in FA and decreases in MD, RD and AD for all tracts except the corpus callosum) between preterm and term-equivalent age as shown in time point one of Table A1. The

slopes were extracted for each of the tracts, to assess the change in the DTI metric with age. In Figure 5, slopes of each tract are plotted to highlight the relative changes across tracts. After including the additional variables (GA, sex and injury), several white matter tracts demonstrated slower maturation of FA in the presence of WMI and IVH/GMH. Slower rates of FA change were found for those with WMI within the left posterior limb of the internal capsule (slope = -0.008, $p = 0.037$ adjusted) as well as the left and right retrolenticular part of the internal capsule (slope = - 0.090, $p = 0.013$; slope = -0.086, $p = 0.014$ adjusted). In addition, a slower rate of FA change was found for those with right-lateralized IVH/GMH in the right posterior thalamic radiation (slope = 0.093, $p = 0.047$ adjusted). No associations of GA or sex were found following multiple comparisons.

Rates of change were calculated from 29 infants with both preterm and term-equivalent scans and pairwise differences between tracts and hemispheres were tested with the Wilcoxon signed rank test. Posterior tracts developed more quickly than anterior tracts as shown in Figure 5. For example, the rate of change of the anterior limb of the internal capsule was significantly slower than the posterior limb of the internal capsule, corona radiata, and thalamic radiation as well as the retrolenticular aspect of the internal capsule ($p < 0.05$ adjusted). In addition, the rate of change of the corpus callosum was slower than all other tracts. Laterality differences were found in the posterior corona radiata, where the rate of FA change in the left hemisphere was slower than the right hemisphere. Significance values for all the pairwise tests are provided in Table A2.

2.5.4 Term-Equivalent to Two Years of Age

The time period from term-equivalent age through to two years of age demonstrated the greatest changes in DTI measures (Figure 3). Across all DTI measures and tracts, significant changes (increases in FA and decreases in MD, RD and AD) were found between scan ages. Three additional white matter tracts were able to be assessed between these two time points, the superior longitudinal fasciculus, the inferior and superior fronto-occipital fasciculus. No associations of gestational age, sex, WMI or IVH/GMH were found following multiple comparisons during this time period.

Figure 5. Rate of change of white matter tracts.

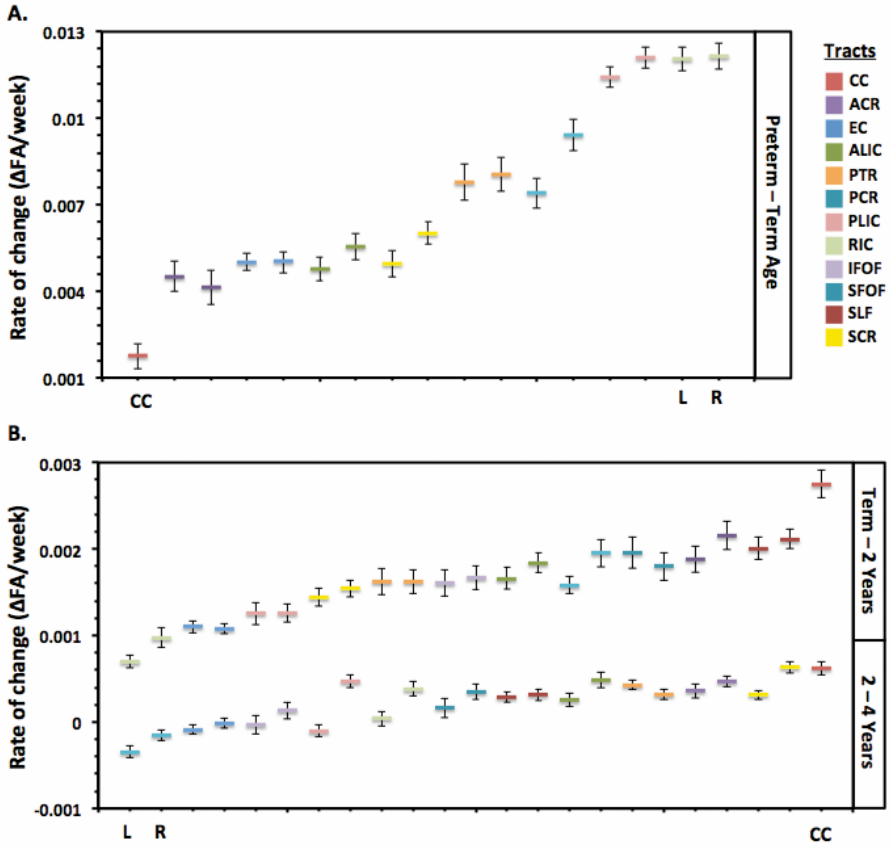

Rates of change and standard errors derived from linear mixed effects models are plotted for each tract (L and R). **A.** The upper points indicate the change in FA per week between preterm and term-equivalent age. **B.** The upper and lower rows of points indicate the change in FA per week between term-equivalent and two years of age, as well as two and four years of age. Colours represent different tracts (see legend).

Pairwise differences between the rates of FA change across tracts and hemispheres were determined from 11 children with scans at both term-equivalent and two years age. In contrast to the preterm period, the rate of change of the anterior limb of the internal capsule demonstrated significantly faster increases of FA in comparison to the posterior limb and retrolenticular part of the internal capsule bilaterally. The rate of FA change was significantly faster in the corpus callosum compared to all other tracts. Furthermore, laterality differences were found in the posterior corona radiata where the left hemisphere developed significantly slower than the right hemisphere. Complete significance values are provided in Table A3.

2.5.5 Two to Four Years of Age

The last time window studied revealed a distinct slowing and plateau of change within the DTI metrics (see Figure 3 and Figure 4). As shown in Table A1, while the majority of tracts are still undergoing significant age-related changes ($p < 0.05$ FDR adjusted), this trend ceased for a number of tracts for the different DTI metrics, but particularly in FA changes, in the left hemisphere within the superior longitudinal fasciculus, superior and inferior fronto-occipital fasciculus, posterior thalamic radiation, as well as the external, posterior limb, and retrolenticular part of the internal capsule. Again, no associations of gestational age, sex, WMI or IVH/GMH were found following multiple comparisons during this time period.

Pairwise differences between tracts and hemispheres were performed for nine children with longitudinal scans between two and four years of age. Laterality differences emerged during this time window where the left posterior limb and retrolenticular portion of the internal capsule and superior corona radiata changed significantly slower than the right (see Table A4).

2.5.6 Associations with Neuropsychological Outcomes

Longitudinal diffusion scans between preterm and term-equivalent age and four-year neuropsychological assessments were acquired in 19 children (median GA: 29 weeks; 13 males). Performance on neuropsychological measures indicated scores at average levels for the majority of the assessments, but with a wide range of ability. Average and standard deviation scores for measures of Full Scale IQ was 96.95(12.98), core language was 96.06(19.53), and visual motor integration was 100.63(10.26). Motor coordination scores were lower than average in our very preterm children compared to the general population, with average scores almost one standard deviation lower than the 50^{th} percentile. A summary of the full measures are provided in Table A5.

The PLS analyses conducted between white matter tract growth across the preterm period and outcome measures revealed associations as shown in Table 4 and Figure 6A and 6B. Of the eight PLS analyses, three analyses resulted in significant first components, all within the left hemisphere. One significant analysis included MD change measures and outcomes corresponding to an eigenvalue of 1.3057, accounting for 90.82% of the total variance. This pattern of association found that slower decreases in the rate of change in MD (calculated as a

less negative value and therefore a higher normalized value and positive value within the figures due to diffusivity decreasing as a function of age) across preterm and term-equivalent age within the left regions of the internal and external capsule corresponded to lower full scale IQ and lower core language scores as shown in Figure 6A. Another significant analysis included AD changes and outcomes corresponding to an eigenvalue of 1.356, accounting for 87.9% of the total variance. This pattern of association found that faster decreases in the rate of change in AD within the left posterior thalamic radiation corresponded to lower scores of full scale IQ and language. Finally, the last significant analysis included RD changes and outcomes with an eigenvalue of 1.261, accounting for 90.45% of the total variance. This pattern of association found that slower decreases in the rate of change in RD within the left regions of the internal and external capsule corresponded to lower scores of full scale IQ (see Figure 6B).

Figure 6. PLS analyses with outcomes.

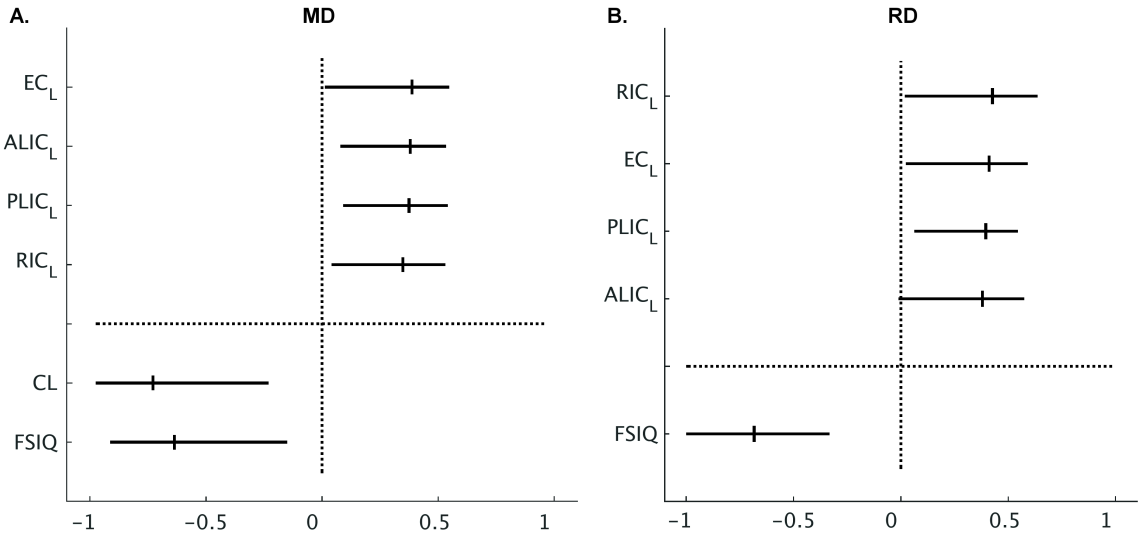

The significant contributions (x-axis) of the independent measures (above dotted line) and dependent measures (below dotted line) for the first components of two significant PLS analyses. The median bootstrapped contribution of each variable is shown as a tick mark on a line representing the 95% prediction interval. Significant contributions to the component were determined using a bootstrap ratio. **A.** In the left hemisphere, slower change of MD measures (visually depicted as a more positive normalized value) of the EC, ALIC, PLIC, and RIC between preterm and term-equivalent age was associated with lower core language (CL) and full scale IQ (FSIQ) scores at 4 years of age. **B.** In the left hemisphere, slower change of RD measures of the RIC, EC, PLIC, and ALIC was associated with lower FSIQ scores.

Table 4. Significant PLS analyses

	Measure	Left MD	Left AD	Left RD
X Variables	Corpus callosum	0.6717	1.0319	0.5860
	Anterior limb of internal capsule	3.8425*	1.3222	2.6045*
	Posterior limb of internal capsule	3.5770*	0.8631	3.6490*
	Retrolenticular internal capsule	3.0278*	0.2102	3.6348*
	Anterior corona radiata	2.4518	-0.4950	1.3908
	Superior corona radiata	1.0739	-0.0498	1.7299
	Posterior corona radiata	-1.3614	0.6662	0.0324
	External capsule	3.2045*	0.4616	3.5612*
	Posterior thalamic radiation	-1.6302	-5.3608*	-0.9440
Y Variables	Full scale IQ	-4.2887*	-6.5287*	-5.4534*
	Core language	-3.2786*	-8.3850*	-0.4222
	Visual motor integration	1.0922	-0.0448	0.2066

** Denotes significant bootstrap ratios*

2.6 Discussion

The evolution of white matter during infancy and childhood in children born very preterm provides a unique opportunity to identify some of the early stages of maturation in the developing brain. In the present study, we provide in vivo evidence of biological changes in white matter beginning from the equivalent of the third trimester. We examined three stages of white matter development based upon our imaging time points and its impact on diffusion measures, which were predominantly characterized by tract-specific increases in FA and decreases of MD, AD and RD. Additionally, we investigated a critical clinical concern regarding the potential impact of white matter development during the preterm period with long-term developmental outcomes in this high-risk population. Associations between MD and RD measures for tracts within the left-lateralized internal and external capsule were associated with intelligence and language outcomes.

Our methodology combining TBSS and validated atlas-based segmentation of the white matter in neonates was chosen to increase the reliability of our diffusion measures and allow us to analyze longitudinal changes in the diffusion measures (Oishi et al., 2011). Extracting values from the centre of each tract avoided partial volume sampling as much as possible, particularly at the youngest time points when myelination is only just starting. Measures of FA have been found to

be the most sensitive for evaluating variances between white matter tracts of infants born very preterm as maturational changes of anisotropy are larger than the other diffusion measures (Partridge et al., 2004). Thus, we focused mostly upon changes in FA in the present study.

The changes in diffusion measures per week were most rapid between preterm and term compared to their maturation after term-equivalent age. This implies that in a given infant typical in utero white matter development is more rapid than ex utero development (Qiu et al., 2015). We found that the posterior limb and retrolenticular part of the internal capsule exhibited the fastest rates of change during the preterm period. Additionally, the posterior tracts demonstrated greater and faster rates of change than the more anterior tracts and corpus callosum (Figures 3,4 and 5). This supports a posterior to anterior gradient of development as well as faster development of projection tracts versus association tracts (Kersbergen et al., 2014; Partridge et al., 2004). Measures of the tracts at term-equivalent age (Figure 3) demonstrate previously documented hierarchies of regions: the highest FA values were found in the posterior limb of the internal capsule and corpus callosum and the lowest FA values in the anterior corona radiata and external capsule (Nossin-Manor et al., 2013; Partridge et al., 2004). Reasons for high FA in the posterior limb of the internal capsule and corpus callosum, however, are due to different factors; the posterior limb of the internal capsule has high FA due to beginning stages of myelination while the corpus callosum is made of parallel fibres only and has more densely packed unmyelinated microstructures anteriorly (Nossin-Manor et al., 2013).

Our study provides novel information regarding longitudinal imaging between term-equivalent and four years of age in children born preterm, as the rates of change of FA varied by tract and age. For example, the posterior corona radiata and limb of the internal capsule matured more slowly relative to the others while the anterior corona radiata and limb of the internal capsule accelerated (Figures 4 and 5). In contrast, the rate of change of the external capsule remained relatively slow and stable throughout this four-year period. In normative studies from birth through four years of age, similar patterns have been reported where the peripheral and association fibres develop later than the projection and commissural fibres, the dynamics of these changes being driven by reduced water content, fibre organization and myelination (Geng et al., 2012; Hermoye et al., 2006).

The maturation of the corpus callosum differed from the other structures measured, as it exhibited the lowest rate of change during the preterm period, but the fastest thereafter (Figure 5). This dramatic switch from before to after term-equivalent age is consistent with the beginning of intense myelination post-term (Geng et al., 2012). Furthermore, the corpus callosum was also distinct due to the rate of FA change differing significantly from all other tracts from birth through two years of age.

Laterality effects were subtle in our findings. In the first two time windows between preterm and two years of age, the rate of FA change in the posterior corona radiata was significantly higher in the right hemisphere. Between two and four years of age, the posterior limb and retrolenticular aspect of the internal capsule as well as the superior corona radiata exhibited higher rates of change in the right than the left hemisphere. As illustrated in Figure 5, the tracts within the right hemisphere had consistently greater rates of FA change than the left, providing additional evidence of laterality effects and possibly earlier right hemispheric development (Chiron et al., 1997). We did not find effects of sex in any of the analyses, consistent with other reports (Akazawa et al., 2016; Geng et al., 2012; Kersbergen et al., 2014). In addition, effects of gestational age were not found, indicating that differing gestational ages between 24 and 32 weeks did not have a substantial impact on the rates at which white matter tracts matured.

Brain injury, which affects up to 50% of very low birth weight infants, adversely affects white matter development (Volpe, 2009). Other studies have found associations between white matter abnormalities and altered DTI measures, primarily at term-equivalent age in regions including the thalamic radiation and cortical spinal tract (Bassi et al., 2011; Counsell et al., 2003; Kersbergen et al., 2015; Liu et al., 2012). In our study, 37% of infants had WMI and approximately 25% had GMH/IVH at birth. Children with WMI exhibited slower changes in FA between preterm and term-equivalent ages in posterior limb and retrolenticular part of the internal capsule. The right posterior thalamic radiation was similarly affected by right-lateralized GMH. This is consistent with the effect of injury severity on DTI values of the left posterior limb of the internal capsule and optic radiation shortly following birth, as WMI was more extensive in the left hemisphere (Pavaine et al., 2015). Injury identified at birth was not associated with cognitive and motor outcomes, but rather persistent identification of WMI at term-equivalent age was associated with problematic behaviours and impaired executive function in our cohort (Young et al., 2016).

Longitudinal changes in diffusion measures during the preterm period were associated with long-term outcomes. Complementary to a previous report of this cohort presenting perinatal deep grey matter growth associations with visual-motor outcomes (Young et al., 2015), we found that white matter maturation was indicative of later cognition. The data-driven, multivariate PLS analyses revealed which combinations of white matter tracts were most correlated with outcomes. Advantages of using this method include more accurate predictions than multiple regression models, more stability in handling co-related variables, and models for multiple dependent measures (Cramer, 1993). We found that slower changes in MD and RD within the left-lateralized internal and external capsule were associated with lower IQ and language scores. These results highlight that deep, medial white matter tracts are most related to long-term outcomes versus more lateral or superficial tracts.

Slower decreases in the rates of MD change found in the PLS analyses, likely driven by RD, may indicate protracted premyelinating and myelinating processes that occur within the affected fibre tracts during the preterm period. Characteristic of typical development, decreasing RD during premyelination corresponds to an increasing presence of oligodendrocytes, water restriction and myelination gliosis (Nossin-Manor et al., 2015). In the preterm brain, oligodendrocytes are particularly vulnerable and sensitive to oxidative stress (Ferriero & Miller, 2010). Disrupted maturational processes in the internal and external capsule, as suggested by the slowest decreases in MD and RD changes, were found in the children with the lowest IQ and language scores, signifying a potential early biomarker for impaired long-term outcomes, concordant with earlier work (Duerden et al., 2013). Similarly, thalamo-cortical tracts, the posterior limb and retrolenticular part of the internal capsule, which project to sensorimotor, language and visual areas are also adversely affected by term-equivalent age and correlate with cognitive outcomes at eighteen months and two years of age (Ball et al., 2012, 2015; Duerden et al., 2015). The left-lateralization of our findings supports differing maturation between the two hemispheres in fetal life (Akazawa et al., 2016; Dubois et al., 2009; Kasprian et al., 2008) and was related to increased susceptibility to cognitive impairments in our cohort.

There are some limitations to consider in the present study. Differences in diffusion protocols (60 direction versus 15 direction) and scanners (3T versus 1.5T) between the four-year time point and the earlier time points may have influenced the data. The number of directions acquired using the 3T scanner was substantially greater, and thus may be more reliable at this

time point. In addition, the number of children who returned for follow-up after the initial time point decreased, with the lowest number at two years of age. This was primarily due to the need to use a sedative during the scanning procedure and/or loss of contact. Furthermore, our diffusion imaging cannot thoroughly investigate subcortical white matter due to the extensive crossing of thin fibres, which may be important for neurocognitive development. Our longitudinal sample that included the preterm, term-equivalent, and four-year developmental outcomes was relatively small and should be acknowledged while interpreting results. It is nevertheless a unique sample in the literature with longitudinal scanning and follow-up.

In conclusion, white matter maturation developed the most rapidly between birth and two years of age in our cohort of children born very preterm. While the patterns of maturation found are similar to what is reported in term-born normative populations, subtle alterations of growth leading to poorer connectivity can have important clinical implications. It is known that white matter microstructure is compromised in children born very preterm, reflected in changes of diffusivity measures. Our study is one of the first to relate early and longitudinal measures of white matter development following very preterm birth to long-term outcomes, offering compelling evidence that early developmental changes are indicative of long-term consequences. Therapeutic targets should therefore be aimed at the earliest stages of development possible.

Chapter 3
Altered White Matter Development in Children Born Very Preterm

Julia M. Young, Marlee M. Vandewouw, Benjamin R. Morgan, Mary Lou Smith, John G. Sled, Margot J. Taylor. (2018). Altered White Matter Development in Children Born Very Preterm. *Brain Structure and Function*, 223(5):2129-2141.

This chapter is a reformatted version of the manuscript published in *Brain Structure and Function.*

3 Altered White Matter Development in Children Born Very Preterm

3.1 Abstract

Children born very preterm at less than 32 weeks' gestational age (GA) are prone to disrupted white matter maturation and impaired cognitive development. The aims of the present study are to identify differences in white matter microstructure and connectivity of children born very preterm compared to term-born children as well as relations between white matter measures with cognitive outcomes and early brain injury. Diffusion images and T1-weighted anatomical MR images were acquired along with developmental assessments in 31 very preterm children (mean GA: 28.76 weeks) and 28 term-born children at 4 years of age. FSL's tract-based spatial statistics was used to create a cohort-specific template and mean fractional anisotropy (FA) skeleton that was applied to each subject's DTI data. Whole brain deterministic tractography was performed and graph theoretical measures of connectivity were calculated based on the number of streamlines between cortical and subcortical nodes derived from the Desikan-Killiany atlas. Between group analyses included FSL Randomise for voxel-wise statistics and permutation testing for connectivity analyses. Within group analyses between FA values and graph measures with IQ, language, and visual-motor scores as well as history of white matter injury (WMI) and germinal matrix/intraventricular haemorrhage (GMH/IVH) were performed. In the children born very preterm, FA values within major white matter tracts were reduced compared to term-born children. Reduced measures of local strength, clustering coefficient, local and global efficiency were present in the children born very preterm within nodes primarily in the lateral frontal, middle and superior temporal, cingulate, precuneus, and lateral occipital regions. Within group analyses revealed associations in term-born children between FA, Verbal IQ, Performance IQ, and Full-scale IQ within regions of the superior longitudinal fasciculus, inferior fronto-occipital fasciculus, forceps minor and forceps major. No associations with outcome were found in the very preterm group. Global efficiency was reduced in the children born very preterm with a history of WMI and GMH/IVH. These findings are evidence for under-developed and less connected white matter in children born very preterm, contributing to our understanding of white matter development within this population.

3.2 Introduction

Premature birth affects cortical and cognitive development by perturbing the critical foundations of early neurodevelopment. Children born very preterm (<32 weeks gestational age (GA)) are at risk for developing difficulties in aspects of cognitive function including intelligence, visual and perceptual abilities, language, attention, learning and memory, processing speed and executive function (Anderson, 2014). By 4 years of age, almost half of those with one developmental impairment also have difficulties in multiple developmental domains (Woodward et al., 2009). Lower cognitive scores in children born preterm have been found to be generally stable beginning from 4 years of age through early adolescence, yet with greater intra- and inter-individual variability (Mangin et al., 2017). Additional behavioural problems such as hyperactivity/inattention, emotional symptoms, and peer problems are also associated with cognitive impairments, which become apparent by 5 years of age (Delobel-Ayoub et al., 2009b). As cognitive difficulties children born very preterm experience are widespread, it is likely that there is a global pattern of cortical dysmaturation involving multiple brain regions.

Disturbances of grey matter development have been associated with the preterm brain. Beginning from infancy, those born very preterm have reduced subcortical and cortical grey matter volumes (Ball et al., 2012; Boardman et al., 2006) as well as altered diffusion properties in grey matter compared to term-born infants (Ball, Srinivasan, et al., 2013). Explanations for these findings in grey matter have been attributed to dysmaturation of white matter. Animal models of the preterm brain have revealed delayed dendritic arborisation and synaptic formations of projection neurons, which undergo critical development during the preterm period (Dean et al., 2013; Mcclendon et al., 2014). In particular, the thalamocortical projections of sensory systems have an intricate relationship with preterm birth (Krsnik, Majić, Vasung, Huang, & Kostović, 2017). Ingrowth of axons from the thalamus to the somatosensory, frontal, and occipital regions are especially active during the time of very preterm birth (23 – 34 post conception weeks) and are vulnerable to early brain injury such as hypoxia-ischemia induced white matter injury (Krsnik et al., 2017).

Diffusion imaging facilitates the study of white matter microstructure on a voxel-wise level by modelling a diffusion tensor to measure water diffusion within the brain (Jones, Knösche, & Turner, 2013). Fractional anisotropy (FA) quantifies the degree of restricted water diffusion

based upon the relation between axial diffusivity (AD) and radial diffusivity (RD), which represent the extent of water mobility along the principle and perpendicular directions of the fibre axis respectively (Jones et al., 2013). With increasing GA and ongoing development, FA is found to increase while RD and MD decreases, due to contributing factors such as increasing myelination, improved coherence of fibres, increasing axonal density, and reduced axonal caliber (Beaulieu, 2002; Jones et al., 2013; Pannek, Scheck, Colditz, Boyd, & Rose, 2014).

In children born very preterm, differences in diffusion properties compared to full-term children have been identified across infancy, late childhood, and adolescence. At term-equivalent age, preterm infants exhibited reduced FA as well as elevated RD within frontal white matter regions (Anjari et al., 2007). Furthermore, voxel-wise whole brain analyses have identified measures of FA and RD in regions of the corpus callosum, internal and external capsule to be correlated with global developmental measures of cognitive and motor outcomes at 2 years of age (Counsell et al., 2008; Duerden et al., 2015; van Kooij et al., 2012). In late childhood, reduced FA has also been reported in regions including the external capsule, superior longitudinal fasciculus, uncinate fasciculus, and inferior fronto-occipital fasciculus (Duerden, Card, Lax, Donner, & Taylor, 2013). Altered FA within these regions in addition to the corpus callosum and internal capsule persists into adolescence (Constable et al., 2008; Loe, Lee, & Feldman, 2013; Mullen et al., 2012; Travis, Adams, Ben-Shachar, & Feldman, 2015; Vanberg et al., 2006).

Tractography methods and graph theoretical analyses using diffusion imaging have contributed to our understanding of topological characteristics of structural brain connectivity across development. The organization of grey matter regions (nodes) and their connections (edges) can be described through graph measures such as strength, how connected nodes are to adjacent nodes, and global efficiency, how integrated and efficient networks are within the whole brain (Bullmore & Sporns, 2012; Rubinov & Sporns, 2010). Local efficiency and clustering coefficient describe segregation, based upon the path length and clustered connectivity between a node`s adjacent neighbours, respectively (Achard & Bullmore, 2007). Increased integration and decreased segregation as well as changes towards a more organized network construction are hallmark features of typical brain development (Cao et al., 2017; Cao, Huang, Peng, Dong, & He, 2016). Accordingly, changes in network properties due to early brain maturation occur in conjunction to changes in whole brain FA (Huang et al., 2015; Yap et al., 2011).

Premature birth impacts the organization of structural connections beginning from birth. Infants imaged within the preterm period demonstrated associations between local connectivity and GA involving the thalamus, cerebellum, superior frontal and cingulate gyrus (Batalle et al., 2017). At preterm birth and childhood, greater GA was related to higher connection strength, clustering coefficient, and global efficiency as well as lower local efficiency (Brown et al., 2014; Pandit et al., 2014; Thompson et al., 2016). With respect to cognitive outcomes, children born very preterm at 7 years of age were found to have associations between impaired performance on intelligence testing with lower connection strength in nodes primarily within the right hemisphere (Thompson et al., 2016).

At present, there is a distinct gap in the literature of children born very preterm during early childhood and before school age. Delayed white matter maturation and impaired outcomes at four years of age provide important indications of children who may experience persistent cognitive difficulties as they enter school age as well as those who begin learning at a disadvantage. The primary aim of the present study was to characterise altered maturation of white matter microstructure and connectivity in children born very preterm compared to full-term children at four years of age. We employed a whole brain approach, utilizing tract-based spatial statistics (TBSS) to analyze DTI metrics and deterministic tractography to analyze graph theoretical measures of connectivity such as strength, clustering coefficient, local and global efficiency between groups. Furthermore, our secondary aim was to examine relations between whole brain white matter measures with developmental outcomes within each group separately. The impact of early brain injury on white matter maturation, such as those with a history of white matter injury (WMI) and germinal matrix/intraventricular haemorrhage (GMH/IVH) detected at birth, was tested in the children born very preterm.

3.3 Methods

3.3.1 Participants

At four years of age, 53 participants born at <32 weeks GA were recruited as a part of a larger longitudinal study, conducted between 2009 and 2014 at the Hospital for Sick Children in Toronto, Canada. Exclusion criteria included those with any known chromosomal or major congenital abnormalities. Twenty-eight full-term children born >37 weeks GA were also

recruited at four years of age. Exclusion criteria for full-term children included prematurity, learning, language, neurological or developmental disabilities as well as MRI incompatibility based upon a screening interview. An informed consent to the study was signed by parents and informed assent was provided by the children. The research ethics board at the Hospital for Sick Children approved the study protocol.

3.3.2 Perinatal Clinical and Radiological Measures

The children born very preterm have clinical information from their stay in the neonatal intensive care unit. Characteristics such as GA, birth weight, head circumference, sex and delivery type (caesarean-section or vaginal) are described from birth. Significant events during pregnancy were also recorded such as premature rupture of membranes (PROM) and intrauterine growth restriction (IUGR). Measures of illness included Apgar scores at 1 and 5 minutes, the Clinical Risk Index for Babies II, patent ductus arteriosus, necrotizing enterocolitis and sepsis (defined as a positive blood or cerebrospinal fluid culture and antibiotic therapy for more than 5 days). Medical treatments including the number of days on positive pressure ventilation, endotracheal tube, continuous positive airway pressure, supplemental oxygen and total parenteral nutrition were also collected. These data are summarized in Table 5.

Paediatric neuroradiologists and neurologists assessed each of the structural T1- and T2-weighted images for the children born very preterm shortly following birth. White matter injury was graded on a scale of 1-3 for no injury, mild to moderate (T1 signal abnormalities in three or fewer areas), and severe (T1 signal abnormalities in >5% of hemisphere) levels of injury (Miller et al., 2003). Presence and grades of germinal matrix/intraventricular haemorrhage (GMH/IVH) on a scale from 0 (no haemorrhage) to 4 (periventricular venous haemorrhagic infarction associated with IVH) corresponding to levels of bleeding within the germinal matrix of the brain were also determined. This was based upon the Papile scale (GMH 1 to 4) for computed tomography findings (Papile et al., 1978) and Volpe scale for cranial ultrasonography findings adapted to MRI findings (IVH 1 to 3, PVHI) (Volpe, 2008). More specifically, GMH1/IVH1 is haemorrhage limited to the germinal matrix, GMH2/IVH2 includes an intraventricular haemorrhagic component, GMH3/IVH3 additionally includes ventriculomegaly, and GMH4/PVHI is characterized by periventricular venous haemorrhagic infarction associated with IVH (Raybaud et al., 2013). At four years of age, paediatric neuroradiologists also assessed each

of the children's structural T1- , T2- weighted and FLAIR images when collected. Any incidental findings were noted.

Table 5. Perinatal clinical and radiological characteristics.

Characteristic	Mean (SD) or number (%)
Gestational Age (weeks)	28.62 (1.75)
Males	18 (58%)
Birth Weight (g)	1152 (257.8)
Head circumference (cm)	25.4 (2.1)
Intrauterine growth restriction	5 (16%)
Cesarean-section delivery	18 (58%)
Multiple births	5 (16%)
Apgar score at 5 min	7.38 (1.5)
CRIB II	6.59 (2.26)
Endotracheal tube days	12..67 (18.32)
Oxygen administration days	15.1 (24.79)
Positive pressure ventilation	13.3 (11.06)
Patent ductus arteriosus (treated)	14 (45.2 %)
Sepsis (cultures positive)	10 (32.3%)
Premature rupture of membranes	3 (9.7%)
Necrotizing entercolitis (stage 2 & 3)	3 (9.7%)
Bronchopulmonary dysplasia	4 (12.9%)
GMH/IVH (Grade 1-2)	7 (22.6%)
GMH/IVH (Grade 3-4)	6 (19.4%)
White Matter lesions	9 (29%)

CRIB II - Clinical Risk Index for Babies; GMH - germinal matrix haemorrhage; IVH – intraventricular haemorrhage

3.3.3 Maternal Education

Levels of maternal education were obtained for all the children. Two categories of education levels were distinguished: the first as those with high school and non-university post-secondary school education and the second as those with university and post-graduate school education.

3.3.4 Developmental Assessments

Developmental assessments were performed at four years of age for the children born very preterm who returned for follow-up as well as the recruited controls. For each assessment, raw scores were converted into standardized scores with a population mean of 100 (50^{th} percentile of typical development) and a standard deviation of 15. Intelligence quotients (IQ) were determined by the Wechsler Preschool and Primary Scales of Intelligence – Third Edition (WPPSI-III; (Wechsler, 2002)) using Canadian norms. Four measures of cognitive abilities were obtained: Verbal IQ (VIQ), Performance IQ (PIQ), Processing Speed (PSQ) and Full-Scale IQ (FSIQ). The Clinical Evaluation of Language Fundamentals – Preschool, Second Edition (CELF-Pre-2; (Semel et al., 2004)) evaluated receptive and expressive language, yielding a core language (CL) summary score. . Visual-motor integration (VMI) ability and supplemental tests of visual perception (VP) and motor coordination (MC) were assessed by the Beery-Buktenica Test of Visual Motor Integration (VMI; Beery, Buktenica, & Beery, 2010).

3.3.5 MRI Data Acquisition

MRI scans were acquired with a 3.0T Siemens Trio scanner and 12 channel head coil. Sixty-direction diffusion (SE-EPI, b-value = 1000) and T1-weighted (MPRAGE) anatomical images (repetition/echo time: 8.8/.087s and 2.3/.00296s; field of view: 244 x 244 x 140mm and 192 x 240 x 256mm; resolution: 2mm isotropic and 1mm isotropic; scan time: 20 min and 5 min, respectively) were obtained when the children were awake while watching a movie or naturally asleep in the evening. All images were inspected for gross motion artefacts and anatomical abnormalities. We obtained T1-weighted images in 43 children born very preterm and diffusion images in 34 children. One child was identified with ventriculomegaly and excluded from analyses. Due to the susceptibility of the diffusion sequence to motion, two children had diffusion data with too much motion. Within the group of children born very preterm, 31 of the diffusion scans were determined to be useable. All 28 full-term children obtained usable diffusion scans.

3.3.6 Diffusion Processing

The diffusion data were pre-processed, which included the alignment of all volumes to a reference volume using FSL tools (Jenkinson et al., 2012) as well as b-vector realignment using custom scripts. Following visual inspection, volumes corrupted with motion were excluded from

an individual's dataset. Up to 30 volumes of the 60-direction sequence were determined to be excluded. Two children were excluded whose data exceeded this threshold. Across groups, the median number of excluded volumes was 3 with a range of 0-24 volumes. The RESTORE algorithm (Chang et al. 2005) was applied to exclude outliers on a voxel-wise basis.

3.3.6.1 Tract-based spatial statistics (TBSS)

DTI metrics (FA, MD, AD, RD) were calculated and extracted from the output of the RESTORE algorithm (Chang et al., 2005). Analyses of the DTI metrics were conducted using TBSS (Smith et al., 2006). A cohort-specific template of the diffusion data was created following co-registration of everyone's diffusion image to each other. Subsequently, a mean fractional anisotropy (FA) skeleton was generated and thresholded at 0.25 to represent the centre of major white matter tracts within the whole brain. The skeleton was applied to each child's FA, MD, AD, and RD data.

3.3.6.2 Connectivity Measures

Structural T1-weighted and diffusion images were co-registered using FSL tools (Jenkinson et al., 2012). The structural images were parcellated to obtain 34 cortical and 7 subcortical regions in MNI space using the Desikan-Killiany atlas (Desikan et al., 2006; Fischl et al., 2002). Whole-brain deterministic tractography was performed on the pre-processed diffusion images between each region pair using the Fiber Assignment by Continuous Tracking (FACT) algorithm (Mori, Crain, Chacko, & Van Zijl, 1999) with a 45 degree angular threshold using Diffusion Toolkit and TrackVis (www. trackvis.org; Wang, Benner, Sorensen, & Wedeen, 2007). The number of streamlines (edges) between parcellated regions (nodes) were extracted using the UCLA Multimodal Connectivity Package (UCMP) (Brown, Rudie, Bandrowski, Van Horn, & Bookheimer, 2012) and normalized by the average volume of region pairs for measures of fibre density. A weighted connectivity matrix was generated containing fibre densities between all pairs of regions. All nodes were organized by their respective lobes. Figure 7 provides a visual representation of methods used to obtain connectivity matrices for each person.

Local and global graph measures of connectivity were calculated using the Brain Connectivity Toolbox in MATLAB (The MathWorks, Inc., Natick, Massachusetts, USA). Local strength, the weighted variant of degree, was calculated by summing all of the edge weights of each node

together to quantify how nodes are structurally connected to adjacent nodes (Rubinov & Sporns, 2010). Weighted local and global efficiency were also calculated (Rubinov & Sporns, 2010). Local efficiency is the average of the inverse minimum path length of each node and global efficiency is the average minimum path length (Achard & Bullmore, 2007). Higher global efficiency indicates more complex networks with short mean path length (Bullmore & Sporns, 2012). Weighted clustering coefficient, the proportion of the node's neighbours that are also neighbours to each other was also calculated (Rubinov & Sporns, 2010).

Figure 7. White matter connectivity processing steps.

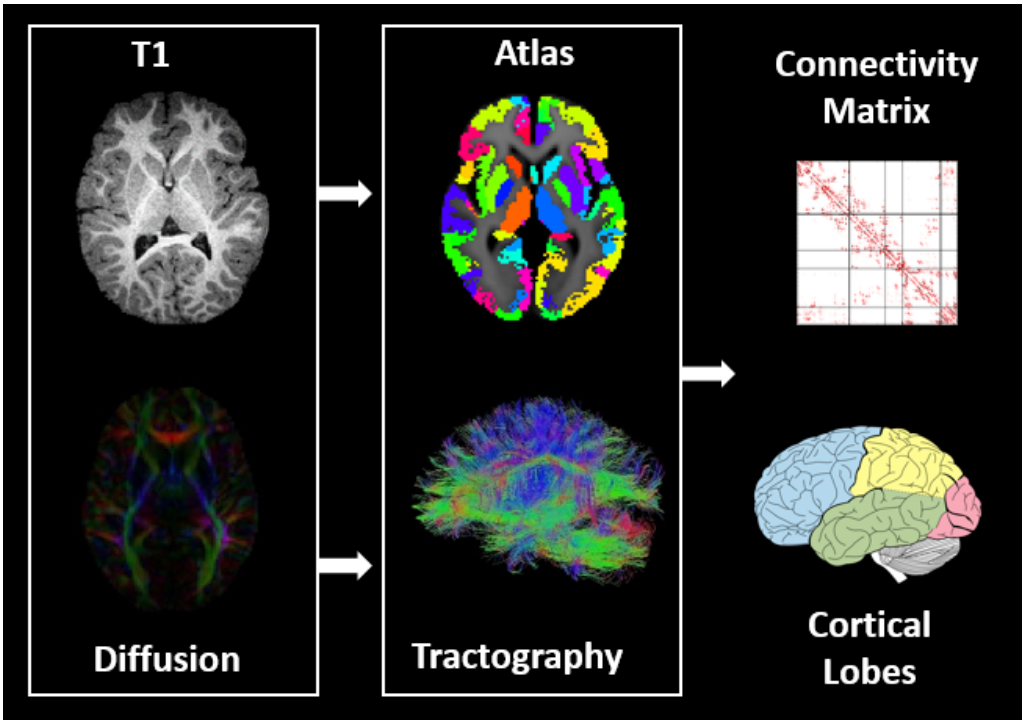

Visual representation of the processing steps to obtain connectivity matrices for each child based on deterministic tractography.

3.4 Statistical Analyses

3.4.1 Participant Characteristics

Differences in the sex ratio and age at scan between the children born very preterm and full-term children were tested using a chi-square and t-test. Additional t-tests were used to assess

differences in maternal education levels with developmental outcomes in the two groups separately as well as differences between groups for each of the developmental outcomes. Significance values were held at $p<0.05$.

3.4.2 TBSS Analyses

Between and within group voxel-wise analyses were performed with FSL Randomise (Anderson & Robinson, 2001) to determine significance, with 5,000 permutations and threshold-free cluster enhancement (Smith & Nichols, 2009). Significance was defined to be $p < 0.05$ following corrections for multiple comparisons. Between group analyses were conducted using a general linear model with group, age at scan, sex and number of excluded volumes due to motion corruption as explanatory variables. This was performed for all DTI metrics: FA, MD, AD and RD. Within the preterm group, additional voxel-wise regression analyses were performed between FA and GA, presence of white matter injury, GMH/IVH, and developmental measures. Within the full-term group, voxel-wise regression analyses were performed between FA and developmental measures.

To visualize significant results based upon the voxel-wise regression analyses, the JHU DTI-based tractography atlas (Mori, Wakana, Van Zijl, & Nagai-Poetscher, 2005) was applied to the FA skeleton to plot FA values within defined white matter tracts and developmental measures with significant voxels based upon the TBSS group difference analysis.

3.4.3 Connectivity Analyses

Local graph measures were calculated for each node and each subject, while global graph measures were calculated for each subject. Both local and global graph measures were averaged across subjects by group. To assess group differences in local graph measures, average values from the control group were subtracted from the average values of the preterm group at each node (e.g. group difference = preterm – control). Thus, negative values at any given node represents reduced local graph measures in the children born very preterm compared to full-term children. To determine statistical significance for individual metrics, permutation testing was performed with two-tailed z-tests following 100,000 permutations to obtain a null distribution of average group difference. Significance was determined based on a false discovery rate (FDR) of 5% to control for multiple comparisons (Benjamini & Hochberg, 1995). To visualize the results,

the group difference values of the graph measures for all the nodes were organized by lobes and subcortical structures. BrainNet Viewer (Xia, Wang, & He, 2013; http://www.nitrc.org/ projects/ bnv/) was used to further depict the nodes with group differences that passed FDR correction.

Associations between graph measures with GA and outcome measures (VIQ, PIQ, FSIQ, and VMI) were tested with Pearson correlations within each group separately. Graph measures and presence of white matter injury and GMH/IVH were further tested with t-tests in the preterm group. Significance was reported at a FDR of 5%. Correlations at $p<0.01$ uncorrected are reported in Supplemental material. R Studio (2015) and MATLAB software were used for statistical analyses.

3.5 Results

3.5.1 Participant Characteristics

Of the 53 children born very preterm who were tested, 31 children (13 females; mean age: 4.2 ± 0.19 years) completed developmental assessments and had usable diffusion images. Perinatal clinical and radiological characteristics for the children born very preterm are provided in Table 5. At four years of age, twelve children born very preterm had incidental findings involving small, focal white matter hyperintensities. Twenty-eight full-term children (15 females; mean age 4.6 ± 0.32 years) were recruited and completed developmental assessments and neuroimaging. No sex differences were found between groups ($p=0.371$) but there was a small difference in age at scan ($p<0.05$). Of the mothers of the children born very preterm, 22.6% had education levels in the first category and 74.2% in the second category. The mothers of the full-term children had education levels of 14.3% in the first category and 82.2% in the second category.

Performance on developmental assessments indicated average levels of ability on most measures, when considering the mean of each group separately as described in Table 6. The only subtest where the children born very preterm were below average as a group compared to the general population was in motor coordination. However, full-term children performed significantly higher than the children born very preterm on all the developmental measures ($p<0.05$) apart from Verbal IQ (see Table 6). There were no differences between the higher and lower maternal education levels and developmental assessments in either group (all $p>0.05$).

Table 6. Developmental assessments at four years of age

	FSIQ	VIQ	PIQ	PSQ	CL	VMI	VP	MC
Preterm	97.0 (12.06)	102.3 (14.72)	96.8 (10.94)	92.7 (16.38)	97.9 (14.82)	99.5 (9.28)	96.2 (18.42)	83.3 (13.78)
Full-term	107.3 (12.89)	107.4 (13.24)	105.2 (12.78)	109.1 (10.06)	109.3 (12.73)	109.0 (8.84)	105.7 (9.61)	95.8 (9.4)
p-value	*0.003*	0.186	*0.005*	*0.0002*	*0.005*	*0.0002*	*0.021*	*0.0001*

Means and standard deviations are reported

3.5.2 TBSS Analyses

Between group analyses revealed significant differences between children born very preterm and full-term within FA and RD images. Full-term children exhibited significantly higher FA than children born very preterm within voxels of most tracts, particularly in the left hemisphere (Figure 8A). These tracts include the bilateral anterior thalamic radiation, corticospinal tract, cingulum, inferior fronto-occipital fasciculus, inferior longitudinal fasciculus, superior longitudinal fasciculus, uncinate fasciculus as well as the forceps major and minor. Within RD images, children born very preterm displayed higher RD than controls within voxels of the corpus callosum, right superior longitudinal fasciculus, and inferior fronto-occipital fasciculus (Figure B1). Small clusters within the forceps minor, right cortical spinal tract, anterior thalamic radiation and superior longitudinal fasciculus were found to have differences in FA and RD where more volumes were removed due to motion corruption (Figure B2 and B3). No significant group differences were found within AD and MD images. There were no voxels where the children born very preterm had higher DTI metrics compared to controls.

Within the preterm group, no significant associations were found between FA and any of the cognitive measures (FSIQ, VIQ, PIQ, PSQ, CL, VMI, VP, and MC), nor significant associations between FA and GA, white matter injury or GMH/IVH. Within the control group, significant positive associations between FA and VIQ, PIQ, and FSIQ were found. Significant clusters of positive associations between FA and VIQ were present within areas of the forceps major and minor, left anterior thalamic radiation, bilateral inferior fronto-occipital fasciculus, and bilateral

Figure 8. TBSS results at four years of age.

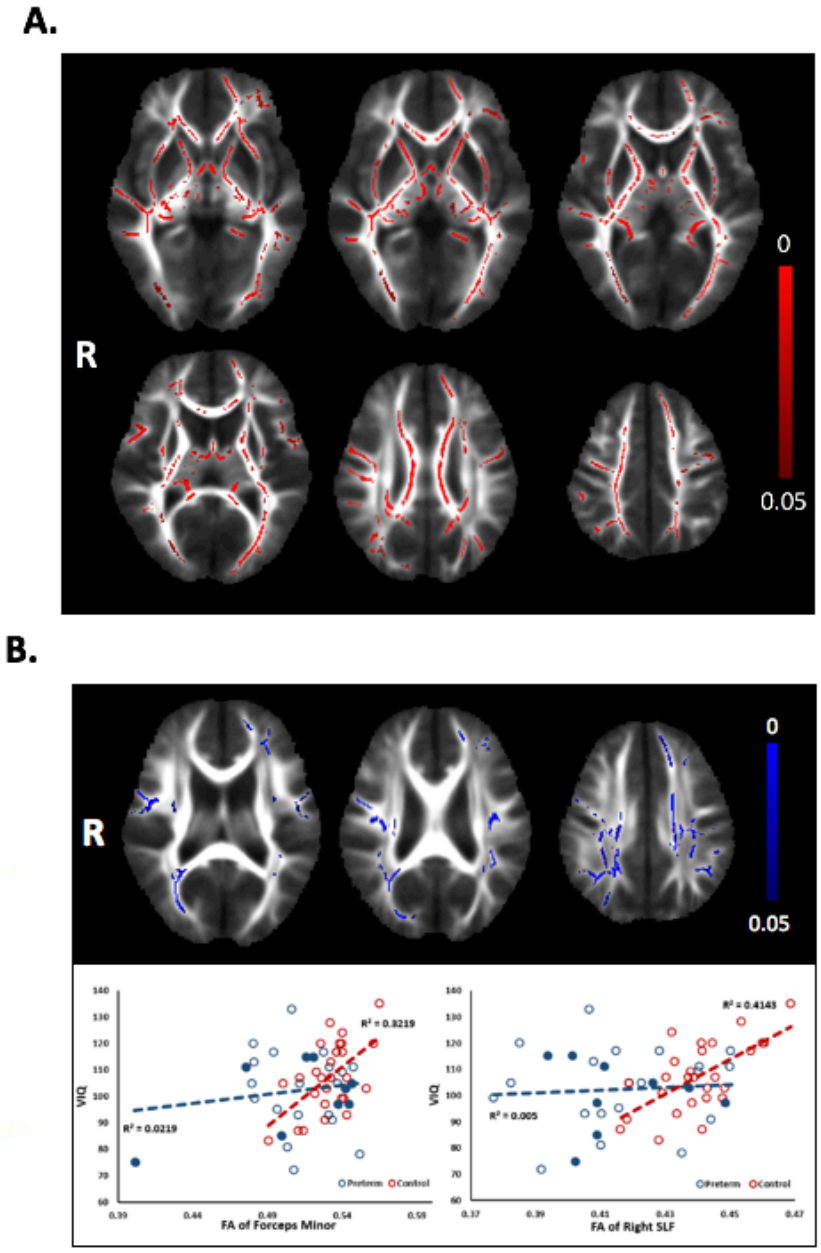

A. TBSS analyses of group differences revealed widespread areas where full-term children have significantly greater measures of FA compared to children born very preterm along the white matter skeleton ($p < 0.05$). Significant voxels are depicted in red. Colour bars indicate p-values. **B.** On the top panel, TBSS analyses identified voxels (in blue) within the full-term group to be significantly associated with VIQ ($p < 0.05$). On the bottom panel, plots indicate the relation between FA within the forceps minor and right superior longitudinal fasciculus (SLF) and VIQ for both the preterm and full-term (control) groups where significant effects were present in the full-term group. Shaded individuals (in blue) indicate those within the preterm group who experienced any degree of white matter injury at birth.

superior longitudinal fasciculus (Figure 8B). To visualize this association, mean FA measures extracted within white matter tracts from the JHU-based tractography atlas (Mori et al., 2005) were plotted with VIQ for each group (Figure 8B). Significant clusters of positive associations between FA, FSIQ, and PIQ were present within the left anterior aspects of the inferior fronto-occipital fasciculus, anterior thalamic radiation and forceps minor as well as the right posterior aspect of the forceps major (Figure B4). There were no associations with PSQ, CL, VMI, VP or MC.

3.5.3 Connectivity Analyses

The average connectivity matrices for each group indicated that proximal regions were more highly connected to one another than distal regions. Thus, short-range connections were much more prevalent than longer-range connections. Overall the entire connectivity matrix was sparse, having 9.49% of region pairs connected (9.42% for preterms, 9.57% for controls). The distribution of the sparsity of graphs was not statistically significant between groups ($p = 0.08$), (Figure B5). Group differences in edge weight were calculated and plotted by node in a connectivity matrix. The average of all the nodal differences by lobe were also plotted in a connectivity matrix as shown in Figure 9A and 9B. Although the pattern of edge weight was one of consistently reduced connectivity in the children born very preterm, these differences did not survive FDR correction.

Between group analyses revealed an overall pattern of reduced strength, local efficiency, and clustering coefficient in the children born very preterm compared to the term-born children (left panel of Figure 10A-C). Following FDR correction across all nodes, strength was significantly reduced in the children born very preterm in the bilateral middle temporal gyrus (Figure 10A). Nodes with significantly reduced local efficiency and clustering coefficient included regions across all lobes, but with the majority in the left hemisphere as well as frontal and temporal regions (Figure 10B and 10C). Common nodes found between measures of local efficiency and clustering coefficient in the left hemisphere include the lateral orbitofrontal, isthmus of the cingulate, precuneus, lateral occipital, middle temporal, superior temporal, and accumbens regions. Common nodes in the right hemisphere include the precentral, isthmus of cingulate, lateral occipital, and banks of superior temporal sulcus regions. A summary of all the significant nodes following FDR correction for strength, local efficiency, and clustering coefficient are

provided in Table 7. Moreover, the children born very preterm demonstrated significantly reduced measures of global efficiency ($p<0.0045$), (Figure B6).

Figure 9. Connectivity results between groups.

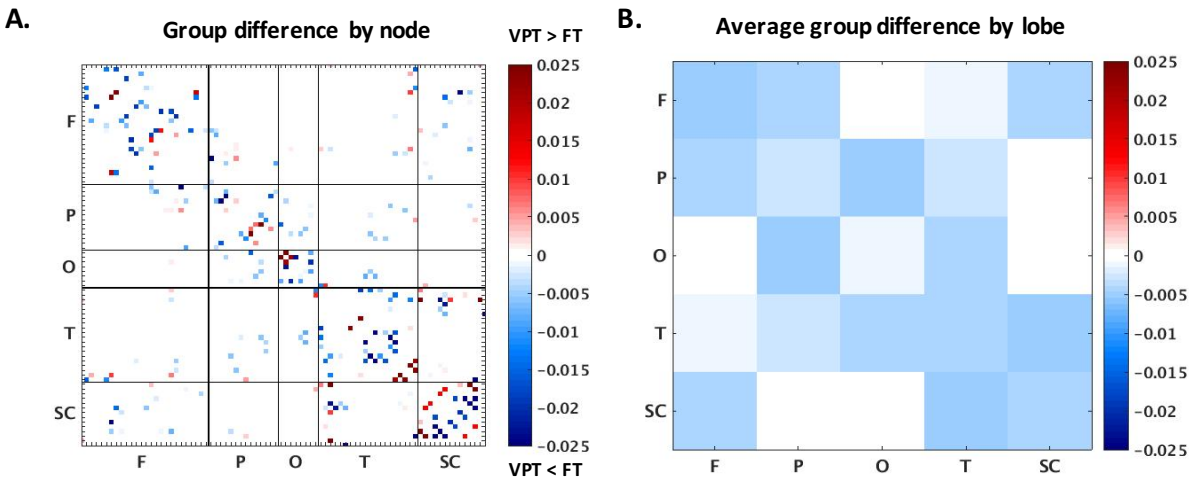

A. Connectivity matrix representing group differences in edge weight, the number of streamlines between parcellated regions normalized by the average volume of region pairs. The blue squares represent edge weight values that are smaller in the children born very preterm compared to the full-term children. Following permutation testing and FDR correction, results did not survive multiple comparisons. **B.** The group differences by node were averaged across lobes, indicating that children born very preterm tend to have reduced edge weights between and within lobes compared to full-term children.

Within group analyses for both the children born very preterm and controls revealed relations between local graph measures of strength, local efficiency, and clustering coefficient with developmental outcomes at the $p<0.01$ uncorrected level (Table B1). In the very preterm group, correlations between local graph measures with GA, white matter injury, and GMH/IVH at the $p<0.01$ uncorrected level are reported in Table A2. With respect to GMH/IVH, there was a trend for the subcortical structures to have reduced local connectivity. However, these within-group analyses did not survive multiple comparisons.

Figure 10. Connectivity results by node.

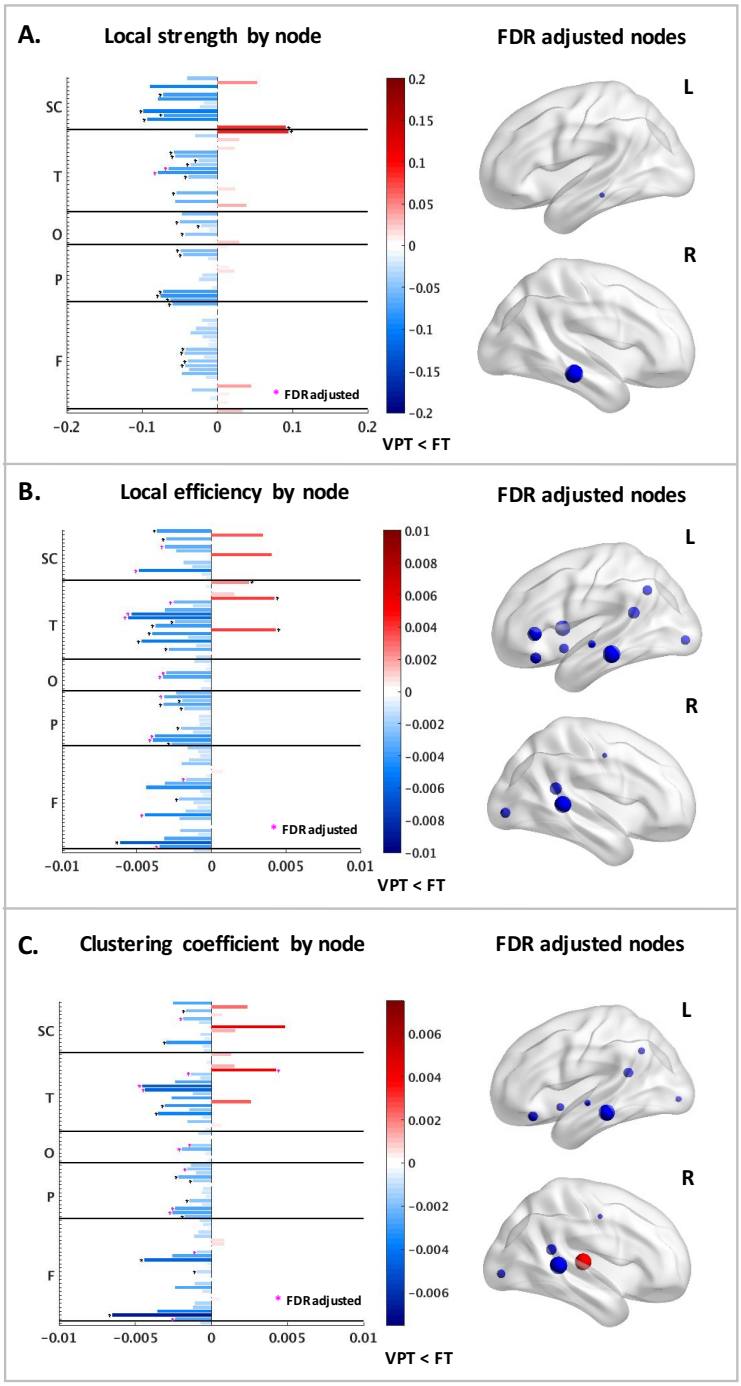

A. Group differences indicate that children born very preterm have reduced strength (shown in blue) compared to full-term children. Nodes that were significantly different following permutation testing ($p < 0.05$) are indicated with black stars. Nodes that survived FDR correction are indicated with pink stars and are plotted on the glass brains. **B.** Group differences of local efficiency by node. **C.** Group differences of clustering coefficient by node. A complete list of the nodes corresponding to the order of regions within the figures from top to bottom is provided in Table B3. Each region is ordered bilaterally (left above right).

Table 7. Significant group differences by node.

Graph Measure	Hemisphere	Region	Mean Difference	q-value
Strength	**Left**	**Middle temporal**	-0.0791	0.0216
	Right	**Middle temporal**	-0.0648	0.0216
Local efficiency	**Left**	**Lateral orbitofrontal**	-0.0035	0.0434
		Pars triangularis	-0.0045	0.0470
		Isthmus of cingulate	-0.0038	0.0139
		Precuneus	-0.0031	0.0102
		Lateral occipital	-0.0030	0.0139
		Middle temporal	-0.0056	0.0139
		Superior temporal	-0.0025	0.0434
		Caudate	-0.0048	0.0434
		Accumbens	-0.0031	0.0470
	Right	**Precentral**	-0.0017	0.0470
		Isthmus of cingulate	-0.0039	0.0434
		Lateral occipital	-0.0032	0.0139
		Banks of superior temporal sulcus	-0.0053	0.0204
Clustering coefficient	**Left**	**Lateral orbitofrontal**	-0.0024	0.0424
		Isthmus of cingulate	-0.0024	0.0424
		Precuneus	-0.0016	0.0110
		Lateral occipital	-0.0013	0.0454
		Middle temporal	-0.0043	0.0110
		Superior temporal	-0.0013	0.0454
		Accumbens	-0.0018	0.0454
	Right	**Precentral**	-0.0009	0.0454
		Isthmus of cingulate	-0.0026	0.0454
		Lateral occipital	-0.0019	0.0110
		Banks of superior temporal sulcus	-0.0045	0.0424
		Tranverse temporal	0.0043	0.0454

Negative mean difference value: Preterm < Full–term; q-value indicates significance at FDR of 5%

Following FDR correction, significant correlations between local efficiency and clustering coefficient with GA remained within the right supramarginal gyrus (*q=0.019* and *q=0.0073,* respectively). Global efficiency was not found to associate with GA or developmental outcomes. However, significant reductions in global efficiency were found in relation to WMI (*p=0.0022*)

and GMH/IVH (*p=0.0138*) indicating that brain injury detected at birth affected the integration of information.

3.6 Discussion

The impact of very preterm birth on the structural organization of white matter during early childhood is widespread and robust. In the present study, we demonstrated that white matter microstructure and connectivity are simultaneously affected in children born very preterm compared to children born full-term. Our results of reduced FA and graph measures of strength, clustering coefficient, local and global efficiency support the idea that this atypical profile of white matter in children born very preterm reflects one that is less mature and less connected than children born at term. Consequently, our findings suggest that the secondary effects of these structural alterations are expressed as poorer performance in cognitive, language, and motor abilities that have a high probability of persisting later in development.

At 4 years of age, white matter maturation is in a period of flux. It is at the beginning of a protracted period of modifications in white matter microstructure and network organization that will persist well into adulthood (Dubois et al., 2014; Hagmann et al., 2010; Paus et al., 2001). The first two years of life are known to be a time of dramatic change in brain development that children experience due to increases in myelination, synaptic and axonal pruning that is reflected in rapid increases of FA and decreases in AD, RD, and MD (Dubois et al., 2014; Young et al., 2017). While the rate of white matter development is not as steep at four years of age as it is from birth to two years of age, the microstructure and network connections are far from reaching their full potential. Parallel processes of myelination will continue to increase as indicated by FA and RD as well as network reorganization towards a more integrated and efficient model of the mature brain (Hagmann et al., 2010; Huang et al., 2015). Children born very preterm demonstrate a delay in these maturational processes, which will have downstream implications in their development of more complex and higher-order cognitive abilities as they encounter more demanding environments and responsibilities.

3.6.1 Differences in white matter microstructure

Understanding the role of white matter in preterm brain development is integral in elucidating the basis for their cortical and cognitive differences. Both human and animal studies have

supported the hypothesis that overall altered neural connectivity, rather than the number of cortical neurons, is the source of reduced cortical growth and adverse outcomes in preterms (Dean et al., 2014; Kapellou et al., 2006). Our findings of reduced FA across the whole brain in 4 year-old children born very preterm compared to those born full-term adds to existing literature that has also found reduced FA within white matter of individuals born preterm at term-equivalent age and older children, adolescents, and young adults (Allin et al., 2011; Constable et al., 2008; Duerden et al., 2013). The extensive differences we found may be contributed by our inclusion of lower functioning children, who often could not tolerate the imaging awake and underwent the scans under natural sleep. This occurred for about a third of the total scans and enabled high-quality imaging in children who would otherwise not be scanned.

Our study also found increased RD in the children born very preterm within the corpus callosum and aspects of the right superior longitudinal fasciculus and inferior fronto-occipital fasciculus. These tracts are involved in inter-hemispheric communication and intellectual abilities (Tamnes et al., 2010). There was an absence of differences in AD and MD. Thus, as the children born very preterm have reduced FA and increased RD, alterations in white matter are likely due to myelin (Anjari et al., 2007; Ball, Srinivasan, et al., 2013; Song et al., 2005). In addition to reduced myelination, other potential reasons for the widespread reductions in FA could be explained by decreased axonal density and fibre coherence as well as increased axonal size (Jones, Knösche, & Turner, 2013). Our findings indicate that children born very preterm at 4 years continue to demonstrate altered white matter microstructure that have been first detected with imaging at term-equivalent age (Anjari et al., 2007) and more importantly do not appear to catch up to their term-born peers following the accelerated period of white matter growth between birth and two years of age.

The children born very preterm included in the present study have non-uniform neonatal clinical courses and incidences of brain injury, representative of the preterm population. Interestingly, we did not find that white matter injury or GMH/IVH directly affected DTI measures following multiple comparisons in our preterm cohort. Furthermore, we did not find a linear relation between DTI metrics and neurodevelopmental outcome measures in the children born very preterm at 4 years of age. This finding contrasts others who have found relations in children born very preterm between FA at term-equivalent age and early childhood cognitive outcomes (Counsell et al., 2008; Duerden et al., 2015b; Keunen et al., 2017; Salvan et al., 2017; Ullman et

al., 2015; van Kooij et al., 2012), as well as FA and cognitive measures in late childhood, adolescence and adulthood (Allin et al., 2011; Constable et al., 2008; Feldman et al., 2012; Feldman, Lee, Yeatman, & Yeom, 2013). This may be due to the timing of sampling, as 4 years of age is a dynamic stage of development and more heterogeneous in preterm children than typically developing children. Furthermore, the children born very preterm displayed more variability in both their DTI and outcome measures. Associations were found in the term-born group between areas of the forceps major and minor, left anterior thalamic radiation, bilateral inferior fronto-occipital fasciculus, and bilateral superior longitudinal fasciculus and VIQ. These tracts facilitate inter-hemispheric communication, connect the thalamus to the frontal lobe, and link the frontal and posterior lobe, which have been shown to be related to verbal intelligence abilities in typically developing individuals from late childhood to adulthood (Tamnes et al., 2010).

3.6.2 Network alterations in children born very preterm

Connectivity within the infant brain facilitates local information transfer such that structural networks are highly segregated into localized clusters with short path lengths between nodes (Cao et al., 2017). Over time, long-range connections begin to form to allow for greater integration of information between more distal structures while short-range connections are simultaneously fortified (Cao et al., 2017). This common developmental phenomenon has been characterized in normative studies (Hagmann et al., 2010) and should also present in children born very preterm as they follow similar trajectories of white matter microstructural maturation and functional connectivity (Cao, He, et al., 2016; Doria et al., 2010; Young et al., 2017). Our results indicate, however, that those who are born very preterm experienced weaker connections relative to term-born children as reflected in their reduced pattern of connections based on graph measures of strength, clustering coefficient, local efficiency and global efficiency. Hence, children born very preterm have network properties that are not only less integrated but also less segregated. It is possible that the very preterm children had weaker network segregation than term-born children following birth and are behind in their development of long-range connections. Thus, in our study, children born very preterm demonstrated less efficient networks and a potential maturational lag for the integration of networks, even if they eventually mature in a similar pattern to term-born children. Thompson and colleagues (2016) reported that children born very preterm had reduced density, global efficiency, yet higher local efficiency at 7 years of

age while we found that our preterm group demonstrated reduced local efficiency. This discrepancy may be due to differences in age or balance between increasing integration and decreasing segregation between the two groups (Hagmann et al., 2010).

The specific nodes that displayed reduced connectivity in the children born very preterm were relatively consistent between the graph measures. The left middle temporal region was affected between strength, local efficiency, and clustering coefficient. We would expect agreement between local efficiency and clustering coefficient, as they are related measures of local information transfer between neighbouring nodes (Achard & Bullmore, 2007). There were also more nodes with group differences in the left hemisphere indicating a weaker connectivity pattern in the left hemisphere, which is typically dominant. Interestingly, the bilateral differences in local efficiency and clustering coefficient were mostly specific to nodes that involved the language network, such as regions within the pars triangularis, middle temporal, superior temporal, and banks of the superior temporal sulcus. Moreover, the right supramarginal region was the most affected node with increasing prematurity. In combination, these findings could provide a structural premise for children born very preterm to develop compensatory atypical language lateralization involving the right-hemisphere, which has been identified in school-age and adolescent preterms (Gozzo et al., 2009; Schafer et al., 2009).

There are some limitations to consider with the present study. The impact of excluding motion corrupted volumes from the data may have impacted the tractography results. In addition, our sample size may have lacked the power to detect associations between connectivity measures and DTI metrics with cognitive outcomes. We were unable to acquire diffusion images for forty-one percent of the children born very preterm who were recruited at four years of age. This was due to a combination of reasons such as parental decline to participate in neuroimaging, the diffusion scans being highly sensitive to motion, as well as noisy and long scan durations. Thus, improved scan protocols with shorter scan times would be highly beneficial in this young population.

3.6.3 Conclusions

In conclusion, we have demonstrated that the pattern of white matter in children born very preterm at 4 years of age is less mature and less organized than term-born children, likely driven by myelination differences. Their white matter development does not appear to catch up

following the rapid maturation of white matter in the first years of life. Furthermore, their structural abnormalities reach beyond locally-reduced diffusion metrics and encompass network-level architectural differences. Our study provides evidence for both altered brain development and poorer cognitive profiles in children born very preterm at this very young age, such that they are already disadvantaged and show signs of delay behind their peers. White matter relations with cognitive outcomes may involve multiple DTI and connectivity measures together, warranting future multivariate analyses with appropriate sample sizes. Importantly, our findings support the need for these children to be followed closely in their first years of life and also provided services such as enrichment programs and early interventions given their poorer cognitive profiles and altered white matter.

Chapter 4
White matter microstructural differences identified using multi-shell diffusion imaging in six-year-old children born very preterm

Julia M. Young, Marlee M. Vandewouw, Sarah Mossad, Benjamin R. Morgan, Wayne Lee, Mary Lou Smith, John G. Sled, Margot J. Taylor. This chapter is a manuscript under revision for *NeuroImage: Clinical*.

4 White matter microstructural differences identified using multi-shell diffusion imaging in six-year-old children born very preterm

4.1 Abstract

The underlying microstructural properties of white matter differences in children born very preterm (<32 weeks gestational age) can be investigated in more depth using multi-shell diffusion imaging. The present study compared white matter across the whole brain using diffusion tensor imaging (DTI) and neurite orientation dispersion and density imaging (NODDI) metrics in children born very preterm and full-term children at six years of age. We also investigated associations between white matter microstructure with early brain injury and developmental outcomes. Multi-shell diffusion imaging, T1-weighted anatomical MR images and developmental assessments were acquired in 23 children born very preterm (16 males; mean scan age: 6.57 ± 0.34 years) and 24 full-term controls (10 males, mean scan age: 6.62 ± 0.37 years). DTI metrics were obtained and neurite orientation dispersion index (ODI) and neurite density (ND) were calculated using the NODDI diffusion model. FSL's tract-based spatial statistics was employed and each subject's DTI data were non-linearly co-registered. A mean fractional anisotropy (FA) skeleton was generated to represent a mask of major white matter tracts, which was then applied to each subject's FA, mean diffusivity (MD), axial diffusivity (AD), radial diffusivity (RD), ODI and ND data. FSL Randomise was used to test between-group differences as well as within-group associations with developmental outcomes and history of early brain injury such as white matter injury and germinal matrix/intraventricular haemorrhage (GMH/IVH). In the children born very preterm, widespread reductions of FA and increased ODI within the corpus callosum and corona radiata were identified. Within-group analyses of the children born very preterm revealed significant positive associations between increasing FA and ND with higher IQ. Lower ODI was found in the internal capsule and corona radiata in those with a history of white matter injury. Increased AD was identified in the corpus callosum, internal capsule and corona radiata for those who had GMH/IVH. Within the full-term group, associations were found between increasing ND and ODI and lower IQ as well as increasing FA and lower visuomotor scores. Measures of ODI and ND provide additional information into the impact of prematurity and early brain injury on white matter microstructure in children born very preterm as well as a thorough depiction of its role in cognitive abilities at six years of age.

4.2 Introduction

Very preterm birth (<32 weeks' gestational age) can disrupt sensitive developmental processes of white matter fibre organization and myelination that occur during the preterm period (Kinney et al., 1988). Other factors such as illness, brain injury and ex-utero environments children born very preterm experience can impact white matter maturation and its supportive role in cognition, as children born very preterm are at greater risk for later neurodevelopmental impairments in cognitive, behavioural, and social/emotional abilities (Dubois et al., 2008; Mangin et al., 2017; Woodward et al., 2009). Understanding the characteristics of white matter fibre organization and myelination in children born very preterm is necessary for elucidating developmental disturbances in these children.

Diffusion tensor imaging (DTI) and its indices of fractional anisotropy (FA), mean diffusivity (MD), axial diffusivity (AD), and radial diffusivity (RD) are commonly used to evaluate white matter structures. Although sensitive in detecting group differences, DTI metrics are nonspecific. Changes and reductions in FA across development can be driven by multiple contributing factors such as myelination, organization of axons, membrane permeability, axon density, partial volume effects, axon size and the number of axons (Jones et al., 2013). Diffusion imaging with multiple b-values provides an opportunity to measure more specific information regarding the microstructure of white matter that can overcome some of the ambiguities of DTI metrics. One such method is the biophysical model, neurite orientation dispersion and density imaging (NODDI) (Zhang et al., 2012), which quantifies structural properties of axons and dendrites (neurites) that FA is unable to infer. The NODDI model differentiates three tissue types: intra-cellular, extra-cellular, and CSF compartments (Zhang et al., 2012). Two primary measures of interest, orientation dispersion index (ODI), and neurite density (ND) are calculated with this method. ODI represents the angular variation of neurite orientations, quantifying the bending and fanning of axons, whereas ND represents the intra-cellular volume fraction, quantifying the number of axons and spaces between the axons (Zhang et al., 2012).

Only a few studies have used multi-shell diffusion imaging with DTI and NODDI metrics to identify early brain maturation and its variability across different tissues. One study identified age-related changes of ODI and ND in grey matter following very preterm birth until term-equivalent age (Eaton-Rosen et al., 2015). During this time, the cortex and thalamus

demonstrated decreases and increases in FA, respectively, yet with different contributions of ODI and ND. Increases in FA within the thalamus were due to increases in ND, reflecting active myelinating processes while decreases in FA within the cortex were due to increases in ODI reflecting microstructural complexity (Eaton-Rosen et al., 2015). During the first month of life in typically developing babies, ODI and ND were also shown to vary across white matter regions concordant with different microstructural properties, different developmental timing of white matter regions, and regional asymmetries (Dean et al., 2017). For instance, the corpus callosum and internal capsules exhibited the lowest axonal ODI, complementing its highly-organized axons, early developmental trajectory and high FA relative to other tracts (Dean et al., 2017; Young et al., 2016). In contrast, tracts that were more peripheral in the brain had higher ODI values, reflecting less mature white matter in those areas (Dean et al., 2017).

Developmental changes in diffusion tensor measures and NODDI measures are not uniform across brain regions. Cross-sectional studies from childhood to adolescence indicate that ND demonstrates stronger age-related changes compared to FA and diffusivity (MD, AD, RD) in both white matter and subcortical grey matter (Genc et al., 2017; Mah, Geeraert, & Lebel, 2017). These studies suggest that early brain development may be primarily driven by axonal packing and increasing myelination. Concurrently, FA was found to be more highly correlated to ODI, despite ODI having weak associations with age in childhood to early adolescence (Mah et al., 2017). Rapid increases in ND occur primarily in childhood, but then slow down throughout adulthood (Chang et al., 2015). This developmental trajectory differs from ODI, which increases more slowly in childhood and then more rapidly in adulthood (Chang et al., 2015).

A recent study by Kelly and colleagues (2016) identified white matter differences using DTI and NODDI metrics in a large retrospective sample of children born very preterm at 7 years of age. Reduced FA was identified in a small cluster within the right hemisphere overlapping the cingulum, inferior longitudinal fasciculus, inferior frontal-occipital fasciculus, uncinate fasciculus, anterior thalamic radiation, and external capsule. In contrast, extensive differences of axon orientation dispersion were identified in about one fifth of the total white matter examined, including areas where FA differences were found. Moreover, the authors identified relations between FA, ODI, and ND with neurodevelopmental outcomes such as IQ, motor abilities, academics, and behavioural measures in the children born very preterm. FA and neurite density

were positively correlated with IQ, demonstrating one of the first studies to relate NODDI measures to cognitive abilities in childhood.

In this prospective study, we assessed white matter development in children born very preterm when the children were 6 years of age. Previously at four years of age, reduced FA within many white matter tracts were found in an overlapping sample compared to full-term matched controls (Young et al., 2018). Relations between IQ were also found at this age in the full-term children but not the children born very preterm (Young et al., 2018). In the present study, our first objective was to identify whether these FA differences were sustained two years later using multi-shell imaging. Our second objective was to calculate NODDI measures of ODI and ND to delineate any additional microstructural white matter differences and their potential contributions to any FA differences found between very preterm and full-term children. In addition, relations between DTI and NODDI measures with developmental outcomes were examined in each group separately. In the children born very preterm, we also investigated relations between the DTI and NODDI measures with prematurity and early brain injury such as white matter injury and germinal matrix/intraventricular haemorrhage. We hypothesized that the measures of ODI and ND would provide greater insight into white matter differences in the children born very preterm and that they would also be sensitive in identifying relations with developmental outcomes such as IQ and visual-motor ability.

4.3 Methods

4.3.1 Participants

Seventy-three children were recruited for this study. Of those, thirty-nine children were born very preterm (<32 weeks GA) and recruited at as a part of an ongoing larger longitudinal study, conducted between 2009 and 2017 at the Hospital for Sick Children in Toronto, Canada. Exclusion criteria for the children born very preterm included those with any known chromosomal or major congenital abnormalities. Thirty-four full-term children (>37 weeks GA) were also recruited. Exclusion criteria for full-term children included prematurity, learning, language, neurological or developmental disabilities, non-English speakers, as well as MRI incompatibility based on a screening interview. An informed consent to the study was signed by parents and informed assent was provided by the children. The research ethics board at the Hospital for Sick Children approved the study protocol.

Table 8. Clinical and radiological characteristics at very preterm birth

Characteristic	Mean (SD) or number (%)
Gestational Age (weeks)	28.8 (1.4)
Males	16 (69.6%)
Birth Weight (g)	1161.6 (233.4)
Head circumference (cm)	25.5 (1.9)
Intrauterine growth restriction	3 (13.0%)
Cesarean-section delivery	17 (73.9%)
Multiple births	5 (21.7%)
Apgar score at 5 min	7.3 (1.7)
CRIB II	7.1 (2.3)
Endotracheal tube days	11.5 (15.5)
Oxygen administration days	15.2 (22)
Positive pressure ventilation	13.4 (10.8)
Patent ductus arteriosus (treated)	6 (26.1%)
Sepsis (cultures positive)	9 (39.1%)
Premature Rupture of Membranes	2 (8.7%)
Necrotizing entercolitis (stage 2 & 3)	3 (13.0%)
Bronchopulmonary dysplasia	4 (17.4%)
GMH/IVH (Grade 1-2)	4 (17.4%)
GMH/IVH (Grade 3-4)	5 (21.7%)
White Matter lesions	8 (34.8%)

CRIB II - Clinical Risk index for Babies; GMH - Germinal Matrix Hemorrhage

4.3.2 Perinatal clinical and radiological measures

Perinatal clinical information was obtained for the children born very preterm during their stay in the neonatal intensive care unit. Information such as demographics, significant events during pregnancy, and medical interventions are summarized in Table 8. Paediatric neuroradiologists and neurologists assessed each of the structural T1- and T2- weighted images for the children born very preterm shortly following birth. The presence of white matter injury and germinal matrix/intraventricular haemorrhage (GMH/IVH) was identified. The grade of GMH/IVH was determined according to the classification by Papile and Volpe for cranial ultrasonography findings adapted to MRI (Papile et al., 1978; Volpe, 2008). At six years of age, paediatric

neuroradiologists also assessed each of the children's structural T1- , T2- weighted and FLAIR images. Any incidental findings were noted.

4.3.3 Developmental Assessments and Maternal Education

Developmental assessments were performed for the children born very preterm who returned for follow-up as well as the recruited controls. For each assessment, raw scores were converted into standardized scores with a population mean of 100 (50^{th} percentile of typical development) and a standard deviation of 15. Intelligence quotients (IQ) were determined by the 2-subtest Wechsler Abbreviated Scale of Intelligence (WASI; Wechsler, 1999) using Canadian norms, which included the vocabulary and matrix reasoning subtests to estimate general intellectual ability. Visual-motor integration (VMI) and supplemental tests of visual perception (VP) and motor coordination (MC) were assessed by the Beery-Buktenica Test of Visual Motor Integration (Beery, Buktenica, & Beery, 2010).

Levels of maternal education were obtained for all the children. Percentages of mothers with high school or college education, university education, and post-graduate education are reported.

4.3.4 MRI Data Acquisition

MRI scans were acquired with a 3T Siemens Trio scanner and 12 channel head coil, and 180 direction diffusion images (SE-EPI, b-values = 700/1000/2850 s/mm^2; repetition time: 10.7/8.8/10.7s; echo time: 0.115/0.087/0.115s; field of view: 244 x244x140mm; resolution: 2mm isotropic; scan time: 40.9 min) were obtained with 26 interleaved b = 0 s/mm^2 volumes. Anatomical T1-weighted (MPRAGE) images (repetition/echo time: 2.3/.00296s; field of view: 192 x 240 x 256mm; resolution: 1mm isotropic; scan time: 5 min) were obtained. All of the scans were collected when the children were awake and watching a movie. Images were inspected for gross motion artefacts and anatomical abnormalities. We obtained 32 T1-weighted images and diffusion data in children born very preterm, and 24 of the children had complete multi-shell scans. One child born very preterm had ventriculomegaly and was excluded from analyses. A total of 30 T1-weighted and diffusion data were obtained in the full-term children, and 24 of the children had complete multi-shell diffusion scans.

4.3.5 Diffusion Processing

FSL tools (Jenkinson et al., 2012) and custom scripts were used to correct for eddy current distortions and head motion. The mean for each b-value (0, 700, 1000, 2850 s/mm^2) was calculated, and transformations between the mean b = 0 image and each mean b-value were obtained using FSL's FLIRT (Jenkinson, Bannister, Brady, & Smith, 2002). Each individual volume was first registered to its corresponding mean image, and then to the mean b = 0 image by applying the previous transformation, while adjusting corresponding b-vectors. Following visual inspection, all volumes for each child were included due the large number of volumes acquired. DTI metrics (FA, MD, AD, RD) were calculated and extracted from the output of the RESTORE algorithm (Chang, Jones, & Pierpaoli, 2005). NODDI measures of orientation dispersion index (ODI) and neurite density (ND) were calculated using all three b-values with the NODDI Matlab toolbox version 1.0 (Zhang et al., 2012).

4.3.6 Tract Based Spatial Statistics (TBSS)

Analyses of the DTI (FA, AD, RD, MD) and NODDI metrics (ODI, ND) were conducted using FSL's TBSS method (Smith et al., 2006). Nonlinear co-registration of all the children's fractional anisotropy (FA) images were performed to each other. One image that was the most representative of the group was used as the target image and then registered to MNI151 standard space. Therefore, each FA image underwent a combined nonlinear registration and linear registration to the target image. A mean of all the FA images and a skeleton representing the centre of major white matter tracts within the brain was generated and thresholded at 0.2. All of the same registrations were applied to each child's MD, AD, RD, ODI, and ND data. Lastly, the skeleton was projected to the data.

4.4 Statistical Analysis

4.4.1 Participant Characteristics

Between the children born very preterm and full-term children, sample differences of male and female sex ratios as well as age at scan were tested using a chi-square and two-tailed t-test, respectively. Group differences in developmental test scores were also tested using two-tailed t-tests. To compare the three maternal education levels (high school or college education, university education, and post-graduate education) between groups, a non-parametric Mann-

Whitney U Test was employed. Moreover, the relation between the three levels of maternal education and developmental test scores were examined using a one-way ANOVA tests for each group separately. Significance values were held at $p<0.05$.

4.4.2 TBSS Analyses

Between and within-group voxel-wise analyses were performed with FSL Randomise (Anderson & Robinson, 2001) using 5,000 permutations and threshold-free cluster enhancement (Smith & Nichols, 2009). Significance was defined to be $p < 0.05$ following corrections for multiple comparisons. Between group analyses were conducted using a general linear model with group, age at scan and sex as explanatory variables. This was performed for all DTI metrics (FA, MD, AD and RD) as well as the NODDI metrics (ODI and ND). Within the preterm group, additional voxel-wise regression analyses were performed between all of the DTI and NODDI metrics with GA, presence of white matter injury, presence of GMH/IVH, and developmental measures (IQ and VMI). Within the full-term group, voxel-wise regression analyses were performed between all of the DTI and NODDI metrics and developmental measures (IQ and VMI).

To visualize significant results based on the voxel-wise regression analyses, the JHU DTI-based labelled atlas (Mori et al., 2005) was applied to the FA skeleton to plot DTI and NODDI values within defined white matter tracts where significant voxels were found based on the TBSS analyses.

4.5 Results

4.5.1 Participant Characteristics

Twenty-three children born very preterm (16 males, 7 females; mean scan age: 6.57 ± 0.34 years; mean gestational age: 28.8 ±1.4 weeks) were included with useable multi-shell diffusion data and developmental assessments. Perinatal clinical and radiological characteristics for the children born very preterm are provided inTable 8. Eight (34.8%) children born very preterm had incidences of white matter lesions and nine (39.1%) had incidences of GMH/IVH of any severity on structural scans following birth. Twenty-four full-term children (10 males, 14 females; mean age: 6.62 ± 0.37 years) completed useable multi-shell diffusion data and developmental assessments. No sex differences were found between the group samples ($X^2(1) = 3.69, p=0.054$). There was also no difference in age at scan between groups ($p=0.697$).

The education levels of the mothers of the children born very preterm were 26.1% high school or college, 60.7% university, and 13% post-graduate. The education levels of the mothers of the full-term children were 21.7% high school or college, 56.5% university, and 21.7% post graduate. There were no differences in education levels between groups ($p=0.645$).

Performance on the neurodevelopmental tests was consistently lower for the children born very preterm than for the full-term children. Compared to the general population, the mean of each measure (IQ, VMI, VP and MC) by group was in the average range apart from MC in the very preterm group, which was in the low average range. The very preterm and full-term group had scores of IQ that were 103.04 (11.75) and 112.36 (13.43), respectively ($p=0.015$). In addition, the very preterm group and full-term group had scores of VMI (96 (8.5) and 102.13 (9.31), respectively) and MC (87.17 (13.58) and 95.08 (10.70), respectively) that were significantly higher in the full-term group ($p=0.023$ and $p=0.036$). Group differences of VP scores were not significant ($p=0.062$) between the very preterm (99.23 (16.77)) and full-term groups (107.17 (13.5)).

In the full-term group, developmental measures were not associated with maternal education levels (all $p>0.05$). In the very preterm group, IQ, VMI, and VP were not associated with maternal education levels (all $p>0.05$); measures of MC were significantly different between maternal education levels in the children born very preterm ($p=0.017$). The children born very preterm with mothers who had post-graduate training had significantly higher MC abilities than both those who had university training ($p=0.017$) and high-school or college level training ($p=0.0277$).

4.5.2 TBSS Between-Group Analyses

Group differences were present between the children born very preterm and full-term children in FA and ODI metrics at $p<0.05$ following multiple comparisons. Full-term children displayed significantly higher FA values than the children born very preterm within the majority of white matter subregions across the white matter skeleton as shown in Figure 11A. The subregions corresponding to the JHU white matter atlas where group differences were found are listed in Table 9 with the number of significant voxels per region. The children born very preterm had significantly higher ODI than the full-term children (Figure 11B) in regions including the corpus callosum (genu, body, and splenium) as well as the posterior thalamic radiation (left

hemisphere), anterior corona radiata (left hemisphere) and bilateral superior corona radiata extending into bilateral areas of the cortical spinal tract. There were no between-group differences found in the other DTI and NODDI metrics (MD, AD, RD, and ND).

Figure 11. FA and ODI TBSS Results at six years of age.

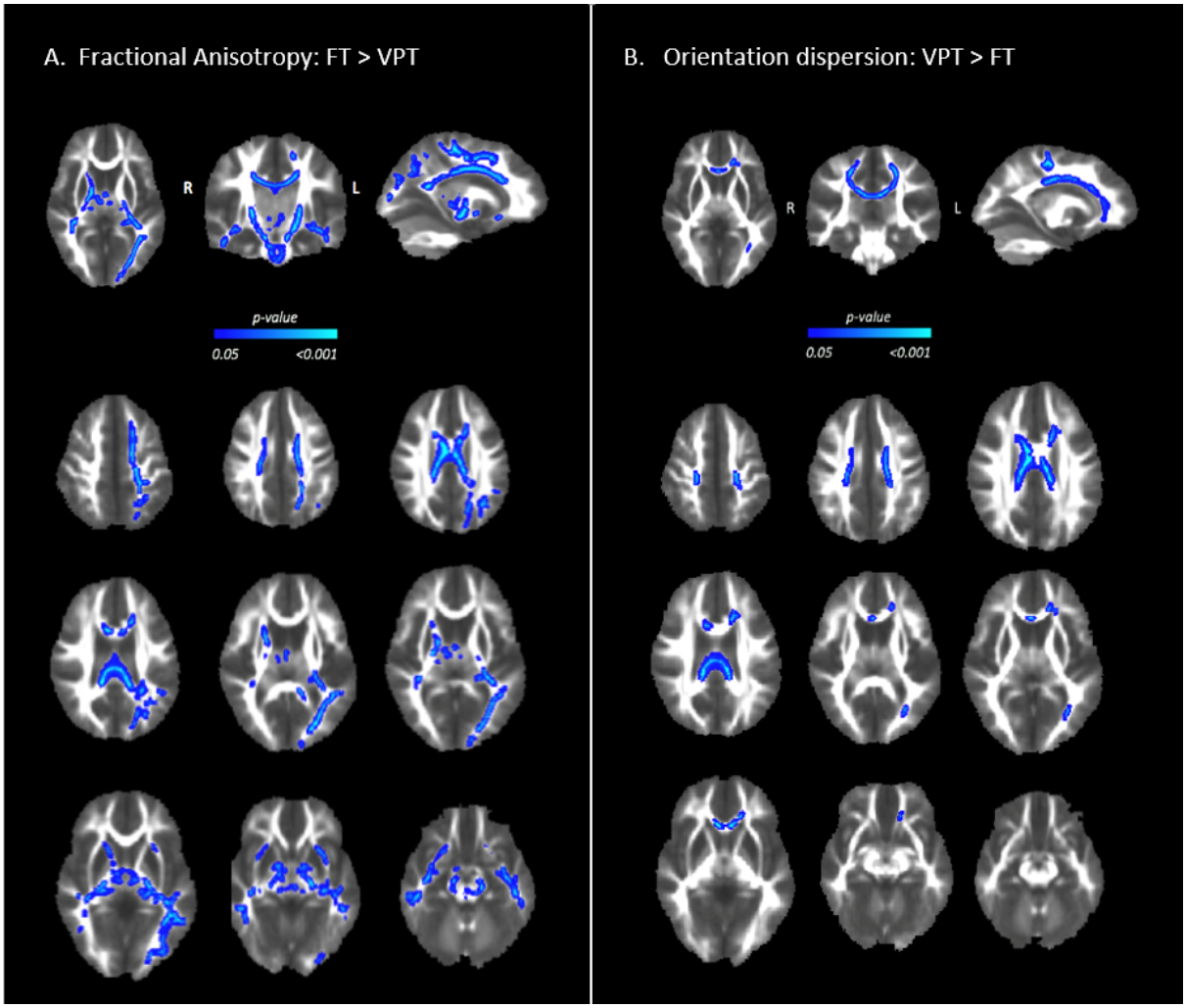

A. TBSS analyses of group differences revealed reduced FA in the children born very preterm compared to the full-term children along the white matter skeleton ($p < 0.05$). Significant voxels are depicted in blue. Colour bars indicate p-values. **B.** Voxels with significantly increased neurite orientation dispersion in the children born very preterm are indicated in blue along the white matter skeleton.

Table 9. Number of significant voxels for between group differences.

White matter Region	L/R	FA: FT>VPT	ODI: VPT>FT
Genu of corpus callosum	-	46	393
Body of corpus callosum	-	1673	1367
Splenium of corpus callosum	-	577	190
Fornix (column and body)	-	121	-
Corticospinal tract	L	66	-
	R	48	-
Cerebral peduncle	L	311	-
	R	258	-
Anterior limb of internal capsule	L	6	-
	R	335	-
Posterior limb of internal capsule	L	166	-
	R	210	-
Retrolenticular part of internal capsule	L	424	-
	R	224	-
Anterior corona radiata	L	99	354
	R	25	-
Superior corona radiata	L	191	137
	R	99	86
Posterior corona radiata	L	289	40
	R	41	25
Posterior thalamic radiation	L	482	91
	R	53	-
Sagittal stratum	L	176	-
	R	-	-
External capsule	L	433	-
	R	69	-
Cingulum (cingulate gyrus)	L	4	-
	R	-	-
Cingulum (hippocampus)	L	-	-
	R	-	-
Superior longitudinal fasciculus	L	75	-
	R	-	-
Superior fronto-occipital fasciculus	L	-	-
	R	-	-
Uncinate fasciculus	L	62	-
	R	58	-

4.5.3 Within-Group Analyses

In the preterm group, many areas of white matter were associated between DTI and NODDI metrics with IQ. Associations were present between increasing FA and ND with higher scores of IQ (see Figure 12A-12B) and associations were found between increasing MD and RD with lower scores of IQ ($p<0.05$) (Figure C1). Associations between RD and IQ were the most significant and demonstrated widespread differences at the $p<0.001$ level.

Figure 12. Within-group TBSS results.

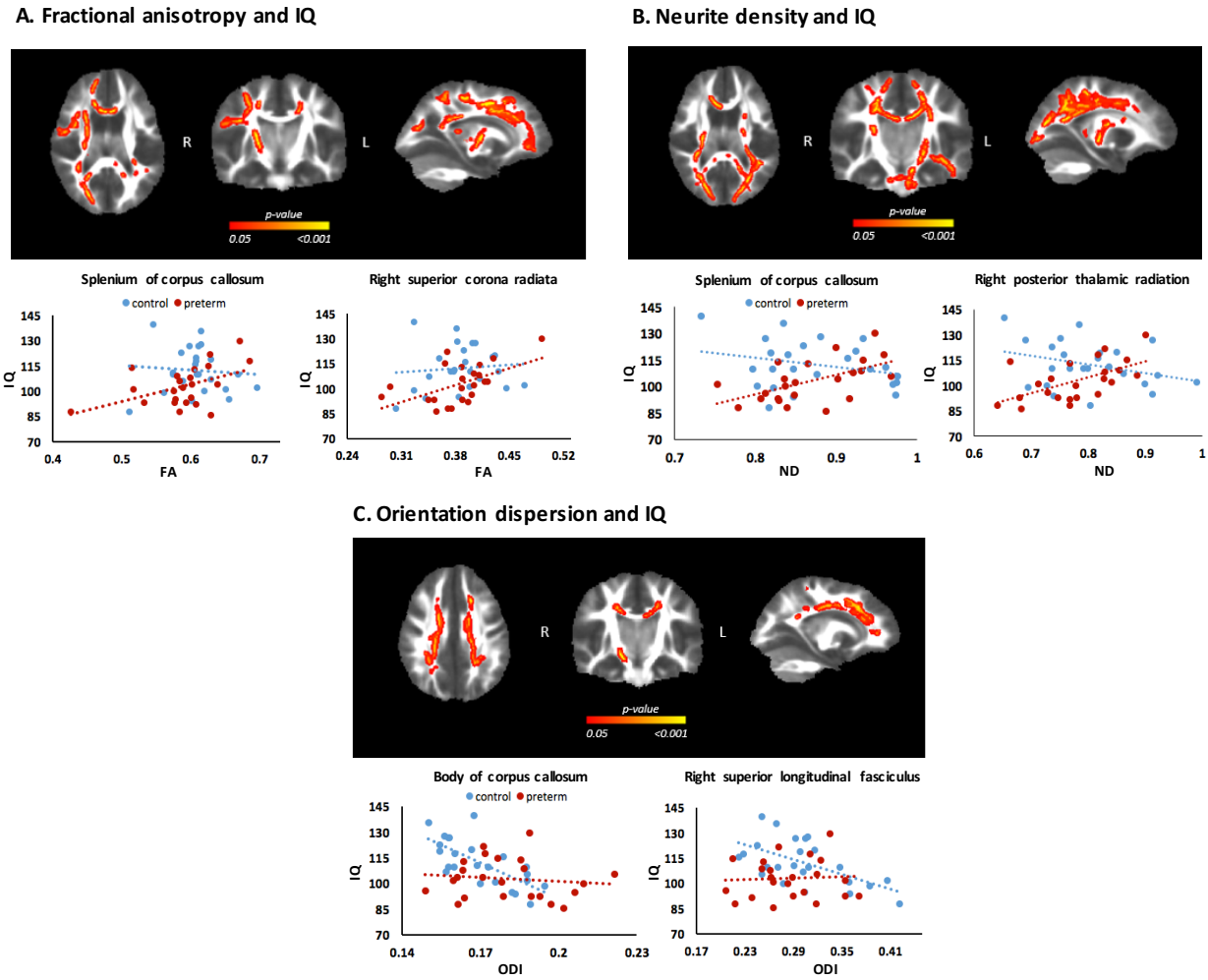

A. Within the group of children born very preterm, TBSS analyses demonstrated significant associations between increasing FA and higher IQ as indicated in red and yellow ($p < 0.05$). Colour bars indicate p-values. The scatter plots below indicate regions where there were significant TBSS findings. Full-term children are shown in blue and children born very preterm are shown in red. **B.** Significant associations were found between increasing neurite density and higher IQ in the children born very preterm ($p < 0.05$). **C.** Significant associations were found between decreasing ODI and lower IQ in the full-term children ($p < 0.05$). The scatter plots below depict the direction of the relationship

Table C1 describes the subregions of white matter that included significant voxels in the very preterm group. No associations were found between the DTI and NODDI metrics with gestational age. With respect to early brain injury, those who had GMH/IVH at birth demonstrated increased AD within areas of the corpus callosum (splenium, body, and genu), bilateral anterior limb and posterior limb of the internal capsule, anterior and superior corona radiata, external capsule, and the left posterior corona radiata ($p<0.05$) (see Figure 13B). Children who had GMH/IVH also demonstrated increased ODI in a few voxels within the body and genu corpus callosum ($p<0.05$). In addition, children born very preterm who had white matter injury, displayed lower ODI in regions such as the right anterior and posterior limb of the internal capsule, and the anterior and superior corona radiata ($p<0.05$) (see Figure 13A).

Figure 13. TBSS results with early brain injury

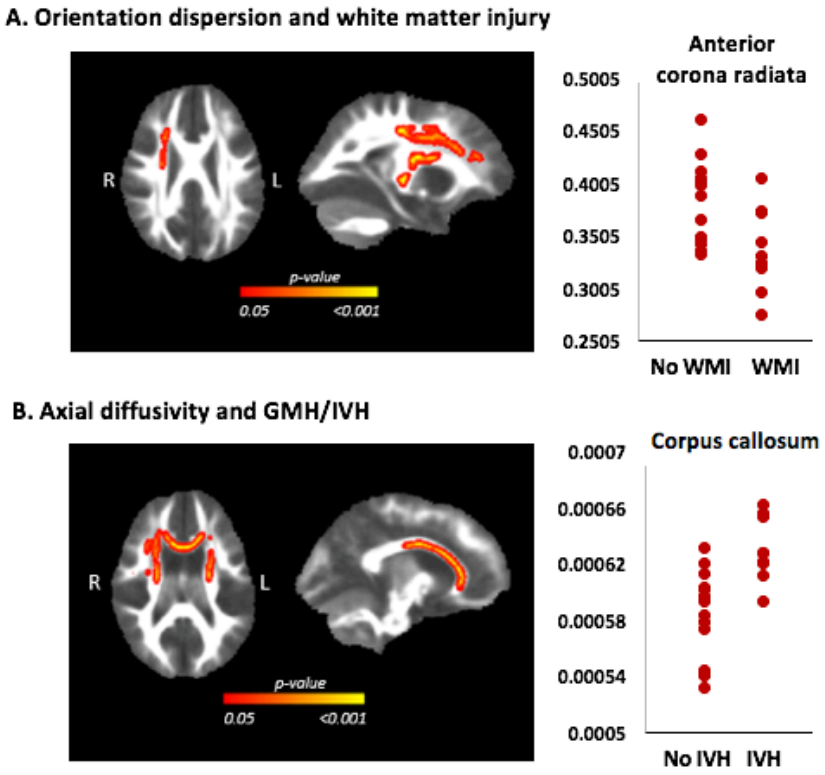

A. TBSS analyses revealed lower neurite orientation dispersion with early white matter injury in the children born very preterm ($p < 0.05$). **B.** Increased axial diffusivity was found in the children born very preterm who experienced GMH/IVH ($p < 0.05$).

In the full-term children, many areas of white matter also showed associations between DTI and NODDI metrics with IQ and VMI. Negative associations were present between increasing ND and ODI and lower scores of IQ ($p<0.05$), shown in Figure C2. Positive associations were found between increasing AD and higher scores of IQ ($p<0.05$) (Figure C2). Table C2 lists the subregions of white matter that included significant voxels in the full-term group. Negative associations were also found between increasing FA and lower scores of VMI while positive associations were found between increasing AD and RD with higher scores of VMI ($p<0.05$). Increasing ND was also found with increasing age in the full-term children ($p<0.05$).

4.6 Discussion

In children born very preterm, fundamental development of white matter differs from full-term children on a microstructural level. Examining these differences using NODDI opens a new perspective into the microstructural components that comprise white matter by quantifying two additional metrics from the traditional diffusion tensor model: neurite orientation dispersion and density. Compared to term-born children at six years of age, we identified widespread reductions of FA and focal increases in neurite orientation dispersion in children born very preterm. Neurite orientation dispersion and density were also associated with cognitive abilities as well as brain injury experienced in the perinatal period in the children born very preterm. These alterations in microstructural properties of white matter that are present in childhood may help explain the origins of developmental differences as well as adverse functional outcomes.

Developmental studies using multi-shell diffusion imaging in young children are sparse and challenging due to long acquisition times. The few existing studies that have applied NODDI to developmental populations have shown utility in understanding early brain development (Tamnes, Roalf, Goddings, & Lebel, 2017). Neurite density has been shown to have a stronger relationship with age than diffusion metrics (FA, MD, ND, RD), thereby an important contributor to increases of FA during childhood within white matter; however, neurite orientation dispersion is more strongly correlated with FA irrespective of age (Chang et al., 2015; Genc et al., 2017; Tamnes et al., 2017; Zhang et al., 2012). Our study is one of the first *prospective* studies in children born very preterm applying NODDI to multi-shell diffusion data. We found widespread reductions of FA in the children born very preterm compared to full-term children at the beginning of school-age, which were consistent with previous findings in an

overlapping cohort of children at 4 years of age as well as an independent cohort of seven to nine-year-old very preterm children (Duerden, Card, Lax, Donner, & Taylor, 2013; Young et al., 2018). The reductions in FA suggest that there may be a sustained maturational lag of white matter development as well as possible differences in the structural architecture of white matter in the children born very preterm.

Increased neurite orientation dispersion was identified within several white matter regions in the children born very preterm. The regions identified were the corpus callosum (genu, body and splenium), corona radiata (anterior, superior, and posterior aspects), and the left posterior thalamic radiation. Most of the significant voxels were identified in the body of the corpus callosum and the left-sided corona radiata and thalamic radiation. The corpus callosum is understood to be a coherent fibre pathway, containing fibres that have consistent directionality along its macroscopic curvature (Budde & Annese, 2013). However, it also exhibits microscopic regional variations in orientation in its medial and lateral aspects (Budde & Annese, 2013). Low orientation dispersion in the corpus callosum has been found during the neonatal period in typically developing neonates, reflecting the very early organization of this fibre pathway (Dean et al., 2017). It is thought that the increased orientation dispersion, indicating greater bending and fanning of axons, in children born very preterm later in childhood may be a product of early disruptions to the organization of its characteristic densely packed parallel fibres prior to or during the neonatal period (Nossin-Manor et al., 2013; Young et al., 2016).

The corona radiata and posterior thalamic radiation are projection fibres that extend towards the cortex from the internal capsule in subcortical regions. These fibres contain thalamic and motor projections involved in sensory and motor function (Catani, Howard, Pajevic, & Jones, 2002). In late childhood and early adolescence, motor fibres within the internal capsule and cortical spinal tract have lower values of orientation dispersion compared to other fibre regions, also reflecting early organization in concordance to that seen in the corpus callosum (Mah et al., 2017). Greater dispersion within the corona radiata and posterior thalamic radiation in the children born very preterm highlights additional vulnerabilities of highly organized white matter structures. It is possible that differences in orientation dispersion are more pronounced in these structures as they are likely to be more coherent and less variable in their composition between individuals. Differences found in these areas support primary disruptions to thalamocortical fibres in early maturation, which are particularly vulnerable during the preterm period when axonal ingrowth

via programmed migration paths outspread to designated regions of the cortical plate (Kostović & Judas, 2002). These deviances can impact secondary organization and further influence susceptibility to adversity with age (Dean et al., 2017; Rae et al., 2017).

The effect of early brain injury was also explored within the group of children born very preterm. Decreased orientation dispersion was found in relation to those who had white matter injury detected on MRI within two weeks of birth. Areas of decreased orientation dispersion were present in the right hemisphere within the anterior and posterior limb of the internal capsule as well as the anterior and superior corona radiata. A histological study of demyelinating white matter lesions from multiple sclerosis spinal cord pathology quantified NODDI metrics and found reduced variability in axonal orientations within the lesions, indicating reduced neurite complexity (Grussu et al., 2017). As reduced orientation dispersion was indicative of pathology in the context of focal demyelination, early white matter injury in the children born very preterm may have a similar effect on the neural architecture of axons with respect to reducing the angular variation of the internal capsule and corona radiata pathways involved in sensorimotor processing. Perinatal GMH/IVH resulted in increased axial diffusivity in the corpus callosum as well as the anterior and posterior limbs of the internal capsule and regions of the corona radiata. GMH/IVH is known to impact the proliferation of oligodendroglial precursor cells that originate in the germinal matrix and later differentiate and migrate into cerebral white matter (Volpe, 2015). From a developmental perspective, these findings may reflect secondary disruptions to neurodevelopment and represent less mature regions of white matter due to GMH/IVH.

In the children born very preterm, intelligence was associated with neurite density rather than neurite orientation dispersion. Moreover, positive associations were present between intelligence, FA, and neurite density as well as negative associations between MD, RD and IQ. Neurite density represents the density of myelinated axons as well as the caliber of myelinated axons (Carper, Treiber, White, Kohli, & Müller, 2017). Thus, reduced neurite density can be consistent with abnormal myelin as well as neuronal loss, with overlapping microstructural contributions to RD (Timmers et al., 2016). Lower intelligence scores in the children born very preterm may be closely related to myelination. In contrast, the full-term children exhibited differing relations with outcomes than the children born very preterm, demonstrating decreasing NODDI metrics and FA with higher scores of intelligence and visual-motor abilities. For instance, lower ODI was associated with higher IQ in regions such as the corpus callosum, corona radiata, and

superior longitudinal fasciculus. The different associations with outcomes between the two groups may be due to different developmental processes contributing to outcomes as well as a sensitive range of microstructural components contributing to cognitive abilities.

A recent study by Kelly and colleagues (2016) also investigated DTI and NODDI metrics using tract-based spatial statistics in a sample of seven-year-old children born very preterm. Parallel findings between our prospective study and their retrospective study are promising for enhancing our understanding of white matter microstructural differences between children born very preterm and full-term children at the beginning of school-age. Results of their study indicated small areas of reduced FA and large areas (about 25 percent) of increased orientation dispersion within white matter in the very preterm born group (Kelly et al., 2016). While our results indicated more FA group differences compared to orientation dispersion, neither study found group-level differences in neurite density, suggesting that the angular variation of axons is an integral contributor to FA differences in this population. Similar to our study, they found that FA and neurite density positively correlated with IQ in the very preterm group while they did not find significant correlations in the full-term group. These structural insights help lay the foundation for understanding functional differences and should be complemented with functional imaging studies.

There are a few limitations to consider. The relatively small sample size was, in part, due to the 40-minute acquisition time of the diffusion protocol with the available 3T scanner. Lower functioning children were unable to complete the scan protocol and were thus under-represented in the current sample. New protocols with faster acquisition times will be integral to expanding the literature using NODDI methods. Another limitation was the loss to follow-up of the longitudinal cohort that has been followed since birth, due to loss of contact and attrition in participation. The original cohort was recruited during their stay in the neonatal intensive care unit six years prior to the current study.

In conclusion, multi-shell diffusion imaging can assist in disentangling the microstructural properties in the white matter of children born very preterm. NODDI metrics of neurite orientation dispersion and neurite density have shown independent associations at the group level as well as with early brain injury and outcomes. Understanding the differences of white matter maturation at the microscale level will increase our ability to identify biophysical elements of

developmental processes that may be therapeutically targeted during the neonatal period in the future.

Chapter 5
General Discussion

5 General Discussion

5.1 Overview of Studies

Based on a longitudinal cohort of children born very preterm, the present thesis provides novel insights of white matter development and its relation to early brain injury and cognitive outcomes. Few studies have investigated whole brain, longitudinal white matter development in a very preterm-born population in conjunction with long-term outcomes during early childhood. This series of studies includes data that begins at preterm birth and extends to 6 years of age, following the children born very preterm from the time of their birth, to term-equivalent age, two years, four years, and six years of age. Moreover, each study incorporates a wealth of multimodal data, including diffusion weighted imaging, perinatal medical history, and measures of developmental outcomes. Elucidating maturational patterns of white matter as well as microstructural and connectivity differences in comparison to term-born children during childhood is important for understanding the consequences of very preterm birth on brain maturation. Furthermore, investigating associations between measures of white matter with early brain injury and cognitive abilities extends our understanding of the close relation between white matter vulnerabilities with functional outcomes.

5.2 Summary of Results

The first study (Chapter 2), "Longitudinal study of white matter development and outcomes in children born very preterm", evaluated maturational changes, or growth, of white matter tracts within cortical and subcortical regions using DTI metrics. Similar to trajectories reported in term-born infants, the most dramatic change in white matter development occurred between birth and two years of age for each tract, indicating an important period of brain development that has been documented in typically developing children (Qiu et al., 2015). Differential maturational patterns between tracts based on changes in DTI metrics also displayed variations in growth between individual tracts over time. During the preterm period (birth to term-equivalent age), faster rates of change in FA were found in the posterior tracts compared to anterior tracts and the corpus callosum. In addition, projection tracts were found to develop faster than association tracts. These changes in white matter microstructure can be attributed to increased myelination, axonal packing and axonal coherence (Lebel & Deoni, 2018).

Evaluating growth of white matter across the preterm period elucidated associations with later developmental outcomes at four years of age. Slower maturational changes in MD and RD within the left-lateralized internal and external capsule during the preterm period was associated with lower intelligence and language scores, likely due to slower or poorer myelination during that time. The left lateralization of our finding suggests that the white matter tracts of the left hemisphere such as the internal and external capsules are maturing more slowly than the right hemisphere, which may indicate an early disruption to typical development. In contrast to previous findings of associations between perinatal deep grey matter growth and visual-motor outcomes (Young et al., 2015), left-lateralized white matter microstructure of the internal and external capsules was associated more with cognitive and language functions as the combination of these projection tracts are one of the first white matter regions to mature and are involved in cognitive and language functions. Visual-motor function was more closely related to growth of the globus pallidus and caudate, attributable to the role of the globus pallidus in motor function. Additional follow-up studies would be beneficial to consider all of these structures together to further determine the associations between structural growth with long-term outcomes in children born very preterm.

These findings provide a potential biomarker of outcomes for children born very preterm shortly following birth, offering important evidence for imaging babies during the preterm period. Furthermore, associations were found between early brain injury and white matter growth. Neonates with white matter lesions detected at birth demonstrated slower changes in FA within the posterior limb of the internal capsule and retrolenticular portion of the internal capsule. Imaging neonates born very preterm shortly following birth can reveal information on the extent of brain injury such as white matter lesions and can provide an important opportunity to influence the clinical care of these babies by understanding more precise changes in brain growth after birth (Guo et al., 2017).

This study is one of the first in the literature to provide detailed investigation of whole brain white matter maturation across the first four years of life in children born very preterm. Longitudinal studies of normative white matter microstructural development within the perinatal period (Dean et al., 2017; Dubois et al., 2008) and during later childhood through adolescence beginning at four years of age are limited (Genc et al., 2017; Krogsrud et al., 2016; Mah et al., 2017). In addition, there are few serial studies investigating white matter maturation during the

perinatal period in preterm neonates (Akazawa et al., 2016; Kersbergen et al., 2014; Partridge et al., 2004). Our study investigated the rate of change of DTI metrics within tracts between preterm and term-equivalent age and identified dynamic changes during the preterm period that varied in association with later outcomes, extending from a previous study of deep grey matter growth within the preterm period in the same cohort (Young et al., 2015). Thus, differences in structural brain growth during this time may also be indicative of further alterations in brain maturation later in childhood.

The second study (Chapter 3), "Altered white matter development in children born very preterm", compared white matter microstructure, connectivity, and cognitive abilities between children born very preterm and term-born children at 4 years of age. As a group, the children born very preterm demonstrated significantly lower cognitive abilities compared to the term-born children in intelligence, core language, visual motor integration, visual perception and motor coordination abilities. The children born very preterm displayed widespread reduced FA and increased RD. Positive associations with increasing FA and verbal IQ, performance IQ, and full-scale IQ were present in the term-born children yet absent in the children born very preterm. In the term-born children, positive associations between FA with verbal and performance IQ were found in regions of the corpus callosum, bilateral inferior fronto-occipital fasciculus and superior longitudinal fasciculus, as well as the left anterior thalamic radiation. Normative samples have also shown associations of verbal intelligence with these regions, particularly the inferior fronto-occipital fasciculus and superior longitudinal fasciculus (Tamnes et al., 2010). More specifically, intelligence scores involving both verbal and non-verbal abilities have been found to be supported by connections between multiple brain regions, particularly with association tracts connecting frontal and occipital cortices (Tamnes et al., 2010). The lack of associations found in the children born very preterm could be because these children have prolonged white matter development supporting cognition in comparison to the full-term children, especially as lower functioning children born very preterm were included in the sample. This hypothesis would require additional longitudinal studies to investigate the developmental trajectory of this relationship.

In addition, the children born very preterm displayed reduced white matter connectivity compared to term-born children reflected by graph theoretical measures of local strength, clustering coefficient, local and global efficiency within nodes such as the frontal, temporal,

cingulate, precuneus and lateral occipital regions. While no associations were found between the graph measures and outcomes in either group, reduced global efficiency was found in the children born very preterm who had a history of white matter lesions and GMH/IVH at birth.

Imaging children at 4 years of age is a practical challenge, and there is no other study to date that has a comparable sample of both children born very preterm and term-born children at this age. Typically, DTI studies of children born very preterm have imaging data at term-equivalent age with outcomes during early childhood (18 months to 5 years of age) or both imaging and psychological data beginning at 6 and 7 years of age (Duerden et al., 2013; Duerden et al., 2015; Kelly et al., 2016; Keunen et al., 2017; Rogers et al., 2013; Travis et al., 2015). Furthermore, studies investigating white matter connectivity have begun at 6 years of age (Kim et al., 2014; Thompson et al., 2016). The present demonstration of widespread reductions in FA and connectivity at 4 years of age in children born very preterm born fills a gap in the developmental literature. Moreover, it provides evidence that their white matter may be less mature, with altered microstructure that do not associate with outcomes in the same manner as is expected in typical development, suggesting more diffuse or distributed involvement of white matter regions with outcomes.

The third study (Chapter 4), "White matter microstructural differences identified using multi-shell diffusion imaging in six-year-old children born very preterm," delved more deeply into the investigation of white matter microstructure differences between term-born children and children born very preterm. This cross-sectional study was performed using 180-direction diffusion imaging, DTI metrics as well as NODDI metrics of axonal orientation dispersion (ODI) and neurite density (ND). In the children born very preterm, widespread reductions of FA across the cortex and increased ODI within the corpus callosum and corona radiata were identified.

The children born very preterm revealed significant positive associations between increasing FA and ND with higher scores of IQ while the term-born children displayed a differing pattern of increasing ND, ODI, and FA with lower IQ and visuomotor scores. These findings suggest that the full-term children may have reached an interim plateau with respect to the relationship between their white matter development and cognitive abilities. The children born very preterm demonstrated a contrasting relation as no associations between outcomes with white matter microstructure were found at 4 years of age while positive associations with outcome were found

at 6 years of age. This could reflect a developmental lag in the children born very preterm. Furthermore, axonal density may also be a more important contribution for cognitive functioning in the children born very preterm whereas neurite orientation dispersion may have more influence on cognitive functioning in the full-term children. Full-term children may have increased sensitivity to microstructural deviances that involve highly organized white matter structures like the corpus callosum and cortical spinal tract.

With respect to early brain injury, lower ODI was found in the internal capsule and corona radiata in the children born very preterm with a history of white matter lesions. Increased AD was also found in the corpus callosum, internal capsule, and corona radiata for those with a history of GMH/IVH. Only one other study has a comparable sample of children born very preterm with respect to age (7 years) as well as NODDI and TBSS methodology (Kelly et al., 2016). The findings within Chapter 4 confirms broadly similar differences in FA and ODI (Kelly et al., 2016). Nevertheless, using NODDI to further inform differences in DTI adds important contributions to the minimally existing development literature incorporating multi-shell diffusion imaging with NODDI metrics.

In combination, the three studies comprehensively characterize changes in white matter over the course of six years. The group of studies comprising the present dissertation also extend the literature by imaging neonates and children born very preterm at younger ages than most. The longitudinal findings indicate that white matter develops in a similar manner to typically developing children (Qiu et al., 2015). However, subtle differences in the rates of white matter change during the perinatal period, particularly within the internal and external capsules, can predict outcomes and likely later developmental growth rates in children born very preterm. Reduced FA identified at term-equivalent age in these regions as well as the corpus callosum reflect differences in maturational patterns occurring prior to term-age (Anjari et al., 2007; Rose et al., 2008). It is evident that children born very preterm continue to display differential white matter maturational patterns as measures of microstructure and connectivity widely diverge from term-born children at 4 years of age. Over time through 6 years of age, differences in microstructure are sustained yet slightly less widespread than what was found at 4 years of age. Fewer differences may be due to other contributing environmental and social factors influencing white matter maturation. Furthermore, white matter microstructural differences vary with age such that some groups have found both decreased and increased FA in middle to late childhood,

adolescence, and young adulthood (Allin et al., 2011; Eikenes, Løhaugen, Brubakk, Skranes, & Håberg, 2011; Nagy et al., 2003; Travis, Adams, Kovachy, Ben-Shachar, & Feldman, 2016). Importantly, the findings from the present dissertation provide early evidence for sustained differences found in white matter later in development.

Early brain injury implicated white matter beginning from birth to six years of age. During the perinatal period, slower rates of FA changes were found within the posterior limb of the internal capsule, retrolenticular part of the internal capsule, and posterior thalamic radiation in the presence of white matter injury and IVH/GMH. At four years of age, reduced global efficiency was found in relation to white matter injury and IVH/GMH. Moreover, increased ODI was identified in the corpus callosum with respect to IVH/GMH. These regions have also been implicated in early brain injury in other studies and identify particularly vulnerable structures for children born very preterm (Bassi et al., 2011; Malavolti et al., 2017).

The two studies at 4 and 6 years of age reported consistently reduced cognitive performance on measures of intelligence, language, and visuomotor abilities. These findings were in line with previous studies also performed with similar ages and cognitive domains (Delobel-Ayoub et al., 2009b; Wolke & Meyer, 1999; Woodward et al., 2009). Lower scores of intelligence, language, and visuomotor ability are also identified during late childhood, adolescence, and young adulthood (Allin et al., 2008; Allin et al., 2011; Anderson, 2014; Foster-Cohen et al., 2007; Foulder-Hughes & Cooke, 2003; Mangin et al., 2017; Reidy et al., 2013; van Noort-van der Spek et al., 2012). With respect to associations between white matter measures and outcomes, there were some discrepancies between the second and third studies. At four years of age, associations between white matter microstructure and cognitive measures were only found in the full-term children. However, at six years of age, associations between white matter microstructure and outcomes were found in both the full-term and children born very preterm, yet in contrasting directions. At six years of age, the findings that the children born very preterm demonstrated microstructural properties such as myelination and neurite density contributing to intelligence is more convincing than our results at four years of age. This may be due to increased imaging resolution as the six-year-old sample was similar in size to the four-year-old group. It is also possible that neither groups had a large enough sample to clearly delineate the associations between white matter measures and outcomes. Other studies in the literature that have also found associations between DTI metrics and outcomes in those born very preterm, yet no associations

in term-born individuals (Allin et al., 2011; Eikenes et al., 2011; Kelly et al., 2016). Thus, white matter associations with outcomes can be variable across the literature due to variations in cohort, imaging protocols, and methodologies.

5.3 Limitations

There are some limitations to consider. One of the main limitations in the first study is that a comparison sample of full-term children was unavailable. Despite this, we could compare the developmental trends in the children born very preterm with the existing literature. There were a few DTI studies of white matter development in normative samples across early childhood (Dean et al., 2017; Dubois et al., 2014; Qiu et al., 2015) as well a post-mortem literature of children over the first two years of life (Kinney et al., 1988). Based on a qualitative comparison with the literature, we could confidently conclude that white matter tracts in children born very preterm follow similar developmental trends to typically developing children, with an overall pattern of increasing maturity in medial versus distal structures and posterior versus anterior regions. However, we were unable to quantitatively assess how white matter development in the children born very preterm may differ from term-born children, particularly in the preterm period.

Another limitation of the first study is that there were different number of children at each time point (birth, term-equivalent age, 2 years and 4 years). This may have impacted the maturational trends between term-equivalent age and 2 years of age, as well as between 2 and 4 years of age. Furthermore, children had a different number of scans depending on the time that the child came back for follow-up as well as different combinations of time points. Thus, we used linear mixed effects models to handle the uneven number of data points at each time point as well as the different number of longitudinal datasets of the children. In addition, it was apparent that large developmental gains were made between term-equivalent age and 2 years of age. It would have been beneficial to have imaging data at 1 year of age, to help characterise the developmental trajectories to build a more representative model of FA changes across the first four years of life. Nevertheless, this is one of the first studies to include longitudinal imaging data in children born very preterm at these time points.

Limitations to consider within the second and third study are primarily concerning the methodologies chosen to analyze the diffusion data and the statistics used to evaluate associations with outcomes. For instance, tract based spatial statistics was utilized to determine

voxel-based differences within the white matter FA skeleton (Smith et al., 2006). This method is robust, reliable, and widely implemented yet has its own shortcomings, one of which is that it only samples the areas of highest FA within a tract to avoid including voxels that may have partial volumes with other tissue such as grey matter. Only including the areas of highest FA captured by the FA skeleton may not be representative of the entire white matter tract, and it is possible that areas of white matter that may contribute to group differences are not being fully explored. Another shortcoming of this method is the possibility that the average group FA skeleton may not register perfectly onto an individual's FA skeleton, particularly in the more peripheral tracts.

In the second study, deterministic tractography was chosen over other tractography methods such as probabilistic tractography. Deterministic tractography uses local fibre orientation information to begin tracts in one or more voxels whereas probabilistic tractography uses the probability that a voxel is connected to the starting point (Jones et al., 2013). Probabilistic tractography may be able to assess a greater pathway of connections while deterministic tractography is more conservative. In general, tractography does not favour long-range connections, which are likely under-represented with both methods (Bassett, Brown, Deshpande, Carlson, & Grafton, 2011). In addition, quantification of white matter connectivity using orientation information from the diffusion images may not be fully accurate of the actual connectivity in the brain (Jones et al., 2013). Relations with outcomes were not found in the second study between the graph theoretical measures of connectivity and developmental outcomes. This negative result may have been due to the relatively small sample size of data acquired at 4 years of age, which may not have had the power to detect these associations. The univariate t-tests between nodal graph measures and outcomes were subject to many multiple comparisons, which likely contributed to our null findings on these tests.

Sample sizes varied across studies and sizes were limited during childhood, largely due to the difficulty in acquiring useable diffusion images. For instance, the first study included neonates shortly following birth (N=75), term-equivalent age (N=39), 2 years of age (N=18), and 4 years of age (N=29). Within the cross-sectional study at 4 years of age, it was possible to scan children under natural sleep, we could obtain imaging data on the children born very preterm who were non-compliant to the scan procedure while they were awake at the initial attempt (N=31). However, at 6 years of age, there was more loss to neuroimaging follow-up in the longitudinal

cohort of children born very preterm at the 6-year time point compared to at 4 years of age, particularly in the group of children born very preterm. The smaller sample size (N=23) was partially due to being unable to scan children at this age who were lower functioning. At 6 years of age, the sleep scan method does not work as the children are more aware of their surroundings and less prone to fall into a deep sleep knowing that they were uncomfortable with being scanned or unable to complete the scan awake.

A potential limitation of the third study is that all the diffusion data (180-directions) acquired were used in the analysis of these children. Unlike the second study, we did not exclude volumes that contained motion because we found that the exclusion of volumes created more biases in the data than when the volumes were included, particularly within the high b-value (b = 2850). This conscious decision was based on testing the effect of excluding volumes on the DTI metrics as well as having many volumes acquired.

With respect to the follow-up of the children born very preterm at 4 and 6 years of age within the second and third study, it was apparent that there was a selection bias in the parents of the children who participated in the studies. It was more common to have mothers participate in the study who had university level or post-graduate level education while it was less common for mothers to have high school or college level education. As such, it is also possible that the children we sampled could have higher cognitive scores than those of the longitudinal cohort who dropped out of the study for various reasons. Thus, it is likely that we are sampling a high-functioning group of children born very preterm.

5.4 Future Directions

The rich longitudinal dataset following the neurodevelopment of children born very preterm that was included in the present dissertation illuminated many further questions for important avenues of inquiry and investigation. For instance, the first study focused only upon the changes in DTI metrics across white matter tracts in cortical regions within the cohort of children born very preterm. It would be of great interest for future studies to compare typically developing fetuses who were imaged in utero during the same preterm period and contrast white matter maturation within neonatal scans between birth and term-equivalent age. The addition of normative information during the preterm period would help to explain how similar or different the maturational patterns may be between the two groups and provide more insight into the

timing as well as the way in which white matter develops differently by term-equivalent age in the very preterm brain. One such study by Thomason and colleagues (2017) imaged fetuses in utero and found that functional connectivity was reduced in the babies that were delivered preterm versus the babies carried to term. Their findings provided evidence for neural pathways to be altered prior to preterm birth and were likely influenced by adverse medical conditions such as infection and inflammation (Thomason et al., 2017). Also, in agreement with their findings, there is a need for further inquiries towards investigating potential negative impacts of medical conditions experienced by the neonates and mothers on long-term white matter development in these children.

The potential for possible interventions during preterm period could positively impact cognitive outcomes for neonates born very preterm. For instance, Kostovic and Judas (2007) speculated that it may be beneficial to use interventions that would stimulate the somatosensory system, such as the thalamocortical system, to promote structural reorganization in areas with identified insults. In addition, the authors suggested that interventions would be optimal for children born very preterm during the preterm period when there is structural plasticity, many synapses, transient neuronal elements such as the subplate are present, and naturally occurring regressive events are declining (Kostović & Judas, 2007). Such interventions have yet to be tested and realized as beneficial for these children yet are nonetheless compelling to consider.

In terms of other useful analyses for diffusion data, network level longitudinal and cross-sectional analyses could potentially better identify clusters of white matter regions that may be related to cognitive ability. Network-level analyses would be analogous to identifying functional networks responsible for cognition, yet with structural metrics such as graph theoretical measures that were calculated in the second study. As the second study subjected each white matter region (node) to univariate analyses, it is possible that it was not sensitive enough at this level. Analytic methods such as Network Based Statistics could identify multiple connections based on graph theoretical measures with cognitive scores as well as between-group differences (Zalesky, Fornito, & Bullmore, 2010). Thompson and colleagues (2016) employed this method in network measures in 7-year-old children born very preterm that could be applied to structural data. They found that a widespread structural network predicted impaired IQ, likely more representative of cognitive function than at the nodal level.

There are few developmental studies using NODDI metrics to investigate white matter maturation in typically developing populations and individuals born very preterm. The third study of the present thesis found differences in FA and axonal organization (ODI) between children born very preterm and term-born children at six years of age using multi-shell diffusion imaging. These findings support the explanation that deviances in the very beginning of white matter maturation, such as during the second and third trimester, are a primary contributing factor to differences captured later in childhood. Future investigations should also utilize early diffusion imaging data to potentially predict differences found later in childhood. Potential differences in imaging protocols that often occur circumstantially over the time span of a longitudinal follow-up study would need to be overcome. Additional multi-shell imaging studies should also be prioritized at earlier ages to obtain more detailed measures of white matter microstructure across development, such as the NODDI metrics.

The multi-shell diffusion data are particularly interesting to explore in terms of the how the NODDI metrics may differ in grey matter between the children born very preterm and the full-term children, which can also provide additional understanding about white matter differences. For instance, the measure of axonal orientation dispersion could provide insight into how white matter influences grey matter development, especially with respect to patterns of dendritic arborisation, which is a marker of grey matter complexity (Chang et al., 2015). Methodological challenges of accurate grey matter cortical registration between subjects would need to be overcome. Additional analysis methods that are relatively new to the field and available for multi-shell diffusion imaging could also be applied to the data for further detailed investigations of white matter microstructure, such as diffusion kurtosis and fixel-based analyses (Jensen, Helpern, Ramani, Lu, & Kaczynski, 2005; Pannek et al., 2018; Raffelt et al., 2017).

Within the scope of the present dissertation, all the three studies included longitudinal and cross-sectional diffusion imaging data, perinatal medical histories and cognitive outcome measures. Other available imaging modalities could be combined with the diffusion data, such as resting state functional magnetic imaging, to explore multimodal structural and functional connectivity changes over time in children born very preterm as well as in contrast to term-born children. Moreover, additional developmental outcome data could be obtained from parent questionnaires regarding measures of behaviour as well as social and executive functioning. These additional measures of behaviour and social functioning would be important to explore in association

between white matter microstructure and connectivity as behavioural, social and executive function difficulties emerge at these ages.

5.5 Implications

Longitudinal studies are valuable in characterising true maturational changes within the cohort of children born very preterm studied. The associations found between slower white matter growth as reflected in slower changes in RD and MD during the perinatal period and lower scores of IQ and language ability at four years of age provides an opportunity to be used as a potential biomarker in the future. If sophisticated MR imaging such as diffusion imaging was performed on every child born very preterm between the time of their birth, term-equivalent age, and one or two- years of age, it may well prove valuable as a predictor of which children are most at risk for neurodevelopmental impairment. Moreover, we could have a better understanding of differential development of white matter tracts perhaps in an analogous way that growth charts are used to track babies' physical development.

Our findings of slower maturation of white matter with outcomes as well as widespread differences found in FA within the 4 and 6 year old children support the previously established hypothesis that responsible cell populations for myelination, such as the pre-oligodendrocyte glial cells, are affected by very preterm birth (Ferriero & Miller, 2010). During the preterm period and early childhood, the developing brain has a tremendous ability for neuroplasticity and reorganization following insults to the brain, such as white matter lesions (Cioni, D'Acunto, & Guzzetta, 2011). This strengthens the notion that the preterm period is a window of opportunity for further research in understanding developmental processes such as the role of the subplate and oligodendrocytes in white matter development.

Our results are largely consistent with the literature yet are nonetheless striking. It is evident that white matter is affected at multiple developmental stages across early childhood and that developmental outcomes are compromised in these children. Thus, there is an increasing importance for early interventions in this population, especially for the children born very preterm who can be identified as being at highest risk for adverse outcomes. A Cochrane review by Spittle and colleagues (2012) covered twenty-five different interventions for preterm infants that targeted parent-infant relationships, infant development, or parent support alone on motor and cognitive outcomes at infancy, preschool age, school age, and early adulthood compared to

standard follow-up medical care. This review demonstrated that early interventions improved cognitive outcomes up to preschool age and some motor abilities up to school age, despite the heterogeneity in the intervention programs studied (Spittle, Orton, Anderson, Boyd, & Doyle, 2012). The findings from the present thesis support these intervention initiatives and provides additional reason to further investigate early interventions targeting white matter development and cognitive abilities.

5.6 Conclusions

In conclusion, the present thesis comprehensively investigated white matter maturation in children born very preterm and its differences from full-term children. Diffusion imaging in the neonatal period and early childhood was sensitive in identifying compromised white matter in this population, as well as its associations with developmental outcomes. Lower cognitive scores in the children born very preterm were found uniformly within the cross-sectional studies, which contribute to the difficulties that these children may encounter to learn and succeed in the short-term as they enter school age, as well as the long-term when they move into adolescence and adulthood. The results of our findings support dysmaturation of white matter occurring very early in development and within the preterm period. Therefore, the present thesis contributes towards the direction in which additional research, medical and psychological attention are needed to further probe specific ways in which white matter maturation and cognitive development can be understood, treated and interventions applied to optimize the brain and cognitive health of children born very preterm.

References

Aarnoudse-Moens, C. S., Duivenvoorden, H. J., Weisglas-Kuperus, N., Van Goudoever, J. B., & Oosterlaan, J. (2012). The profile of executive function in very preterm children at 4 to 12 years. *Developmental Medicine and Child Neurology*, *54*(3), 247–253. http://doi.org/10.1111/j.1469-8749.2011.04150.x

Achard, S., & Bullmore, E. (2007). Efficiency and cost of economical brain functional networks. *PLoS Computational Biology*, *3*(2), 0174–0183. http://doi.org/10.1371/journal.pcbi.0030017

Akazawa, K., Chang, L., Yamakawa, R., Hayama, S., Buchthal, S., Alicata, D., … Oishi, K. (2016). Probabilistic maps of the white matter tracts with known associated functions on the neonatal brain atlas : Application to evaluate longitudinal developmental trajectories in term-born and preterm-born infants. *NeuroImage*, *128*, 167–179. http://doi.org/10.1016/j.neuroimage.2015.12.026

Allen, M. C. (2002). Preterm outcomes research: A critical component of neonatal intensive care. *Mental Retardation and Developmental Disabilities Research Reviews*, *8*, 221–233. http://doi.org/10.1002/mrdd.10044

Allin, M. P. G., Kontis, D., Walshe, M., Wyatt, J., Barker, G. J., Kanaan, R. A. A., … Nosarti, C. (2011). White matter and cognition in adults who were born preterm. *PLoS ONE*, *6*(10), 1–9. http://doi.org/10.1371/journal.pone.0024525

Allin, M., Walshe, M., Fern, A., Nosarti, C., Cuddy, M., Rifkin, L., … Wyatt, J. (2008). Cognitive maturation in preterm and term born adolescents. *Journal of Neurology, Neurosurgery, and Psychiatry*, *79*(4), 381–386. http://doi.org/10.1136/jnnp.2006.110858

Anderson, M. J., & Robinson, J. (2001). Permutation tests for linear models. *Australian & New Zealand Journal of Statistics*, *43*(1), 75–88. http://doi.org/10.1111/1467-842X.00156

Anderson, P. J. (2014). Neuropsychological outcomes of children born very preterm. *Seminars in Fetal & Neonatal Medicine*, *19*(2), 90–6. http://doi.org/10.1016/j.siny.2013.11.012

Anjari, M., Srinivasan, L., Allsop, J. M., Hajnal, J. V, Rutherford, M. A., Edwards, D. A., &

Counsell, S. J. (2007). Diffusion tensor imaging with tract-based spatial statistics reveals local white matter abnormalities in preterm infants. *NeuroImage*, *35*(3), 1021–7. http://doi.org/10.1016/j.neuroimage.2007.01.035

Back, S. A. (2017). White matter injury in the preterm infant: pathology and mechanisms. *Acta Neuropathologica*, *134*(3), 331–349. http://doi.org/10.1007/s00401-017-1718-6

Ball, G., Boardman, J. P., Aljabar, P., Pandit, A., Arichi, T., Merchant, N., … Counsell, S. J. (2013). The influence of preterm birth on the developing thalamocortical connectome. *Cortex*, *49*(6), 1711–1721. http://doi.org/10.1016/j.cortex.2012.07.006

Ball, G., Boardman, J. P., Rueckert, D., Aljabar, P., Arichi, T., Merchant, N., … Counsell, S. J. (2012). The effect of preterm birth on thalamic and cortical development. *Cerebral Cortex*, *22*(5), 1016–1024. http://doi.org/10.1093/cercor/bhr176

Ball, G., Pazderova, L., Chew, A., Tusor, N., Merchant, N., Arichi, T., … Counsell, S. J. (2015). Thalamocortical connectivity predicts cognition in children born preterm. *Cerebral Cortex*, *25*(11), 4310–4318. http://doi.org/10.1093/cercor/bhu331

Ball, G., Srinivasan, L., Aljabar, P., Counsell, S. J., Durighel, G., Hajnal, J. V, … Edwards, a D. (2013). Development of cortical microstructure in the preterm human brain. *Proceedings of the National Academy of Sciences of the United States of America*, *110*(23), 9541–6. http://doi.org/10.1073/pnas.1301652110

Barnett, M. L., Tusor, N., Ball, G., Chew, A., Falconer, S., Aljabar, P., … Counsell, S. J. (2017). Exploring the multiple-hit hypothesis of preterm white matter damage using diffusion MRI. *NeuroImage: Clinical*, *17*, 596–606. http://doi.org/10.1016/j.nicl.2017.11.017

Bassett, D. S., Brown, J. A., Deshpande, V., Carlson, J. M., & Grafton, S. T. (2011). Conserved and variable architecture of human white matter connectivity. *NeuroImage*, *54*(2), 1262–1279. http://doi.org/10.1016/j.neuroimage.2010.09.006

Bassi, L., Chew, A., Merchant, N., Ball, G., Ramenghi, L., Boardman, J., … Counsell, S. J. (2011). Diffusion tensor imaging in preterm infants with punctate white matter lesions. *Pediatric Research*, *69*(6), 561–566.

Batalle, D., Hughes, E. J., Zhang, H., Tournier, J.-D., Tusor, N., Aljabar, P., … Counsell, S. J. (2017). Early development of structural networks and the impact of prematurity on brain connectivity. *NeuroImage*, *149*, 379–392. http://doi.org/10.1016/j.neuroimage.2017.01.065

Beaulieu, C. (2002). The basis of anisotropic water diffusion in the nervous system - A technical review. *NMR in Biomedicine*, *15*(7–8), 435–455. http://doi.org/10.1002/nbm.782

Beery, K., Buktenica, N., & Beery, N. (2010). *Beery-Buktenica Test of Visual Motor Integration*. San Antonio, TX: The Psychological Corporation.

Benjamini, Y., & Hochberg, Y. (1995). Controlling the false discovery rate: A practical and powerful approach to multiple testing. *Journal of Royal Statistical Society*, *57*(1), 289–300.

Bhutta, A. T., Cleves, M. a, Casey, P. H., Cradock, M. M., & Anand, K. J. S. (2002). Cognitive and behavioral outcomes of school-aged children who were born preterm: a meta-analysis. *JAMA : The Journal of the American Medical Association*, *288*(6), 728–37. http://www.ncbi.nlm.nih.gov/pubmed/12169077

Blencowe, H., Cousens, S., Oestergaard, M. Z., Chou, D., Moller, A.-B., Narwal, R., … Lawn, J. E. (2012). National, regional, and worldwide estimates of preterm birth rates in the year 2010 with time trends since 1990 for selected countries: a systematic analysis and implications. *Lancet*, *379*, 2162–72. http://doi.org/10.1016/S0140-6736(12)60820-4

Boardman, J. P., Counsell, S. J., Rueckert, D., Kapellou, O., Bhatia, K. K., Aljabar, P., … Edwards, a D. (2006). Abnormal deep grey matter development following preterm birth detected using deformation-based morphometry. *NeuroImage*, *32*(1), 70–78. http://doi.org/10.1016/j.neuroimage.2006.03.029

Böhm, B., Katz-Salamon, M., Smedler, Ann-Charlotte; Lagercrantz, H., & Forssberg, H. (2002). Developmental risks and protective factors for influencing cognitive outcome at children. *Developmental Medicine and Child Neurology*, *44*, 508–516.

Bolisetty, S., Dhawan, A., Abdel-Latif, M., Bajuk, B., Stack, J., & Lui, K. (2014). Intraventricular Hemorrhage and Neurodevelopmental Outcomes in Extreme Preterm Infants. *Pediatrics*, *133*(1), 55–62. http://doi.org/10.1542/peds.2013-0372

Bracewell, M., & Marlow, N. (2002). Patterns of motor disability in very preterm children. *Mental Retardation and Developmental Disabilities Research Reviews*, *8*(4), 241–248. http://doi.org/10.1002/mrdd.10049

Brouwer, A., Groenendaal, F., van Haastert, I. L., Rademaker, K., Hanlo, P., & de Vries, L. (2008). Neurodevelopmental outcome of preterm infants with severe intraventricular hemorrhage and therapy for post-hemorrhagic ventricular dilatation. *The Journal of Pediatrics*, *152*(5), 648–654. http://doi.org/10.1016/j.jpeds.2007.10.005

Brouwer, A. J., Groenendaal, F., Benders, M. J. N. L., & De Vries, L. S. (2014). Early and late complications of germinal matrix-intraventricular haemorrhage in the preterm infant: What is new? *Neonatology*, *106*(4), 296–303. http://doi.org/10.1159/000365127

Brouwer, A. J., Van Stam, C., Uniken Venema, M., Koopman, C., Groenendaal, F., & De Vries, L. S. (2012). Cognitive and neurological outcome at the age of 5-8 years of preterm infants with post-hemorrhagic ventricular dilatation requiring neurosurgical intervention. *Neonatology*, *101*(3), 210–216. http://doi.org/10.1159/000331797

Brown, C. J., Miller, S. P., Booth, B. G., Andrews, S., Chau, V., Poskitt, K. J., & Hamarneh, G. (2014). NeuroImage Structural network analysis of brain development in young preterm neonates. *NeuroImage*, *101*, 667–680. http://doi.org/10.1016/j.neuroimage.2014.07.030

Brown, J. A., Rudie, J. D., Bandrowski, A., Van Horn, J. D., & Bookheimer, S. Y. (2012). The UCLA multimodal connectivity database: a web-based platform for brain connectivity matrix sharing and analysis. *Frontiers in Neuroinformatics*, *6*(28), 1–17. http://doi.org/10.3389/fninf.2012.00028

Budde, M. D., & Annese, J. (2013). Quantification of anisotropy and fiber orientation in human brain histological sections. *Frontiers in Integrative Neuroscience*, *7*, 3. http://doi.org/10.3389/fnint.2013.00003

Bullmore, E. T., & Sporns, O. (2009). Complex brain networks: graph theoretical analysis of structural and functional systems. *Nature Reviews. Neuroscience*, *10*(3), 186–98. http://doi.org/10.1038/nrn2575

Bullmore, E. T., & Sporns, O. (2012). The economy of brain network organization. *Nature Reviews. Neuroscience*, *13*(5), 336–49. http://doi.org/10.1038/nrn3214

Caldinelli, C., Froudist-Walsh, S., Karolis, V., Tseng, C. E., Allin, M. P., Walshe, M., … Nosarti, C. (2017). White matter alterations to cingulum and fornix following very preterm birth and their relationship with cognitive functions. *NeuroImage*, *150*, 373–382. http://doi.org/10.1016/j.neuroimage.2017.02.026

Cao, M., He, Y., Dai, Z., Liao, X., Jeon, T., Ouyang, M., … Huang, H. (2016). Early Development of Functional Network Segregation Revealed by Connectomic Analysis of the Preterm Human Brain. *Cerebral Cortex*, 1–15. http://doi.org/10.1093/cercor/bhw038

Cao, M., Huang, H., & He, Y. (2017). Developmental Connectomics from Infancy through Early Childhood. *Trends in Neurosciences*, *40*(8), 494–506. http://doi.org/10.1016/j.tins.2017.06.003

Cao, M., Huang, H., Peng, Y., Dong, Q., & He, Y. (2016). Toward Developmental Connectomics of the Human Brain. *Frontiers in Neuroanatomy*, *10*(25). http://doi.org/10.3389/fnana.2016.00025

Capute, A. J., Shapiro, B. K., Palmer, F. B., Ross, A., & Wachtel, R. C. (1985). Normal gross motor development: The influences pfrace, sex and socio-economic status. *Developmental Medicine & Child Neurology*, *27*(5), 635–643. Retrieved from http://doi.wiley.com/10.1111/j.1469-8749.1985.tb14136.x

Carper, R. A., Treiber, J. M., White, N. S., Kohli, J. S., & Müller, R. A. (2017). Restriction spectrum imaging as a potential measure of cortical neurite density in autism. *Frontiers in Neuroscience*, *10*, 610. http://doi.org/10.3389/fnins.2016.00610

Catani, M., Howard, R. J., Pajevic, S., & Jones, D. K. (2002). Virtual in Vivo interactive dissection of white matter fasciculi in the human brain. *NeuroImage*, *17*(1), 77–94. http://doi.org/10.1006/nimg.2002.1136

Chang, L.-C., Jones, D. K., & Pierpaoli, C. (2005). RESTORE: Robust estimation of tensors by outlier rejection. *Magnetic Resonance in Medicine*, *53*(5), 1088–1095.

http://doi.org/10.1002/mrm.20426

Chang, Y. S., Owen, J. P., Pojman, N. J., Thieu, T., Bukshpun, P., Wakahiro, M. L. J., … Mukherjee, P. (2015). White matter changes of neurite density and fiber orientation dispersion during human brain maturation. *PLoS ONE*, *10*(6), e0123656. http://doi.org/10.1371/journal.pone.0123656

Chiron, C., Jambaque, I., Nabbout, R., Lounes, R., Syrota, a., & Dulac, O. (1997). The right brain hemisphere is dominant in human infants. *Brain*, *120*(6), 1057–1065. http://doi.org/10.1093/brain/120.6.1057

Cioni, G., D'Acunto, G., & Guzzetta, A. (2011). Perinatal brain damage in children. Neuroplasticity, early intervention, and molecular mechanisms of recovery. *Progress in Brain Research*, *189*, 139–154. http://doi.org/10.1016/B978-0-444-53884-0.00022-1

Constable, R. T., Ment, L. R., Vohr, B. R., Kesler, S. R., Fulbright, R. K., Lacadie, C., … Reiss, A. R. (2008). Prematurely Born Children Demonstrate White Matter Microstructural Differences at 12 Years of Age, Relative to Term Control Subjects: An Investigation of Group and Gender Effects. *Pediatrics*, *121*(2), 306–316. http://doi.org/10.1542/peds.2007-0414

Counsell, S. J., Allsop, J. M., Harrison, M. C., Larkman, D. J., Kennea, N. L., Kapellou, O., … Rutherford, M. A. (2003). Diffusion-weighted imaging of the brain in preterm infants with focal and diffuse white matter abnormality. *Pediatrics*, *112*(1), 1–7.

Counsell, S. J., Edwards, a D., Chew, A. T. M., Anjari, M., Dyet, L. E., Srinivasan, L., … Cowan, F. M. (2008). Specific relations between neurodevelopmental abilities and white matter microstructure in children born preterm. *Brain*, *131*, 3201–8. http://doi.org/10.1093/brain/awn268

Cramer, R. D. (1993). Partial least square (PLS): Its strengths and limitations. *Perspectives in Drug Discovery and Design*, *1*, 269–278.

Cusson, R. M. (2003). Factors Influencing Language Development in Preterm Infants. *Journal of Obstetric, Gynecologic, and Neonatal Nursing*, *32*(3), 402–409.

http://doi.org/10.1177/0884217503253530

De Bruïne, F. T., Van Wezel-Meijler, G., Leijser, L. M., Steggerda, S. J., Van Den Berg-Huysmans, A. a., Rijken, M., … Van Der Grond, J. (2013). Tractography of white-matter tracts in very preterm infants: A 2-year follow-up study. *Developmental Medicine and Child Neurology*, *55*(5), 427–433. http://doi.org/10.1111/dmcn.12099

de Kieviet, J. F., Piek, J. P., Aarnoudse-Moens, C. S., & Oosterlaan, J. (2009). Motor Development in Very Preterm and Very Low-Birth-Weight Children From Birth to Adolescence. *Jama*, *302*(20), 2235–2242. http://doi.org/10.1001/jama.2009.1708

de Laat, S. A. A., Essink-Bot, M. L., van Wassenaer-Leemhuis, A. G., & Vrijkotte, T. G. (2016). Effect of socioeconomic status on psychosocial problems in 5- to 6-year-old preterm- and term-born children: the ABCD study. *European Child and Adolescent Psychiatry*, *25*(7), 757–767. http://doi.org/10.1007/s00787-015-0791-4

Dean, D. C., O'Muircheartaigh, J., Dirks, H., Waskiewicz, N., Lehman, K., Walker, L., … Deoni, S. C. L. (2014). Modeling healthy male white matter and myelin development: 3 through 60 months of age. *NeuroImage*, *84*, 742–752. http://doi.org/10.1016/j.neuroimage.2013.09.058

Dean, D. C., Planalp, E. M., Wooten, W., Adluru, N., Kecskemeti, S. R., Frye, C., … Alexander, A. L. (2017). Mapping White Matter Microstructure in the One Month Human Brain. *Scientific Reports*, *7*(1), 1–14. http://doi.org/10.1038/s41598-017-09915-6

Dean, J. M., Bennet, L., Back, S. a, McClendon, E., Riddle, A., & Gunn, A. J. (2014). What brakes the preterm brain? An arresting story. *Pediatric Research*, *75*(1–2), 227–33. http://doi.org/10.1038/pr.2013.189

Dean, J. M., Mcclendon, E., Hansen, K., Azimi-zonooz, A., Chen, K., Riddle, A., … Back, S. A. (2013). Prenatal Cerebral Ischemia Disrupts MRI-Defined Cortical Micrtostructure Through Disturbances in Neuronal Arborization. *Science Translational Medicine*, *5*(168), 1–22. http://doi.org/10.1126/scitranslmed.3004669.Prenatal

Delobel-Ayoub, M., Arnaud, C., White-Koning, M., Casper, C., Pierrat, V., Garel, M., …

Larroque, B. (2009a). Behavioral problems and cognitive performance at 5 years of age after very preterm birth: the EPIPAGE Study. *Pediatrics*, *123*(6), 1485–1492. http://doi.org/10.1542/peds.2008-1216

Delobel-Ayoub, M., Arnaud, C., White-Koning, M., Casper, C., Pierrat, V., Garel, M., … Larroque, B. (2009b). Behavioral problems and cognitive performance at 5 years of age after very preterm birth: the EPIPAGE Study. *Pediatrics*, *123*(6), 1485–1492. http://doi.org/10.1542/peds.2008-1216

Deoni, S. C. L., Dean, D. C., O'Muircheartaigh, J., Dirks, H., & Jerskey, B. a. (2012). Investigating white matter development in infancy and early childhood using myelin water faction and relaxation time mapping. *NeuroImage*, *63*(3), 1038–1053. http://doi.org/10.1016/j.neuroimage.2012.07.037

Desikan, R. S., Se, F., Fischl, B., Quinn, B. T., Dickerson, B. C., Blacker, D., … Killiany, R. J. (2006). An automated labeling system for subdividing the human cerebral cortex on MRI scans into gyral based regions of interest. *NeuroImage*, *31*, 968–980. http://doi.org/10.1016/j.neuroimage.2006.01.021

Doria, V., Beckmann, C. F., Arichi, T., Merchant, N., Groppo, M., Turkheimer, F. E., … Edwards, A. D. (2010). Emergence of resting state networks in the preterm human brain. *Proceedings of the National Academy of Sciences*, *107*(46), 20015–20020. http://doi.org/10.1073/pnas.1007921107

Dubois, J., Dehaene-Lambertz, G., Kulikova, S., Poupon, C., Hüppi, P. S., & Hertz-Pannier, L. (2014). The early development of brain white matter: a review of imaging studies in fetuses, newborns and infants. *Neuroscience*, *276*, 48–71. http://doi.org/10.1016/j.neuroscience.2013.12.044

Dubois, J., Dehaene-Lambertz, G., Perrin, M., Mangin, J. F., Cointepas, Y., Duchesnay, E., … Hertz-Pannier, L. (2008). Asynchrony of the early maturation of white matter bundles in healthy infants: Quantitative landmarks revealed noninvasively by diffusion tensor imaging. *Human Brain Mapping*, *29*(1), 14–27. http://doi.org/10.1002/hbm.20363

Dubois, J., Hertz-Pannier, L., Cachia, a., Mangin, J. F., Le Bihan, D., & Dehaene-Lambertz, G.

(2009). Structural asymmetries in the infant language and sensori-motor networks. *Cerebral Cortex*, *19*(2), 414–423. http://doi.org/10.1093/cercor/bhn097

Dubois, J., Hertz-Pannier, L., Dehaene-Lambertz, G., Cointepas, Y., & Le Bihan, D. (2006). Assessment of the early organization and maturation of infants' cerebral white matter fiber bundles: a feasibility study using quantitative diffusion tensor imaging and tractography. *NeuroImage*, *30*(4), 1121–32. http://doi.org/10.1016/j.neuroimage.2005.11.022

Duerden, E., Card, D., Lax, I. D., Donner, E. J., & Taylor, M. J. (2013). Alterations in frontostriatal pathways in children born very preterm. *Developmental Medicine and Child Neurology*, *55*(10), 952–958. http://doi.org/10.1111/dmcn.12198

Duerden, E. G., Foong, J., Chau, V., Branson, H., Poskitt, K. J., Grunau, R. E., … Miller, S. P. (2015). Tract-based spatial statistics in preterm-born neonates predicts cognitive and motor outcomes at 18 months. *American Journal of Neuroradiology*, *36*(8), 1565–1571. http://doi.org/10.3174/ajnr.A4312

Duerden, E. G., Grunau, R. E., Guo, T., Foong, J., Pearson, A., Au-Young, S., … Miller, S. P. (2018). Early procedural pain is associated with regionally-specific alterations in thalamic development in preterm neonates. *The Journal of Neuroscience*, *38*(4), 867–17. http://doi.org/10.1523/JNEUROSCI.0867-17.2017

Eaton-rosen, Z., Melbourne, A., Orasanu, E., Cardoso, M. J., Modat, M., Bainbridge, A., … Ourselin, S. (2015). NeuroImage Longitudinal measurement of the developing grey matter in preterm subjects using multi-modal MRI. *NeuroImage*, *111*, 580–589. http://doi.org/10.1016/j.neuroimage.2015.02.010

Eikenes, L., Løhaugen, G. C., Brubakk, A. M., Skranes, J., & Håberg, A. K. (2011). Young adults born preterm with very low birth weight demonstrate widespread white matter alterations on brain DTI. *NeuroImage*, *54*(3), 1774–1785. http://doi.org/10.1016/j.neuroimage.2010.10.037

Estep, M. E., Smyser, C. D., Anderson, P. J., Ortinau, C. M., Wallendorf, M., Katzman, C. S., … Shimony, J. S. (2014). Diffusion tractography and neuromotor outcome in very preterm children with white matter abnormalities. *Pediatric Research*, *76*(1), 86–92.

http://doi.org/10.1038/pr.2014.45

Feldman, H. M., Lee, E. S., Loe, I. M., Yeom, K. W., Grill-Spector, K., & Luna, B. (2012). White matter microstructure on diffusion tensor imaging is associated with conventional magnetic resonance imaging findings and cognitive function in adolescents born preterm. *Developmental Medicine and Child Neurology*, *54*(9), 809–814. http://doi.org/10.1111/j.1469-8749.2012.04378.x

Feldman, H. M., Lee, E. S., Yeatman, J. D., & Yeom, K. W. (2013). Language and reading skills in school-aged children and adolescents born preterm are associated with white matter properties on diffusion tensor imaging, *50*(14), 3348–3362. http://doi.org/10.1016/j.neuropsychologia.2012.10.014.Language

Ferriero, D. M., & Miller, S. P. (2010). Imaging selective vulnerability in the developing nervous system. *Journal of Anatomy*, *217*(4), 429–435. http://doi.org/10.1111/j.1469-7580.2010.01226.x

Fischl, B., Salat, D. H., Busa, E., Albert, M., Dieterich, M., Haselgrove, C., … Dale, A. M. (2002). Whole brain segmentation: Neurotechnique automated labeling of neuroanatomical structures in the human brain. *Neuron*, *33*(3), 341–355. http://doi.org/10.1016/S0896-6273(02)00569-X

Foster-Cohen, S., Edgin, J. O., Champion, P. R., & Woodward, L. J. (2007). Early delayed language development in very preterm infants: Evidence from the MacArthur-Bates CDI. *Journal of Child Language*, *34*(3), 655–675. http://doi.org/10.1017/S0305000907008070

Foulder-Hughes, L. A., & Cooke, R. W. (2003). Motor, cognitive, and behavioural disorders in children born very preterm. *Dev Med Child Neurol*, *45*(2), 97–103. http://doi.org/10.1111/j.1469-8749.2003.tb00912.x

Futagi, Y., Suzuki, Y., Toribe, Y., Nakano, H., & Morimoto, K. (2005). Neurodevelopmental outcome in children with posthemorrhagic hydrocephalus. *Pediatric Neurology*, *33*(1), 26–32. http://doi.org/10.1016/j.pediatrneurol.2005.01.008

Gayraud, F., & Kern, S. (2007). Influence of preterm birth on early lexical and grammatical

acquisition. *First Language*, *27*(2), 159–173. http://doi.org/10.1177/0142723706075790

Genc, S., Malpas, C. B., Holland, S. K., Beare, R., & Silk, T. J. (2017). Neurite density index is sensitive to age related differences in the developing brain. *NeuroImage*, *148*, 373–380. http://doi.org/10.1016/j.neuroimage.2017.01.023

Geng, X., Gouttard, S., Sharma, Geng X, Gouttard S, Sharma A, Gu H, Styner M, Lin W, et al. Q. tract-based white matter development from birth to age two years. N. 2012; 61: 542–557. A., Gu, H., Styner, M., Lin, W., … Gilmore, J. H. (2012). Quantitative tract-based white matter development from birth to age two years. *Neuroimage*, *61*(3), 542–557. http://doi.org/10.1016/j.neuroimage.2012.03.057.Quantitative

Glass, T. J. A., Chau, V., Gardiner, J., Foong, J., Vinall, J., Zwicker, J. G., … Miller, S. P. (2017). Severe retinopathy of prematurity predicts delayed white matter maturation and poorer neurodevelopment. *Archives of Disease in Childhood: Fetal and Neonatal Edition*, *102*(6), F532–F537. http://doi.org/10.1136/archdischild-2016-312533

Glass, T. J. A., Chau, V., Grunau, R. E., Synnes, A., Guo, T., Duerden, E. G., … Miller, S. P. (2018). Multiple Postnatal Infections in Newborns Born Preterm Predict Delayed Maturation of Motor Pathways at Term-Equivalent Age with Poorer Motor Outcomes at 3 Years. *Journal of Pediatrics*, *196*, 91–97. http://doi.org/10.1016/j.jpeds.2017.12.041

Goldenberg, R. L., Culhane, J. F., Iams, J. D., & Romero, R. (2008). Epidemiology and Causes of Preterm Birth. *Lancet*, *371*, 75–84. http://doi.org/10.1097/01.aoa.0000344666.82463.8d

Gozzo, Y., Vohr, B., Lacadie, C., Hampson, M., Katz, K. H., Maller-Kesselman, J., … Ment, L. R. (2009). Alterations in neural connectivity in preterm children at school age. *NeuroImage*, *48*(2), 458–63. http://doi.org/10.1016/j.neuroimage.2009.06.046

Grussu, F., Schneider, T., Tur, C., Yates, R. L., Tachrount, M., Ianuş, A., … Gandini Wheeler-Kingshott, C. A. M. (2017). Neurite dispersion: a new marker of multiple sclerosis spinal cord pathology? *Annals of Clinical and Translational Neurology*, *4*(9), 663–679. http://doi.org/10.1002/acn3.445

Guo, T., Duerden, E. G., Adams, E., Chau, V., Branson, H. M., Chakravarty, M. M., … Miller,

S. P. (2017). Quantitative assessment of white matter injury in preterm neonates: Association with outcomes. *Neurology*, *88*(7), 614–622. http://doi.org/10.1212/WNL.0000000000003606

Hagmann, P., Sporns, O., Madan, N., Cammoun, L., Pienaar, R., Wedeen, V. J., … Grant, P. E. (2010). White matter maturation reshapes structural connectivity in the late developing human brain. *Proceedings of the National Academy of Sciences of the United States of America*, *107*(44), 19067–72. http://doi.org/10.1073/pnas.1009073107

Hermoye, L., Saint-Martin, C., Cosnard, G., Lee, S. K., Kim, J., Nassogne, M. C., … Mori, S. (2006). Pediatric diffusion tensor imaging: Normal database and observation of the white matter maturation in early childhood. *NeuroImage*, *29*(2), 493–504. http://doi.org/10.1016/j.neuroimage.2005.08.017

Holwerda, J. C., Van Braeckel, K. N. J. A., Roze, E., Hoving, E. W., Maathuis, C. G. B., Brouwer, O. F., … Bos, A. F. (2016). Functional outcome at school age of neonatal post-hemorrhagic ventricular dilatation. *Early Human Development*, *96*, 15–20. http://doi.org/10.1016/j.earlhumdev.2016.02.005

Howe, T. H., Sheu, C. F., Hsu, Y. W., Wang, T. N., & Wang, L. W. (2016). Predicting neurodevelopmental outcomes at preschool age for children with very low birth weight. *Research in Developmental Disabilities*, *48*, 231–241. http://doi.org/10.1016/j.ridd.2015.11.003

Huang, H., Shu, N., Mishra, V., Jeon, T., Chalak, L., Wang, Z. J., … He, Y. (2015). Development of human brain structural networks through infancy and childhood. *Cerebral Cortex*, *25*(5), 1389–1404. http://doi.org/10.1093/cercor/bht335

Huppi, P., Schuknecht, B., Boesch, C., Bossi, E., Felblinger, J., Fusch, C., & Herschkowitz, N. (1996). Structural and neurobehavioral delay in postnatal brain development of preterm infants. *Pediatric Research*, *39*(5), 895–901.

Huttenlocher, P. R., & Bonnier, C. (1991). Effects of changes in the periphery on development of the corticospinal motor system in the rat. *Developmental Brain Research*, *60*(2), 253–260. http://doi.org/10.1016/0165-3806(91)90054-M

Inder, T. E., Huppi, P. S., Warfield, S., Kikinis, R., Zientara, G. P., Barnes, P. D., … Volpe, J. J. (1999). Periventricular white matter injury in the premature infant is followed by reduced cerebral cortical gray matter volume at term. *Annals of Neurology*, *46*(5), 755–760. Retrieved from http://www.ncbi.nlm.nih.gov/pubmed/10553993

Inder, T. E., Warfield, S. K., Wang, H., Hüppi, P. S., & Volpe, J. J. (2005). Abnormal cerebral structure is present at term in premature infants. *Pediatrics*, *115*(2), 286–94. http://doi.org/10.1542/peds.2004-0326

Innocenti, G. M., & Price, D. J. (2005). Exuberance in the development of cortical networks. *Nature Reviews Neuroscience*, *6*(12), 955–965. http://doi.org/10.1038/nrn1790

Jary, S., De Carli, A., Ramenghi, L. A., & Whitelaw, A. (2012). Impaired brain growth and neurodevelopment in preterm infants with posthaemorrhagic ventricular dilatation. *Acta Paediatrica, International Journal of Paediatrics*, *101*(7), 743–748. http://doi.org/10.1111/j.1651-2227.2012.02686.x

Jenkinson, M., Bannister, P., Brady, M., & Smith, S. (2002). Improved Optimization for the Robust and Accurate Linear Registration and Motion Correction of Brain Images Improved Optimization for the Robust and Accurate Linear Registration and Motion Correction of Brain Images. *NeuroImage*, *17*, 825–841. http://doi.org/10.1006/nimg.2002.1132

Jenkinson, M., Beckmann, C. F., Behrens, T. E. J., Woolrich, M. W., & Smith, S. M. (2012). FSL. *NeuroImage*, *62*(2), 782–790. http://doi.org/10.1016/j.neuroimage.2011.09.015

Jensen, J. H., Helpern, J. A., Ramani, A., Lu, H., & Kaczynski, K. (2005). Diffusional kurtosis imaging: The quantification of non-Gaussian water diffusion by means of magnetic resonance imaging. *Magnetic Resonance in Medicine*, *53*(6), 1432–1440. http://doi.org/10.1002/mrm.20508

Jones, D. K., Knösche, T. R., & Turner, R. (2013). White matter integrity, fiber count, and other fallacies: the do's and don'ts of diffusion MRI. *NeuroImage*, *73*, 239–54. http://doi.org/10.1016/j.neuroimage.2012.06.081

Kanold, P. O., & Luhmann, H. J. (2010). The subplate and early cortical circuits. *Annual Review*

of Neuroscience, *33*, 23–48. http://doi.org/10.1146/annurev-neuro-060909-153244

Kapellou, O., Counsell, S. J., Kennea, N., Dyet, L., Saeed, N., Stark, J., … Edwards, A. D. (2006). Abnormal cortical development after premature birth shown by altered allometric scaling of brain growth. *PLoS Medicine*, *3*(8), 1382–1390. http://doi.org/10.1371/journal.pmed.0030265

Karolis, V. R., Froudist-Walsh, S., Brittain, P. J., Kroll, J., Ball, G., Edwards, A. D., … Nosarti, C. (2016). Reinforcement of the Brain's Rich-Club Architecture Following Early Neurodevelopmental Disruption Caused by Very Preterm Birth. *Cerebral Cortex*, *26*(3), 1322–1335. http://doi.org/10.1093/cercor/bhv305

Karolis, V. R., Froudist-Walsh, S., Kroll, J., Brittain, P. J., Jane Tseng, C.-E., Nam, K.-W., … Nosarti, C. (2017). Volumetric grey matter alterations in adolescents and adults born very preterm suggest accelerated brain maturation. *NeuroImage*, *163*, 379–389. http://doi.org/10.1101/127365

Kasprian, G., Brugger, P. C., Weber, M., Krssák, M., Krampl, E., Herold, C., & Prayer, D. (2008). In utero tractography of fetal white matter development. *NeuroImage*, *43*(2), 213–224. http://doi.org/10.1016/j.neuroimage.2008.07.026

Kelly, C. E., Thompson, D. K., Chen, J., Leemans, A., Adamson, C. L., Inder, T. E., … Anderson, P. J. (2016). Axon density and axon orientation dispersion in children born preterm. *Human Brain Mapping*, *37*(9), 3080–3102. http://doi.org/10.1002/hbm.23227

Kersbergen, K. J., de Vries, L. S., Groenendaal, F., van Haastert, I. C., Chew, A. T. M., Makropoulos, A., … Counsell, S. J. (2015). Corticospinal tract injury precedes thalamic volume reduction in preterm infants with cystic periventricular leukomalacia. *The Journal of Pediatrics*, *167*(2), 260–268.e3. http://doi.org/10.1016/j.jpeds.2015.05.013

Kersbergen, K. J., Leemans, A., Groenendaal, F., van der Aa, N. E., Viergever, M. a., de Vries, L. S., & Benders, M. J. N. L. (2014). Microstructural brain development between 30 and 40 weeks corrected age in a longitudinal cohort of extremely preterm infants. *NeuroImage*, *103*, 214–224. http://doi.org/10.1016/j.neuroimage.2014.09.039

Kesler, S. R., Ment, L. R., Vohr, B., Pajot, S. K., Schneider, K. C., Katz, K. H., … Reiss, A. L. (2004). Volumetric analysis of regional cerebral development in preterm children. *Pediatric Neurology*, *31*(5), 318–325. http://doi.org/10.1016/j.pediatrneurol.2004.06.008

Keunen, K., Benders, M. J., Leemans, A., Fieret-Van Stam, P. C., Scholtens, L. H., Viergever, M. A., … van den Heuvel, M. P. (2017). White matter maturation in the neonatal brain is predictive of school age cognitive capacities in children born very preterm. *Developmental Medicine & Child Neurology*, *59*(9), 939–946. http://doi.org/10.1111/dmcn.13487

Kim, D. J., Davis, E. P., Sandman, C. A., Sporns, O., O'Donnell, B. F., Buss, C., & Hetrick, W. P. (2014). Longer gestation is associated with more efficient brain networks in preadolescent children. *NeuroImage*, *100*, 619–627. http://doi.org/10.1016/j.neuroimage.2014.06.048

Kinney, H. C., Brody, B., Kloman, A., & Gilles, F. (1988). Sequnce of Central Nervous System Myelination in Human Infancy. II Patterns of Myelination in Autopsied Infants. *Journal of Neuropathology and Experimental Neurology*, *47*(3), 217–234.

Knickmeyer, R. C., Gouttard, S., Kang, C., Evans, D., Wilber, K., Smith, J. K., … Gilmore, J. H. (2008). A structural MRI study of human brain development from birth to 2 years. *The Journal of Neuroscience : The Official Journal of the Society for Neuroscience*, *28*(47), 12176–82. http://doi.org/10.1523/JNEUROSCI.3479-08.2008

Korzeniewski, S. J., Romero, R., Cortez, J., Pappas, A., Schwartz, A. G., Kim, C. J., … Hassan, S. S. (2014). A "multi-hit" model of neonatal white matter injury: Cumulative contributions of chronic placental inflammation, acute fetal inflammation and postnatal inflammatory events. *Journal of Perinatal Medicine*, *42*(6), 731–743. http://doi.org/10.1515/jpm-2014-0250

Kostović, I., & Jovanov-Milosević, N. (2006). The development of cerebral connections during the first 20-45 weeks' gestation. *Seminars in Fetal & Neonatal Medicine*, *11*(6), 415–422. http://doi.org/10.1016/j.siny.2006.07.001

Kostović, I., & Judas, M. (2002). Correlation between the sequential ingrowth of afferents and transient patterns of cortical lamination in preterm infants. *The Anatomical Record*, *267*(1),

1–6. http://doi.org/10.1002/ar.10069

Kostović, I., & Judas, M. (2007). Transient patterns of cortical lamination during prenatal life: do they have implications for treatment? *Neuroscience and Biobehavioral Reviews*, *31*(8), 1157–68. http://doi.org/10.1016/j.neubiorev.2007.04.018

Kostovic, I., Kostovic-Srzentic, Benjak, V., Jovanovov-Milosevic, N., & Radoš, M. (2014). Developmental dynamics of radial vulnerability in the cerebral compartments in preterm infants and neonates. *Frontiers in Neurology*, *5*, 139. http://doi.org/10.3389/fneur.2014.00139

Kostovic, I., & Vasung, L. (2009). Insights From In Vitro Fetal Magnetic Resonance Imaging of Cerebral Development. *Seminars in Perinatology*, *33*(4), 220–233. http://doi.org/10.1053/j.semperi.2009.04.003

Kramer, M. S., Goulet, L., Lydon, J., Séguin, L., McNamara, H., Dassa, C., … Koren, G. (2001). Socio-economic disparities in preterm birth: causal pathways and mechanisms. *Paediatric and Perinatal Epidemiology*, *15*(Suppl 2), 104–123. http://doi.org/10.1046/j.1365-3016.2001.00012.x

Krogsrud, S. K., Fjell, A. M., Tamnes, C. K., Grydeland, H., Mork, L., Due-tønnessen, P., … Walhovd, K. B. (2016). Changes in white matter microstructure in the developing brain — A longitudinal diffusion tensor imaging study of children from 4 to 11 years of age. *NeuroImage*, *124*, 473–486. http://doi.org/10.1016/j.neuroimage.2015.09.017

Krsnik, Ž., Majić, V., Vasung, L., Huang, H., & Kostović, I. (2017). Growth of Thalamocortical Fibers to the Somatosensory Cortex in the Human Fetal Brain. *Frontiers in Neuroscience*, *11*(233), 1–17. http://doi.org/10.3389/fnins.2017.00233

Kuklisova-Murgasova, M., Aljabar, P., Srinivasan, L., Counsell, S. J., Doria, V., Serag, A., … Rueckert, D. (2011). A dynamic 4D probabilistic atlas of the developing brain. *NeuroImage*, *54*(4), 2750–2763. http://doi.org/10.1016/j.neuroimage.2010.10.019

Laugier, O., Garcia, P., Boucékine, M., Daguzan, A., Tardieu, S., Sambuc, R., & Boubred, F. (2017). Influence of Socioeconomic Context on the Rehospitalization Rates of Infants Born

Preterm. *The Journal of Pediatrics*, *190*, 174–179.e.1. http://doi.org/10.1016/j.jpeds.2017.08.001

Lebel, C., & Deoni, S. (2018). The development of brain white matter microstructure. *NeuroImage*, *S1053-8119*(17), 31121–7. http://doi.org/10.1016/j.neuroimage.2017.12.097

Leijser, L. M., Miller, S. P., van Wezel-Meijler, G., Brouwer, A. J., Traubici, J., van Haastert, I. C., … de Vries, L. S. (2018). Posthemorrhagic ventricular dilatation in preterm infants. *Neurology*, *90*(8), e698–e706. http://doi.org/10.1212/WNL.0000000000004984

Lerch, J. P., Sled, J. G., & Henkelman, R. M. (2011). MRI Phenotyping of Genetically Altered Mice. *Methods in Molecular BIology*, *711*(1), 349–361. http://doi.org/10.1007/978-1-61737-992-5

Li, K., Sun, Z., Han, Y., Gao, L., Yuan, L., & Zeng, D. (2015). Fractional anisotropy alterations in individuals born preterm: a diffusion tensor imaging meta-analysis. *Developmental Medicine & Child Neurology*, *57*, 328–338. http://doi.org/10.1111/dmcn.12618

Limperopoulos, C. (2005). Impaired Trophic Interactions Between the Cerebellum and the Cerebrum Among Preterm Infants. *Pediatrics*, *116*(4), 844–850. http://doi.org/10.1542/peds.2004-2282

Lind, A., Parkkola, R., Lehtonen, L., Munck, P., Maunu, J., Lapinleimu, H., & Haataja, L. (2011). Associations between regional brain volumes at term-equivalent age and development at 2 years of age in preterm children. *Pediatric Radiology*, *41*(8), 953–961. http://doi.org/10.1007/s00247-011-2071-x

Linsell, L., Malouf, R., Morris, J., Kurinczuk, J. J., & Marlow, N. (2015). Prognostic Factors for Poor Cognitive Development in Children Born Very Preterm or With Very Low Birth Weight: A Systematic Review. *JAMA Pediatrics*, *169*(10), 1–11. http://doi.org/10.1001/jamapediatrics.2015.2175

Liu, Y., Aeby, A., Balériaux, D., David, P., Absil, J., De Maertelaer, V., … Metens, T. (2012). White matter abnormalities are related to microstructural changes in preterm neonates at term-equivalent age: a diffusion tensor imaging and probabilistic tractography study. *AJNR.*

American Journal of Neuroradiology, *33*(5), 839–45. http://doi.org/10.3174/ajnr.A2872

Loe, I. M., Lee, E. S., & Feldman, H. M. (2013). Attention and Internalizing Behaviors in Relation to White Matter in Children Born Preterm. *Journal of Developmental and Behavioral Pediatrics : JDBP*, *34*(3), 156–164. http://doi.org/10.1016/j.biotechadv.2011.08.021.Secreted

Mah, A., Geeraert, B., & Lebel, C. (2017). Detailing neuroanatomical development in late childhood and early adolescence using NODDI. *PLoS ONE*, *12*(8), e0182340.

Malavolti, A. M., Chau, V., Brown-Lum, M., Poskitt, K. J., Brant, R., Synnes, A., … Miller, S. P. (2017). Association between corpus callosum development on magnetic resonance imaging and diffusion tensor imaging, and neurodevelopmental outcome in neonates born very preterm. *Developmental Medicine and Child Neurology*, *59*(4), 433–440. http://doi.org/10.1111/dmcn.13364

Mangin, K. S., Horwood, L. J., & Woodward, L. J. (2017). Cognitive Development Trajectories of Very Preterm and Typically Developing Children. *Child Development*, *88*(1), 282–298. http://doi.org/10.1111/cdev.12585

Marin-Padilla, M. (1970). Prenatal and early postnatal ontogenesis of the human motor cortex: A Golgi study. I. The sequential development of the cortical layers. *Brain Research*, *23*(2), 167–183. http://doi.org/10.1016/0006-8993(70)90037-5

Maritz, J. (1985). Models and the use of signed rank tests. *Statistics in Medicine*, *4*(2), 145–153.

Marlow, N. (2004). Neurocognitive outcome after very preterm birth. *Archives of Disease in Childhood. Fetal and Neonatal Edition*, *89*, F224–F228. http://doi.org/10.1136/adc.2003.019752

Mcclendon, E., Ph, D., Chen, K., Gong, X., Sharifnia, E., Hagen, M., … Ph, D. (2014). Prenatal cerebral ischemia triggers dysmaturation of caudate projection neurons. *Annals of Neurology*, *75*(4), 508–524. http://doi.org/10.1002/ana.24100.Prenatal

McCormick, M. C. (1985). The Contribution of Low Birth Weight to Infant Mortality and Childhood Morbidity. *New England Journal of Medicine*, *312*, 82–90.

McDonald, S. D., Han, Z., Mulla, S., & Beyene, J. (2010). Overweight and obesity in mothers and risk of preterm birth and low birth weight infants: systematic review and meta-analyses. *Bmj*, *341*, c3428. http://doi.org/10.1136/bmj.c3428

McIntosh, A. R., & Mišić, B. (2013). Multivariate statistical analyses for neuroimaging data. *Annual Review of Psychology*, *64*, 499–525. http://doi.org/10.1146/annurev-psych-113011-143804

McLoyd, V. C. (1998). Socioeconomic Disadvantage and Child Development. *American Psychologist*, *53*(2), 185–204. http://doi.org/10.1037/0003-066X.53.2.185

Ment, L. R., Kesler, S., Vohr, B., Katz, K. H., Baumgartner, H., Schneider, K. C., … Reiss, A. L. (2009). Longitudinal brain volume changes in preterm and term control subjects during late childhood and adolescence. *Pediatrics*, *123*(2), 503–11. http://doi.org/10.1542/peds.2008-0025

Mento, G., & Nosarti, C. (2015). The case of late preterm birth: Sliding forwards the critical window for cognitive outcome risk. *Translational Pediatrics*, *4*(3), 214–218. http://doi.org/10.3978/j.issn.2224-4336.2015.06.02

Mewes, A. U., Huppi, P. S., Als, H., Rybicki, F. J., Inder, T., McAnulty, G. B., … Warfield, S. K. (2006). Regional brain development in serial magnetic resonance imaging of low-risk preterm infants. *Pediatrics*, *118*, 23–33.

Miller, S. P., Cozzio, C. C., Goldstein, R. B., Ferriero, D. M., Partridge, J. C., Vigneron, D. B., & Barkovich, A. J. (2003). Comparing the diagnosis of white matter injury in premature newborns with serial MR imaging and transfontanel ultrasonography findings. *American Journal of Neuroradiology*, *24*(8), 1661–1669. Retrieved from http://www.ncbi.nlm.nih.gov/pubmed/13679289

Miller, S. P., Ferriero, D. M., Leonard, C., Piecuch, R., Glidden, D. V, Partridge, J. C., … Barkovich, A. J. (2005). Early brain injury in premature newborns detected with magnetic resonance imaging is associated with adverse early neurodevelopmental outcome. *Journal of Pediatrics*, *147*(5), 609–16.

Monson, B. B., Anderson, P. J., Matthews, L. G., Neil, J. J., Kapur, K., Cheong, J. L. Y., … Inder, T. E. (2016). Examination of the pattern of growth of cerebral tissue volumes from hospital discharge to early childhood in very preterm infants. *JAMA Pediatrics*, *170*(8), 772–779. http://doi.org/10.1001/jamapediatrics.2016.0781

Mori, S., Crain, B. J., Chacko, V. P., & Van Zijl, P. C. M. (1999). Three-dimensional tracking of axonal projections in the brain by magnetic resonance imaging. *Annals of Neurology*, *45*(2), 265–269. http://doi.org/10.1002/1531-8249

Mori, S., Wakana, S., Van Zijl, P. C. M., & Nagai-Poetscher, L. M. (2005). *MRI Atlas of Human White Matter*. Amsterdam, The Netherlands: Elsevier.

Morita, T., Morimoto, M., Yamada, K., Hasegawa, T., Morioka, S., Kidowaki, S., … Hosoi, H. (2015). Low-grade intraventricular hemorrhage disrupts cerebellar white matter in preterm infants: evidence from diffusion tensor imaging. *Neuroradiology*, *57*(5), 507–514. http://doi.org/10.1007/s00234-015-1487-7

Moseley, M., Cohen, Y., Kucharczyk, J., Mintorovitch, J., Asgari, H., Wendland, M., … Norman, D. (1990). Diffusion-weighted MR imaging of anisotropic water diffusion in cat central nervous system. *Radiology*, *176*(2), 469–45.

Muglia, L. J., & Katz, M. (2010). The enigma of spontaneous preterm birth. *The New England Journal of Medicine*, *362*(6), 529–535. http://doi.org/10.1056/NEJMra0904308

Mukerji, A., Shah, V., & Shah, P. S. (2015). Periventricular/Intraventricular Hemorrhage and Neurodevelopmental Outcomes: A Meta-analysis. *Pediatrics*, *136*(6), 1132–1143. http://doi.org/10.1542/peds.2015-0944

Mullen, K. M., Vohr, B. R., Katz, K. H., Schneider, K. C., Lacadie, C., Hampson, M., … Ment, L. R. (2012). Preterm Birth Results in Alterations in Neural Connectivity at Age 16 Years. *NeuroImage*, *54*(4), 2563–2570. http://doi.org/10.1016/j.neuroimage.2010.11.019.Preterm

Mürner-Lavanchy, I., Steinlin, M., Nelle, M., Rummel, C., Perrig, W. J., Schroth, G., & Everts, R. (2014). Delay of cortical thinning in very preterm born children. *Early Human Development*, *90*(9), 443–450. http://doi.org/10.1016/j.earlhumdev.2014.05.013

Murphy, B. P., Inder, T. E., Rooks, V., Taylor, G. A., Anderson, N. J., Mogridge, N., … Volpe, J. J. (2002). Posthaemorrhagic ventricular dilatation in the premature infant: natural history and predictors of outcome. *Arch Dis Child Fetal Neonatal Ed*, *87*(1), F37-41. http://doi.org/10.1136/fn.87.1.F37

Nagy, Z., Ashburner, J., Andersson, J., Jbabdi, S., Draganski, B., Skare, S., … Lagercrantz, H. (2009). Structural Correlates of Preterm Birth in the Adolescent Brain. *Pediatrics*, *124*(5), e964–e972. http://doi.org/10.1542/peds.2008-3801

Nagy, Z., Westerberg, H., Skare, S., Andersson, J. L., Lilja, A., Flodmark, O., … Klingberg, T. (2003). Preterm Children Have Disturbances of White Matter at 11 Years of Age as Shown by Diffusion Tensor Imaging. *Pediatric Research*, *54*(5), 672–679. http://doi.org/10.1203/01.PDR.0000084083.71422.16

Nam, K. W., Castellanos, N., Simmons, A., Froudist-Walsh, S., Allin, M. P., Walshe, M., … Nosarti, C. (2015). Alterations in cortical thickness development in preterm-born individuals: Implications for high-order cognitive functions. *NeuroImage*, *115*, 64–75. http://doi.org/10.1016/j.neuroimage.2015.04.015

Nosarti, C., Rushe, T. M., Woodruff, P. W. R., Stewart, A. L., Rifkin, L., & Murray, R. M. (2004). Corpus callosum size and very preterm birth: Relationship to neuropsychological outcome. *Brain*, *127*(9), 2080–2089. http://doi.org/10.1093/brain/awh230

Nossin-Manor, R., Card, D., Morris, D., Noormohamed, S., Shroff, M. M., Whyte, H. E. A., … Sled, J. G. (2013). Quantitative MRI in the very preterm brain: Assessing tissue organization and myelination using magnetization transfer, diffusion tensor and T1 imaging. *NeuroImage*, (64), 505–516.

Nossin-Manor, R., Card, D., Raybaud, C., Taylor, M. J., & Sled, J. G. (2015). Cerebral maturation in the early preterm period—A magnetization transfer and diffusion tensor imaging study using voxel-based analysis. *NeuroImage*, *112*, 30–42. http://doi.org/10.1016/j.neuroimage.2015.02.051

Oishi, K., Mori, S., Donohue, P. K., Ernst, T., Anderson, L., Buchthal, S., … Chang, L. (2011). Multi-contrast human neonatal brain atlas: Application to normal neonate development

analysis. *Neuroimage*, *56*(1), 8–20. http://doi.org/10.1016/j.neuroimage.2011.01.051.Multi-Contrast

Oudgenoeg-Paz, O., Mulder, H., Jongmans, M. J., van der Ham, I. J. M., & Van der Stigchel, S. (2017). The link between motor and cognitive development in children born preterm and/or with low birth weight: A review of current evidence. *Neuroscience & Biobehavioral Reviews*, *80*(May), 382–393. http://doi.org/10.1016/j.neubiorev.2017.06.009

Pandit, A. S., Robinson, E., Aljabar, P., Ball, G., Gousias, I. S., Wang, Z., … Edwards, A. D. (2014). Whole-brain mapping of structural connectivity in infants reveals altered connection strength associated with growth and preterm birth. *Cerebral Cortex*, *24*(9), 2324–2333. http://doi.org/10.1093/cercor/bht086

Pannek, K., Fripp, J., George, J. M., Fiori, S., Colditz, P. B., Boyd, R. N., & Rose, S. E. (2018). Fixel-based analysis reveals alterations is brain microstructure and macrostructure of preterm-born infants at term equivalent age. *NeuroImage: Clinical*, *18*, 51–59. http://doi.org/10.1016/j.nicl.2018.01.003

Pannek, K., Scheck, S. M., Colditz, P. B., Boyd, R. N., & Rose, S. E. (2014). Magnetic resonance diffusion tractography of the preterm infant brain: A systematic review. *Developmental Medicine and Child Neurology*, *56*(2), 113–124. http://doi.org/10.1111/dmcn.12250

Papile, L. A., Burstein, J., Burstein, R., & Koffler, H. (1978). Incidence and evolution of subependymal and intraventricular hemorrhage: a study of infants with birth weights less than 1,500 gm. *The Journal of Pediatrics*, *92*(4), 529–534. http://doi.org/10.1016/S0022-3476(78)80282-0

Pappas, A., Adams-Chapman, I., Shankaran, S., McDonald, S. A., Stoll, B. J., Laptook, A. R., … Higgins, R. D. (2018). Neurodevelopmental and Behavioral Outcomes in Extremely Premature Neonates With Ventriculomegaly in the Absence of Periventricular-Intraventricular Hemorrhage. *JAMA Pediatrics*, *172*(1), 32–42. http://doi.org/10.1001/jamapediatrics.2017.3545

Partridge, S. C., Mukherjee, P., Henry, R. G., Miller, S. P., Berman, J. I., Jin, H., … Vigneron,

D. B. (2004). Diffusion tensor imaging: serial quantitation of white matter tract maturity in premature newborns. *NeuroImage*, *22*(3), 1302–14. http://doi.org/10.1016/j.neuroimage.2004.02.038

Paus, T., Collins, D. L., Evans, A. C., Leonard, G., Pike, B., & Zijdenbos, A. (2001). Maturation of white matter in the human brain : A review of magnetic resonance studies. *Brain Research Bulletin*, *54*(3), 255–266.

Pavaine, J., Young, J. M., Morgan, B. R., Shroff, M., Raybaud, C., & Taylor, M. J. (2016). Diffusion tensor imaging-based assessment of white matter tracts and visual-motor outcomes in very preterm neonates. *Neuroradiology*. 58(3), 301-310. http://doi.org/10.1007/s00234-015-1625-2

Peterson, B. S., Vohr, B., Staib, L. H., Cannistraci, C. J., Dolberg, A., Schneider, K. C., … Ment, L. R. (2000). Regional brain volume abnormalities and long-term cognitive outcome in preterm infants. *JAMA: Journal of the American Medical Association*, *284*(15), 1939–1947. Retrieved from http://www.ncbi.nlm.nih.gov/pubmed/11035890

Piek, J. P., Dawson, L., Smith, L. M., & Gasson, N. (2008). The role of early fine and gross motor development on later motor and cognitive ability. *Human Movement Science*, *27*(5), 668–681. http://doi.org/10.1016/j.humov.2007.11.002

Pierrat, V., Marchand-Martin, L., Arnaud, C., Kaminski, M., Resche-Rigon, M., Lebeaux, C., … Ancel, P.-Y. (2017). Neurodevelopmental outcome at 2 years for preterm children born at 22 to 34 weeks' gestation in France in 2011: EPIPAGE-2 cohort study. *BMJ*, *358*, j3448. http://doi.org/10.1136/bmj.j3448

Piper, M. C., Byrne, P. J., Darrah, J., & Watt, M. J. (1989). Gross and fine motor development of preterm infants at eight and 12 months age. *Developmental Medicine & Child Neurology*, *31*, 591–597.

Public Health Agency of Canada. (2008). *Canadian Perinatal Health Report*.

Public Health Agency of Canada. (2017). *Perinatal Health Indicators for Canada 2017*.

Purisch, S. E., & Gyamfi-Bannerman, C. (2017). Epidemiology of preterm birth. *Seminars in*

Perinatology, *41*(7), 387–391. http://doi.org/10.1053/j.semperi.2017.07.009

Putnick, D. L., Bornstein, M. H., Eryigit-Madzwamuse, S., & Wolke, D. (2017). Long-Term Stability of Language Performance in Very Preterm, Moderate-Late Preterm, and Term Children. *The Journal of Pediatrics*, *181*, 74–79e3. http://doi.org/10.1016/j.jpeds.2016.09.006

Qiu, A., Mori, S., & Miller, M. I. (2015). Diffusion tensor imaging for understanding brain development in early life. *Annual Review of Psychology*, *66*(1), 853–876. http://doi.org/10.1146/annurev-psych-010814-015340

Rae, C. L., Davies, G., Garfinkel, S. N., Gabel, M. C., Dowell, N. G., Cercignani, M., … Critchley, H. D. (2017). Deficits in Neurite Density Underlie White Matter Structure Abnormalities in First-Episode Psychosis. *Biological Psychiatry*, *82*(10), 716–725. http://doi.org/10.1016/j.biopsych.2017.02.008

Raffelt, D. A., Tournier, J. D., Smith, R. E., Vaughan, D. N., Jackson, G., Ridgway, G. R., & Connelly, A. (2017). Investigating white matter fibre density and morphology using fixel-based analysis. *NeuroImage*, *144*, 58–73. http://doi.org/10.1016/j.neuroimage.2016.09.029

Rakic, P. (1988). Specification of cerebral cortical areas. *Science*, *241*(4862), 170–176. Retrieved from http://www.ncbi.nlm.nih.gov/pubmed/3291116

Ratnarajah, N., Rifkin-graboi, A., Fortier, M. V, Seng, Y., Kwek, K., Saw, S., … Qiu, A. (2013). NeuroImage Structural connectivity asymmetry in the neonatal brain. *NeuroImage*, *75*, 187–194. http://doi.org/10.1016/j.neuroimage.2013.02.052

Raybaud, C., Ahmad, T., Rastegar, N., Shroff, M., & Al Nassar, M. (2013). The premature brain: Developmental and lesional anatomy. *Neuroradiology*, *55*(Suppl 2), S23–S40. http://doi.org/10.1007/s00234-013-1231-0

Reidy, N., Morgan, A., Thompson, D. K., Inder, T. E., Doyle, L. W., & Anderson, P. J. (2013). Impaired Language Abilities and White Matter Abnormalities in Children Born Very Preterm and/or Very Low Birth Weight. *The Journal of Pediatrics*, *162*(4), 719–24. http://doi.org/10.1016/j.jpeds.2012.10.017

Reubsaet, P., Brouwer, A. J., van Haastert, I. C., Brouwer, M. J., Koopman, C., Groenendaal, F., & de Vries, L. S. (2017). The Impact of Low-Grade Germinal Matrix-Intraventricular Hemorrhage on Neurodevelopmental Outcome of Very Preterm Infants. *Neonatology*, *112*(3), 203–210. http://doi.org/10.1159/000472246

Rogers, C. E., Anderson, P. J., Thompson, D. K., Kidokoro, H., Wallendorf, M., Treyvaud, K., … Inder, Terrie, E. (2013). Regional Cerebral Development at Term Relates to School-Age Social-Emotional Development in Very Preterm Children. *Journal of the American Academy of Child & Adolescent Psychiatry*, *51*(2), 181–191. http://doi.org/10.1016/j.jaac.2011.11.009.Regional

Romero, R., Dey, S. K., & FIsher, S. J. (2015). Preterm Labor: One Syndrome, Many Causes. *Science*, *345*(6198), 760–765. http://doi.org/10.1126/science.1251816.Preterm

Rose, S. E., Hatzigeorgiou, X., Strudwick, M. W., Durbridge, G., Davies, P. S. W., & Colditz, P. B. (2008). Altered white matter diffusion anisotropy in normal and preterm infants at term-equivalent age. *Magnetic Resonance in Medicine*, *60*(4), 761–767. http://doi.org/10.1002/mrm.21689

Roze, E., Benders, M. J., Kersbergen, K. J., van der Aa, N. E., Groenendaal, F., van Haastert, I. C., … de Vries, L. S. (2015). Neonatal DTI early after birth predicts motor outcome in preterm infants with periventricular hemorrhagic infarction. *Pediatric Research*, *78*(3), 298–303. http://doi.org/10.1038/pr.2015.94

Rubinov, M., & Sporns, O. (2010). Complex network measures of brain connectivity: Uses and interpretations. *NeuroImage*, *52*(3), 1059–1069. http://doi.org/10.1016/j.neuroimage.2009.10.003

Sadeghi, N., Prastawa, M., Fletcher, P. T., Wolff, J., Gilmore, J. H., & Gerig, G. (2013). Regional characterization of longitudinal DT-MRI to study white matter maturation of the early developing brain. *NeuroImage*, *68*, 236–247. http://doi.org/10.1016/j.neuroimage.2012.11.040

Saigal, S., & Doyle, L. W. (2008). An overview of mortality and sequelae of preterm birth from infancy to adulthood. *Lancet*, *371*, 261–69. http://doi.org/10.1016/S0140-6736(08)60136-1

Salvan, P., Tournier, J. D., Batalle, D., Falconer, S., Chew, A., Kennea, N., … Counsell, S. J. (2017). Language ability in preterm children is associated with arcuate fasciculi microstructure at term. *Human Brain Mapping*, *38*(8), 3836–3847. http://doi.org/10.1002/hbm.23632

Schafer, R. J., Lacadie, C., Vohr, B., Kesler, S. R., Katz, K. H., Schneider, K. C., … Ment, L. R. (2009). Alterations in functional connectivity for language in prematurely born adolescents. *Brain*, *132*, 661–670. http://doi.org/10.1093/brain/awn353

Schneider, J., Duerden, E. G., Guo, T., Ng, K., Hagmann, P., Graz, M. B., … Miller, S. P. (2017). Procedural Pain and Oral Glucose in Preterm Neonates. *Pain*, *159*(3), 515–525. http://doi.org/10.1097/j.pain.0000000000001123

Schneider, J., Fischer Fumeaux, C. J., Duerden, E. G., Guo, T., Foong, J., Graz, M. B., … Miller, S. P. (2018). Nutrient Intake in the First Two Weeks of Life and Brain Growth in Preterm Neonates. *Pediatrics*, *141*(3), e20172169. http://doi.org/10.1542/peds.2017-2169

Semel, E., Wiig, E., & Secord, W. (2004). *Clinical Evaluation of Language Fundamentals-Preschool* (2nd Editio). San Antonio, TX: The Psychological Corporation.

Shim, S.-Y., Jeong, H.-J., Son, D. W., Chung, M., Park, S., & Cho, Z.-H. (2014). Serial diffusion tensor images during infancy and their relationship to neuromotor outcomes in preterm infants. *Neonatology*, *106*(4), 348–54. http://doi.org/10.1159/000363218

Simmons, L. E., Rubens, C. E., Darmstadt, G. L., & Gravett, M. G. (2010). Preventing Preterm Birth and Neonatal Mortality: Exploring the Epidemiology, Causes, and Interventions. *Seminars in Perinatology*, *34*(6), 408–415. http://doi.org/10.1053/j.semperi.2010.09.005

Smith, S. M., Jenkinson, M., Johansen-Berg, H., Rueckert, D., Nichols, T. E., Mackay, C. E., … Behrens, T. E. J. (2006). Tract-based spatial statistics: Voxelwise analysis of multi-subject diffusion data. *NeuroImage*, *31*(4), 1487–1505. http://doi.org/10.1016/j.neuroimage.2006.02.024

Smith, S. M., & Nichols, T. E. (2009). Threshold-free cluster enhancement: Addressing problems of smoothing, threshold dependence and localisation in cluster inference.

NeuroImage, *44*(1), 83–98. http://doi.org/10.1016/j.neuroimage.2008.03.061

Soares, J. M., Marques, P., Alves, V., & Sousa, N. (2013). A hitchhiker's guide to diffusion tensor imaging. *Frontiers in Neuroscience*, *7*(31), 1–14. http://doi.org/10.3389/fnins.2013.00031

Song, S. K., Yoshino, J., Le, T. Q., Lin, S. J., Sun, S. W., Cross, A. H., & Armstrong, R. C. (2005). Demyelination increases radial diffusivity in corpus callosum of mouse brain. *NeuroImage*, *26*(1), 132–140. http://doi.org/10.1016/j.neuroimage.2005.01.028

Song, S., Sun, S., Ju, W., Lin, S., Cross, A. H., & Neufeld, A. H. (2003). Diffusion tensor imaging detects and differentiates axon and myelin degeneration in mouse optic nerve after retinal ischemia, *20*, 1714–1722. http://doi.org/10.1016/j.neuroimage.2003.07.005

Spittle, A., Orton, J., Anderson, P., Boyd, R., & Doyle, L. W. (2012). Early developmental intervention programmes post-hospital discharge to prevent motor and cognitive impairments in preterm infants. *Cochrane Database of Systematic Reviews*, (11). http://doi.org/10.1002/14651858.CD005495.pub3

Staneva, A., Bogossian, F., Pritchard, M., & Wittkowski, A. (2015). The effects of maternal depression, anxiety, and perceived stress during pregnancy on preterm birth: A systematic review. *Women and Birth*, *28*(3), 179–193. http://doi.org/10.1016/j.wombi.2015.02.003

Stiles, J., & Jernigan, T. L. (2010). The basics of brain development. *Neuropsychology Review*, *20*(4), 327–348. http://doi.org/10.1007/s11065-010-9148-4

Synnes, A., Luu, T. M., Moddemann, D., Church, P., Lee, D., Vincer, M., … Lee, S. K. (2017). Determinants of developmental outcomes in a very preterm Canadian cohort. *Archives of Disease in Childhood - Fetal and Neonatal Edition*, *102*(3), F235–F234. http://doi.org/10.1136/archdischild-2016-311228

Tam, E. W. Y., Miller, S. P., Studholme, C., Chau, V., Glidden, D., Poskitt, K. J., … Barkovich, A. J. (2011). Differential effects of intraventricular hemorrhage and white matter injury on preterm cerebellar growth. *Journal of Pediatrics*, *158*(3), 366–371. http://doi.org/10.1016/j.jpeds.2010.09.005

Tamnes, C. K., Ostby, Y., Walhovd, K. B., Westlye, L. T., Due-Tonnessen, P., & Fjell, A. M. (2010). Intellectual abilities and white matter microstructure in development: A diffusion tensor imaging study. *Human Brain Mapping*, *31*(10), 1609–1625. http://doi.org/10.1002/hbm.20962

Tamnes, C. K., Roalf, D. R., Goddings, A.-L., & Lebel, C. (2017). Diffusion MRI of white matter microstructure development in childhood and adolescence: Methods, challenges and progress. *Developmental Cognitive Neuroscience*, *S1878-9293*(17), 30008–7. http://doi.org/10.1016/j.dcn.2017.12.002

Thomason, M. E., Scheinost, D., Manning, J. H., Grove, L. E., Hect, J., Marshall, N., … Romero, R. (2017). Weak functional connectivity in the human fetal brain prior to preterm birth. *Scientific Reports*, *7*, 1–10. http://doi.org/10.1038/srep39286

Thompson, D. K., Chen, J., Beare, R., Adamson, C. L., Ellis, R., Ahmadzai, Z. M., … Anderson, P. J. (2016). Structural connectivity relates to perinatal factors and functional impairment at 7 years in children born very preterm. *NeuroImage*, *134*, 328–337. http://doi.org/10.1016/j.neuroimage.2016.03.070

Thomsen, C. (1987). From the Department of Magnetic Resonance and the Department of Clinical Physiology in Vivo Measurement of Water Self Diffusion in. *Acta Radiologica*, *28*, 353–361.

Timmers, I., Roebroeck, A., Bastiani, M., Jansma, B., Rubio-Gozalbo, E., & Zhang, H. (2016). Assessing microstructural substrates of white matter abnormalities: A Comparative study using DTI and NODDI. *PLoS ONE*, *11*(12), e0167884. http://doi.org/10.1371/journal.pone.0167884

Travis, K. E., Adams, J. N., Ben-Shachar, M., & Feldman, H. M. (2015a). Decreased and Increased Anisotropy along Major Cerebral White Matter Tracts in Preterm Children and Adolescents. *Plos One*, *10*(11), e0142860. http://doi.org/10.1371/journal.pone.0142860

Travis, K. E., Adams, J. N., Ben-Shachar, M., & Feldman, H. M. (2015b). Decreased and Increased Anisotropy along Major Cerebral White Matter Tracts in Preterm Children and Adolescents. *Plos One*, *10*(11), e0142860. http://doi.org/10.1371/journal.pone.0142860

Travis, K. E., Adams, J. N., Kovachy, V. N., Ben-Shachar, M., & Feldman, H. M. (2016). White matter properties differ in 6-year old Readers and Pre-readers. *Brain Structure and Function*, *222*(4), 1–19. http://doi.org/10.1007/s00429-016-1302-1

Tyson, J. E., Parikh, N. A., Langer, J., Green, C., & Higgins, R. D. (2008). Intensive Care for Extreme Prematurity - Moving Beyong Gestational Age. *New England Journal of Medicine*, *358*(16), 1672–1681. http://doi.org/10.1016/j.biotechadv.2011.08.021

Ullman, H., Spencer-Smith, M., Thompson, D. K., Doyle, L. W., Inder, T. E., Anderson, P. J., & Klingberg, T. (2015). Neonatal MRI is associated with future cognition and academic achievement in preterm children. *Brain*, *138*(11), 3251–62. http://doi.org/10.1093/brain/awv244

Van Baar, A. L., Ultee, K., Gunning, W. B., Soepatmi, S., & De Leeuw, R. (2006). Developmental course of very preterm children in relation to school outcome. *Journal of Developmental and Physical Disabilities*, *18*(3), 273–293. http://doi.org/10.1007/s10882-006-9016-6

van den Heuvel, M. P., Kersbergen, K. J., de Reus, M. A., Keunen, K., Kahn, R. S., Groenendaal, F., … Benders, M. J. N. L. (2015). The Neonatal Connectome During Preterm Brain Development. *Cerebral Cortex*, *25*(9), 3000–3013. http://doi.org/10.1093/cercor/bhu095

van der Knaap, M. S., Valk, J., Bakker, C. J., Schooneveld, M., Faber, J. A. J., Willemse, J., & Gooskens, R. H. J. M. (1991). Myelination As an Expression of the Functional Maturity of the Brain. *Developmental Medicine & Child Neurology*, *33*(10), 849–857. http://doi.org/10.1111/j.1469-8749.1991.tb14793.x

van Kooij, B. J. M., de Vries, L. S., Ball, G., van Haastert, I. C., Benders, M. J. N. L., Groenendaal, F., & Counsell, S. J. (2012). Neonatal tract-based spatial statistics findings and outcome in preterm infants. *AJNR. American Journal of Neuroradiology*, *33*(1), 188–94. http://doi.org/10.3174/ajnr.A2723

van Noort-van der Spek, I. L., Franken, M.-C. J. P., & Weisglas-Kuperus, N. (2012). Language Functions in Preterm-Born Children: A Systematic Review and Meta-analysis. *Pediatrics*,

129(4), 745–754. http://doi.org/10.1542/peds.2011-1728

Vangberg, T. R., Skranes, J., Dale, A. M., Martinussen, M., Brubakk, A. M., & Haraldseth, O. (2006). Changes in white matter diffusion anisotropy in adolescents born prematurely. *NeuroImage*, *32*(4), 1538–1548. http://doi.org/10.1016/j.neuroimage.2006.04.230

Volpe, J. J. (2008). Intracranial hemorrhage: Germinal matrix- intraventricular hemorrhage of the premature infant. In *Neurology of the Newborn* (Fifth Edit, pp. 517–588). Philadelphia, USA: Saunders.

Volpe, J. J. (2009). Brain injury in premature infants: a complex amalgam of destructive and developmental disturbances. *Lancet Neurology*, *8*(1), 110–124. http://doi.org/10.1016/S1474-4422(08)70294-1

Volpe, J. J. (2013). Cerebral White Matter Injury of the Premature Infant − More Common Than You Think. *Pediatrics*, *112*(1), 176–180.

Volpe, J. J. (2015). Impaired Neurodevelopmental Outcome After Mild Germinal Matrix-Intraventricular Hemorrhage. *Pediatrics*, *136*(6), 1185–1187. http://doi.org/10.1542/peds.2015-3553

Wang, R., Benner, T., Sorensen, A. G., & Wedeen, V. J. (2007). Diffusion Toolkit : A Software Package for Diffusion Imaging Data Processing and Tractography. *Proc. Intl. Soc. Mag. Reson. Med.*, *15*, 3720.

Wechsler, D. (1999). Wechsler Abbreviated Scales of Intelligence (WASI). *San Antonio, TX: The Psychological Corporation*.

Wechsler, D. (2002). *Wechsler Preschool and Primary Scales of Intelligence 3rd Edition* (3rd ed.). San Antonio, TX: The Psychological Corporation.

WHO. (1977). WHO: recommended definitions, terminology and format for statistical tables related to the perinatal period and use of a new certificate for cause of perinatal deaths. Modifications recommended by FIGO as amended October 14, 1976. *Acta Obstet Gynecol Scand*, (56), 247–253.

Wild, K. T., Betancourt, L. M., Brodsky, N. L., & Hurt, H. (2013). The effect of socioeconomic status on the language outcome of preterm infants at toddler age. *Early Human Development*, *89*(9), 743–746. http://doi.org/10.1016/j.earlhumdev.2013.05.008

Wolke, D., & Meyer, R. (1999). Cognitive status, language attainment, and prereading skills of 6-year-old very preterm children and their peers: the Bavarian Longitudinal Study. *Developmental Medicine and Child Neurology*, *41*(2), 94–109. Retrieved from http://www.ncbi.nlm.nih.gov/pubmed/10075095

Wong, H. S., Santhakumaran, S., Cowan, F. M., & Modi, N. (2016). Developmental Assessments in Preterm Children : A Meta-analysis. *Pediatrics*, *138*(2), 1–12. http://doi.org/10.1542/peds.2016-0251

Woodward, L. J., Moor, S., Hood, K. M., Champion, P. R., Foster-Cohen, S., Inder, T. E., & Austin, N. C. (2009). Very preterm children show impairments across multiple neurodevelopmental domains by age 4 years. *Archives of Disease in Childhood. Fetal and Neonatal Edition*, *94*(5), F339–F344. http://doi.org/10.1136/adc.2008.146282

Xia, M., Wang, J., & He, Y. (2013). BrainNet Viewer: A Network Visualization Tool for Human Brain Connectomics. *PLoS ONE*, *8*(7), e68910. http://doi.org/10.1371/journal.pone.0068910

Yap, P. T., Fan, Y., Chen, Y., Gilmore, J. H., Lin, W., & Shen, D. (2011). Development trends of white matter connectivity in the first years of life. *PLoS ONE*, *6*(9), e24678. http://doi.org/10.1371/journal.pone.0024678

Young, J. M., Morgan, B. R., Powell, T. L., Moore, A. M., Whyte, H. E. A., Smith, M. L., & Taylor, M. J. (2016). Associations of perinatal clinical and magnetic resonance imaging measures with developmental outcomes in children born very preterm. *The Journal of Pediatrics*, *170*, 90–96. http://doi.org/10.1016/j.jpeds.2015.11.044

Young, J. M., Morgan, B. R., Whyte, H. E. A., Lee, W., Smith, M. Lou, Raybaud, C., … Taylor, M. J. (2017). Longitudinal Study of White Matter Development and Outcomes in Children Born Very Preterm. *Cerebral Cortex*, *27*(8), 4094–4105. http://doi.org/10.1093/cercor/bhw221

Young, J. M., Powell, T. L., Morgan, B. R., Card, D., Lee, W., Smith, M. L., … Taylor, M. J. (2015). Deep grey matter growth predicts neurodevelopmental outcomes in very preterm children. *NeuroImage*, *111*, 360–368. http://doi.org/10.1016/j.neuroimage.2015.02.030

Young, J., Vandewouw, M., Morgan, B., Smith, M.L., Sled, J., & Taylor, M. (2018). Altered white matter development in children born very preterm. *Brain Structure and Function*, *223*(5), 2129–2141. http://doi.org/10.1007/s00429-018-1614-4

Zalesky, A., Fornito, A., & Bullmore, E. T. (2010). Network-based statistic: Identifying differences in brain networks. *NeuroImage*, *53*(4), 1197–1207. http://doi.org/10.1016/j.neuroimage.2010.06.041

Zhang, H., Schneider, T., Wheeler-Kingshott, C. A., & Alexander, D. C. (2012). NODDI: Practical in vivo neurite orientation dispersion and density imaging of the human brain. *NeuroImage*, *61*(4), 1000–1016. http://doi.org/10.1016/j.neuroimage.2012.03.072

Zubiaurre-Elorza, L., Soria-Pastor, S., Junqué, C., Fernandez-Espejo, D., Segarra, D., Bargalló, N., … Macaya, A. (2012). Thalamic changes in a preterm sample with periventricular leukomalacia: correlation with white-matter integrity and cognitive outcome at school age. *Pediatric Research*, *71*(4), 354–360. http://doi.org/10.1038/pr.2011.70

Appendix A

Figure A1. Flow chart of samples for each time point

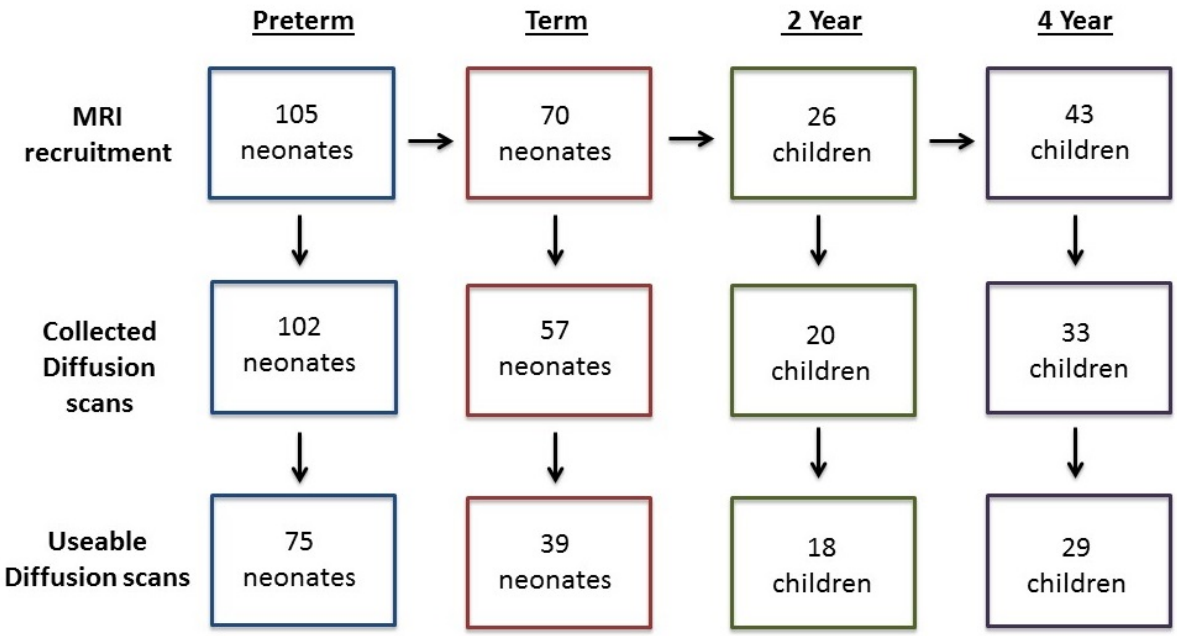

Table A1. Slopes of tracts by scan age

		CC	ALIC		PLIC		RIC		EC		ACR	
Metric	Time point		L	R	L	R	L	R	L	R	L	R
FA	1	0.0017457	0.0047809	0.0055562	0.0114212	0.0120973	0.0120588	0.0121494	0.0050122	0.0050396	0.0045053	0.0041362
	2	0.0027527	0.0016605	0.0018406	0.0012511	0.0012614	0.0007024	0.0009768	0.0011003	0.0010761	0.0018855	0.0021545
	3	0.0006222	0.0002591	0.0004849	-0.0001027	0.0004689	0.0000402	0.0003828	-0.0000865	-0.0000154	0.0003581	0.0004676
MD	1	0.0000026	-0.0000187	-0.0000231	-0.0000233	-0.0000230	-0.0000176	-0.0000146	-0.0000199	-0.0000206	-0.0000205	-0.0000220
	2	-0.0000091	-0.0000005	-0.0000005	-0.0000004	-0.0000004	-0.0000004	-0.0000004	-0.0000005	-0.0000005	-0.0000007	-0.0000008
	3	-0.0000010	-0.0000006	-0.0000011	-0.0000001	-0.0000011	-0.0000003	-0.0000010	-0.0000004	-0.0000011	-0.0000013	-0.0000013
AD	1	0.0000075	-0.0000063	-0.0000120	-0.0000225	-0.0000220	-0.0000096	-0.0000056	-0.0000117	-0.0000116	-0.0000201	-0.0000211
	2	-0.0000092	-0.0000055	-0.0000049	-0.0000048	-0.0000049	-0.0000051	-0.0000056	-0.0000056	-0.0000055	-0.0000070	-0.0000071
	3	-0.0000006	-0.0000006	-0.0000012	-0.0000002	-0.0000013	-0.0000004	-0.0000011	-0.0000006	-0.0000015	-0.0000015	-0.0000014
RD	1	0.0000001	-0.0000253	-0.0000287	-0.0000239	-0.0000237	-0.0000215	-0.0000193	-0.0000242	-0.0000254	-0.0000208	-0.0000223
	2	-0.0000090	-0.0000050	-0.0000048	-0.0000034	-0.0000034	-0.0000033	-0.0000038	-0.0000052	-0.0000050	-0.0000074	-0.0000079
	3	-0.0000012	-0.0000006	-0.0000011	0.0000000	-0.0000010	-0.0000003	-0.0000010	-0.0000003	-0.0000009	-0.0000013	-0.0000013

		PCR		SCR		PTR		SLF		SFOF		IFOF	
Metric	Time point	L	R	L	R	L	R	L	R	L	R	L	R
FA	1	0.0073996	0.0094267	0.0049554	0.0060216	0.0077787	0.0080582						
	2	0.0015832	0.0019492	0.0014460	0.0015458	0.0016244	0.0016185	0.0020063	0.0021146	0.0019593	0.0017981	0.0016075	0.0016685
	3	-0.0003430	-0.0001525	0.0003102	0.0006314	0.0004281	0.0003213	0.0002909	0.0003165	0.0001642	0.0003515	-0.0000353	0.0001318
MD	1	0.0000201	-0.0000275	-0.0000236	-0.0000254	-0.0000176	-0.0000196						
	2	-0.0000006	-0.0000006	-0.0000007	-0.0000007	-0.0000008	-0.0000008	-0.0000009	-0.0000008	-0.0000007	-0.0000007	-0.0000005	-0.0000005
	3	-0.0000001	-0.0000007	-0.0000006	-0.0000013	-0.0000004	-0.0000004	-0.0000002	-0.0000003	-0.0000010	-0.0000014	-0.0000008	-0.0000013
AD	1	-0.0000161	-0.0000219	-0.0000244	-0.0000266	-0.0000157	-0.0000165						
	2	-0.0000065	-0.0000065	-0.0000079	-0.0000077	-0.0000094	-0.0000092	-0.0000093	-0.0000083	-0.0000063	-0.0000067	-0.0000047	-0.0000048
	3	-0.0000006	-0.0000011	-0.0000005	-0.0000013	0.0000000	-0.0000001	0.0000001	-0.0000001	-0.0000013	-0.0000018	-0.0000012	-0.0000017
RD	1	-0.0000223	-0.0000304	-0.0000232	-0.0000248	-0.0000184	-0.0000212						
	2	-0.0000056	-0.0000061	-0.0000068	-0.0000067	-0.0000077	-0.0000073	-0.0000088	-0.0000085	-0.0000068	-0.0000065	-0.0000051	-0.0000052
	3	0.0000001	-0.0000004	-0.0000006	-0.0000013	-0.0000006	-0.0000005	-0.0000004	-0.0000005	-0.0000008	-0.0000012	-0.0000006	-0.0000010

Bolded values denotes p <0.05 FDR adjusted. Slopes derived from mixed effects models.

Table A2. Wilcoxon Pairwise Tests of FA Measures at Time Point 1

Tract	ALIC L	ALIC R	PLIC L	PLIC R	RIC L	RIC R	ACR L	ACR R	SCR L	SCR R	PCR L	PCR R	EC L	EC R	PTR L	PTR R
CC	0.0004277	0.0000918	0.0000002	0.0000002	0.0000002	0.0000002	0.0022848	0.0208971	0.0002600	0.0000132	0.0000004	0.0000002	0.0002590	0.0001994	0.0004290	0.0000139
ALIC L		0.2045695	0.0000002	0.0000002	0.0000012	0.0000005	0.1376503	0.0552762	0.9041326	0.2473454	0.0173465	0.0004715	0.8890600	0.8422737	0.0131291	0.0131291
ALIC R			0.0000004	0.0000002	0.0000132	0.0000078	0.0208971	0.0348379	0.2716611	0.6883538	0.0771585	0.0002347	0.3483774	0.5585029	0.0098617	0.0089188
PLIC L				0.1198400	0.1966736	0.3014855	0.0000002	0.0000002	0.0000002	0.0000002	0.0000132	0.1152455	0.0000002	0.0000002	0.0007976	0.0069064
PLIC R					0.7371737	0.5743629	0.0000002	0.0000002	0.0000002	0.0000002	0.0000016	0.0153211	0.0000002	0.0000002	0.0001994	0.0003852
RIC L						0.9304911	0.0000007	0.0000005	0.0000002	0.0000002	0.0000002	0.0080854	0.0000003	0.0000002	0.0000030	0.0000306
RIC R							0.0000004	0.0000004	0.0000004	0.0000002	0.0000020	0.0011891	0.0000002	0.0000002	0.0000039	0.0000078
ACR L								0.6410436	0.5478069	0.0560421	0.0052670	0.0000501	0.4689168	0.2005851	0.0046866	0.0055366
ACR R									0.2045695	0.0552762	0.0095712	0.0000501	0.2478875	0.1451022	0.0051307	0.0031802
SCR L										0.0838880	0.0006756	0.0000501	0.9538431	0.7255637	0.0069064	0.0069064
SCR R											0.0882895	0.0001051	0.1258933	0.2005851	0.0069064	0.0065998
PCR L												0.0095712	0.0098617	0.0162097	0.2224569	0.1593373
PCR R													0.0000589	0.0001763	0.0510522	0.1593373
EC L														0.5869889	0.0046866	0.0038979
EC R															0.0095712	0.0075242
PTR L																0.2132246

All p-values are FDR adjusted

Table A3. Wilcoxon Pairwise Tests of FA Measures at Time Point 2

Tract	ALIC L	ALIC R	PLIC L	PLIC R	RIC L	RIC R	ACR L	ACR R	SCR L	SCR R	PCR L	PCR R	EC L	EC R	PTR L	PTR R	SLF L	SLF R	SFOF L	SFOF R	IFOF L	IFOF R
CC	0.0065998	0.0200398	0.0065998	0.0065998	0.0065998	0.0065998	0.0065998	0.0200398	0.0065998	0.0095712	0.0095712	0.2920887	0.0095712	0.0095712	0.0095712	0.0153671	0.0323843	0.0648641	0.2254643	0.0153671	0.0153671	0.0065998
ALIC L		0.8277794	0.0200398	0.0525880	0.0065998	0.0095712	0.1974150	0.1218534	0.4689168	0.6699787	1.0000000	0.2603749	0.0248800	0.0179118	0.7777308	0.7777308	0.1668215	0.1218534	0.1218534	0.6699787	0.9795318	1.0000000
ALIC R			0.0323843	0.0153671	0.0065998	0.0065998	0.4689168	0.2603749	0.3359660	0.6222369	0.9304911	0.2920887	0.0131291	0.0131291	0.6641955	0.4689168	0.4689168	0.2254643	0.1974150	0.7777308	0.9795318	0.6699787
PLIC L				0.4689168	0.0248800	0.0648641	0.0648641	0.0430868	0.5716506	0.2920887	0.1974150	0.0430868	0.3761847	0.1182197	0.5359520	0.8277794	0.0200398	0.0131291	0.0525880	0.1409852	0.3359660	0.1974150
PLIC R					0.0248800	0.2603749	0.0819379	0.0200398	0.1974150	0.0525880	0.0200398	0.0095712	0.4805389	0.0560421	0.5359520	0.3359660	0.0153671	0.0095712	0.0323843	0.0648641	0.2920887	0.1409852
RIC L						0.1668215	0.0095712	0.0095712	0.0065998	0.0065998	0.0065998	0.0095712	0.0095712	0.0248800	0.0248800	0.0095712	0.0095712	0.0065998	0.0065998	0.0153671	0.0153671	0.0095712
RIC R							0.0248800	0.0153671	0.0248800	0.0323843	0.0095712	0.0065998	0.5986771	0.8871559	0.1723435	0.1014768	0.0153671	0.0095712	0.0200398	0.0525880	0.0819379	0.0153671
ACR L								0.4266237	0.1014768	0.1409852	0.4266237	0.4689168	0.0179118	0.0430868	0.2860894	0.3359660	0.9304911	0.2254643	0.4266237	0.5262107	0.6699787	0.6222369
ACR R									0.0323843	0.0525880	0.1409852	0.8746987	0.0131291	0.0131291	0.0095712	0.1014768	0.5262107	0.8746987	0.7777308	0.1014768	0.4266237	0.1974150
SCR L										0.6699787	0.3793389	0.0153671	0.0131291	0.0323843	0.8871559	0.9304911	0.0525880	0.0065998	0.0248800	0.2254643	0.6222369	0.8277794
SCR R											0.4689168	0.0323843	0.0131291	0.0323843	1.0000000	0.8746987	0.0819379	0.0065998	0.0819379	0.2920887	0.8277794	0.6222369
PCR L												0.0200398	0.0248800	0.0179118	0.7777308	0.5716506	0.2254643	0.0153671	0.1409852	0.8277794	0.8746987	0.8746987
PCR R													0.0248800	0.0095712	0.1182197	0.0200398	0.5716506	1.0000000	0.9304911	0.2920887	0.4266237	0.2603749
EC L														0.7216727	0.3279138	0.0560421	0.0095712	0.0095712	0.0248800	0.0095712	0.1182197	0.0323843
EC R															0.2044715	0.0248800	0.0095712	0.0095712	0.0430868	0.0095712	0.1723435	0.0560421
PTR L																0.7216727	0.0560421	0.0179118	0.0944243	0.2860894	0.9394600	0.9394600
PTR R																	0.1409852	0.0095712	0.1014768	0.7777308	0.7777308	0.8746987
SLF L																		0.2920887	0.4266237	0.0648641	0.4266237	0.2603749
SLF R																			0.7777308	0.1668215	0.2920887	0.1014768
SFOF L																				0.2603749	0.2920887	0.1218534
SFOF R																					0.7336978	0.5262107
IFOF L																						0.6699787

All p-values are FDR adjusted

Table A4. Wilcoxon Pairwise Tests of FA Measures at Time Point 3

Tract	ALIC L	ALIC R	PLIC L	PLIC R	RIC L	RIC R	ACR L	ACR R	SCR L	SCR R	PCR L	PCR R	EC L	EC R	PTR L	PTR R	SLF L	SLF R	SFOF L	SFOF R	IFOF L	IFOF R
CC	0.1014768	0.4065549	**0.0131291**	0.2920887	**0.0208971**	0.1284346	0.1615921	0.2920887	**0.0430868**	0.8719083	**0.0131291**	**0.0131291**	**0.0131291**	**0.0131291**	0.1014768	**0.0430868**	**0.0131291**	0.1014768	0.1615921	0.0771585	**0.0430868**	0.0560421
ALIC L		0.3429487	**0.0287185**	0.4689168	**0.0131291**	1.0000000	0.6693466	0.1014768	0.5986771	0.1284346	**0.0208971**	0.0560421	**0.0208971**	0.0560421	0.8018449	0.9304911	0.4689168	0.9304911	0.5986771	0.9304911	**0.0287185**	0.1615921
ALIC R			**0.0208971**	0.5986771	**0.0208971**	0.5308031	0.6693466	1.0000000	0.2920887	0.7359870	**0.0208971**	**0.0208971**	**0.0287185**	**0.0208971**	0.4689168	0.2018385	0.4689168	0.3429487	0.3429487	0.2018385	**0.0287185**	**0.0208971**
PLIC L				**0.0131291**	0.8018449	**0.0287185**	**0.0131291**	**0.0131291**	**0.0131291**	**0.0131291**	0.1014768	1.0000000	0.7359870	0.9304911	**0.0131291**	**0.0131291**	0.0560421	**0.0208971**	0.3429487	**0.0287185**	0.8719083	0.2920887
PLIC R					**0.0430868**	0.6693466	0.8018449	0.6693466	0.4065549	0.1014768	**0.0131291**	**0.0131291**	**0.0208971**	**0.0131291**	0.7359870	0.4689168	0.2478875	0.5308031	0.4689168	0.4689168	0.0771585	0.1284346
RIC L						**0.0287185**	**0.0430868**	**0.0131291**	0.2018385	**0.0208971**	0.1284346	0.7359870	0.7359870	0.9304911	**0.0430868**	0.1284346	0.3429487	0.0560421	0.2018385	**0.0430868**	0.8719083	0.7359870
RIC R							0.7359870	0.2920887	0.6693466	0.1284346	**0.0131291**	**0.0131291**	**0.0208971**	**0.0208971**	0.5308031	0.9304911	0.5986771	0.8719083	0.7359870	0.7359870	0.1615921	0.4065549
ACR L								0.2920887	0.6693466	0.3429487	**0.0131291**	**0.0131291**	**0.0131291**	**0.0208971**	0.8018449	0.8719083	0.3429487	0.8018449	0.5308031	0.8018449	0.0771585	0.2920887
ACR R									0.1615921	0.5308031	**0.0131291**	**0.0131291**	**0.0131291**	**0.0131291**	0.9304911	0.2018385	0.1284346	0.2018385	0.2478875	**0.0287185**	**0.0287185**	**0.0287185**
SCR L										**0.0131291**	**0.0131291**	**0.0131291**	**0.0131291**	**0.0131291**	0.5308031	0.5986771	0.5986771	0.8719083	0.8719083	1.0000000	**0.0430868**	0.4065549
SCR R											**0.0131291**	**0.0131291**	**0.0131291**	**0.0131291**	0.0560421	0.1284346	0.0430868	0.1284346	0.0560421	0.1014768	**0.0131291**	**0.0430868**
PCR L												0.0771585	**0.0430868**	**0.0430868**	**0.0131291**	**0.0131291**	**0.0131291**	**0.0131291**	**0.0430868**	**0.0208971**	0.2018385	0.1284346
PCR R													0.8719083	0.5308031	**0.0131291**	**0.0131291**	0.0560421	**0.0131291**	0.1284346	**0.0208971**	0.8719083	0.2920887
EC L														0.4689168	**0.0131291**	**0.0208971**	**0.0131291**	**0.0131291**	0.1014768	0.0208971	0.6693466	0.1615921
EC R															**0.0131291**	**0.0131291**	0.0771585	0.0560421	0.2920887	**0.0430868**	0.9304911	0.5308031
PTR L																0.8018449	0.3429487	0.7359870	0.5308031	0.6693466	**0.0430868**	0.1615921
PTR R																	0.5308031	1.0000000	0.7359870	0.8719083	0.1284346	0.4689168
SLF L																		0.5308031	0.8018449	0.8018449	0.2018385	0.6693466
SLF R																			0.4689168	0.9304911	0.1284346	0.2920887
SFOF L																				0.8018449	0.3429487	0.5986771
SFOF R																					0.1284346	0.1284346
IFOF L																						0.2478875

All p-values are FDR adjusted

Table A5. Neuropsychological Assessments

Assessment	N	Average (SD)	Range
Verbal IQ	19	100.21 (15.31)	72 - 120
Performance IQ	19	96.63 (12.29)	75 - 115
Full Scale IQ*	19	96.95 (12.98)	73 - 115
Core language*	18	96.06 (19.53)	57 - 121
Visual motor integration*	19	100.63 (10.26)	85 - 119
Visual perception	17	96.24 (16.11)	67 - 117
Motor coordination	19	87.47 (18.49)	58 - 126

**Measures used in PLS analyses*

Appendix B

Figure B1. Greater RD in children born very preterm compared to full-term children

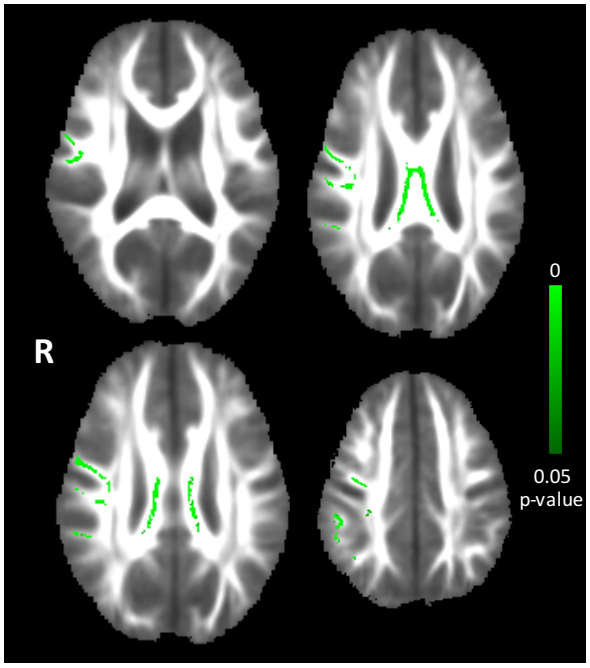

*p-values are shown with colour bar

Figure B2. Effect of excluded volumes across groups on FA

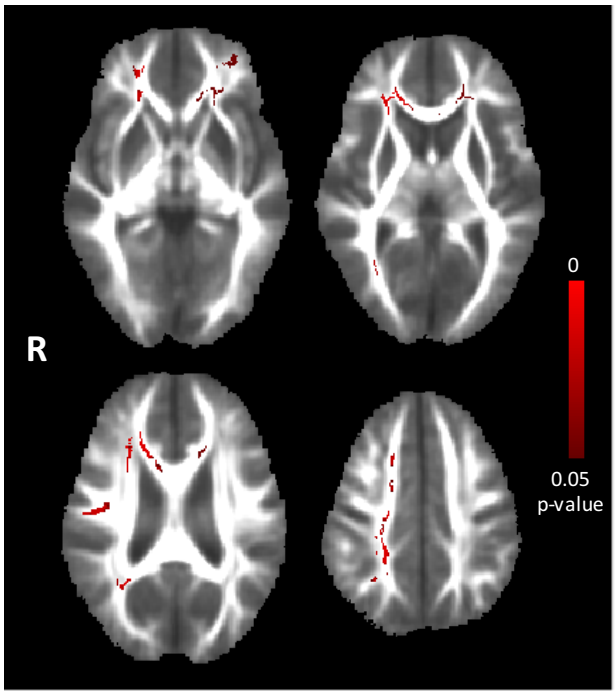

Figure B3. Effect of excluded volumes across groups on RD

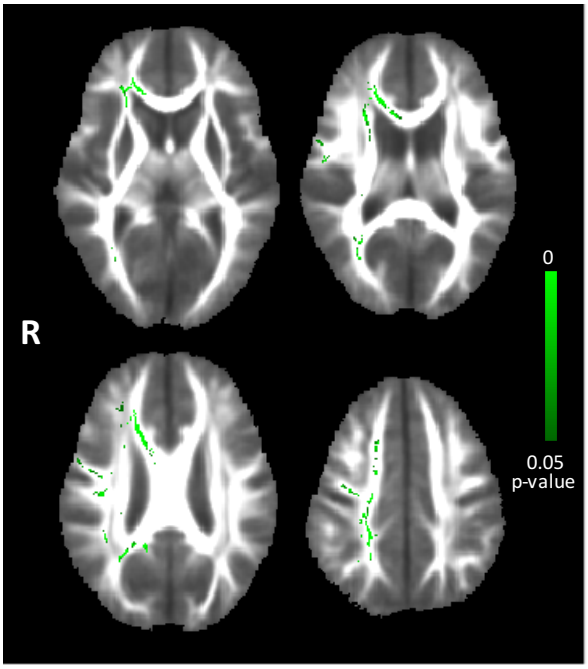

Figure B4. Associations between term-born children and FSIQ

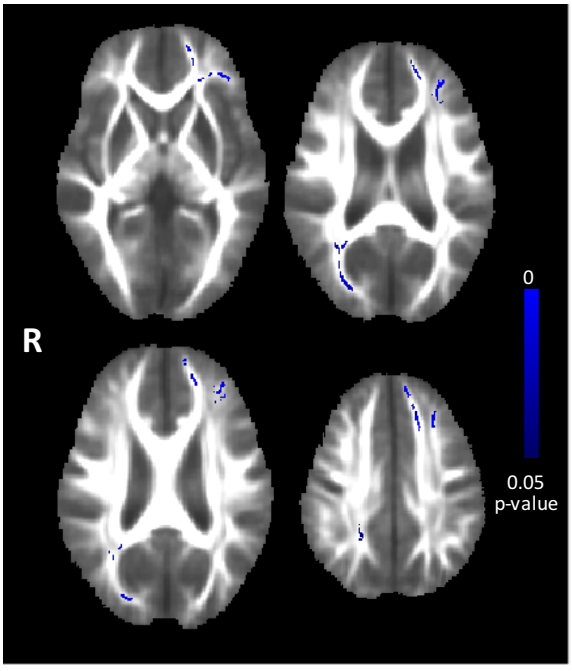

Figure B5. Histogram of the sparsity of connectivity matrices between groups.

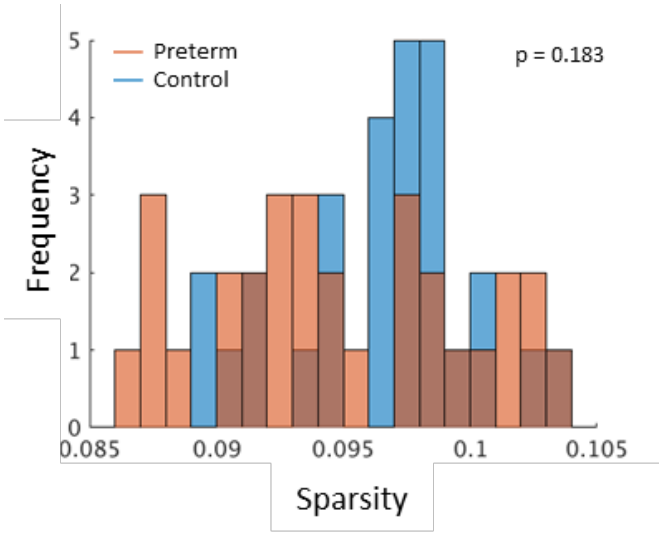

Figure B6. Differences in global efficiency between groups

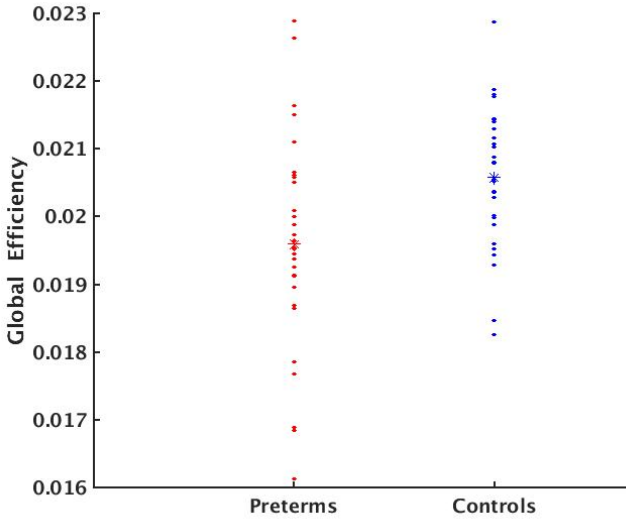

Table B1. Within group relations with developmental outcomes

Group	Graph Measure	Hemisphere	Region	Outcome measure	p-value
Preterm	Strength	Left	Lingual	PIQ	*0.0085*
			Anterior cingulate	FSIQ	*0.0086*
		Right	Frontal pole	PIQ	*0.0029*
			Lingual	CL	*0.0068*
	Local efficiency	Left	Superior parietal	VMI	*0.0010*
			Accumbens	VIQ	*0.0024*
		Right	Supramarginal	CL	*0.0068*
Term	Strength	Left	Anterior cingulate	VIQ	*0.0070*
		Right	Thalamus	VMI	*0.0024*
	Local efficiency	Right	Fusiform	CL	*0.0078*
	Clustering coefficient	Left	Isthmus of the cingulate	CL	*0.0086*
		Right	Posterior cingulate	PIQ	*0.0046*
			Posterior cingulate	FSIQ	*0.0090*
			Fusiform	CL	*0.0088*

Analyses are reported at the p < 0.01 uncorrected level

Table B2. Reduced connectivity in children born very preterm

Group	Graph Measure	Hemisphere	Region	Type	p-value
Preterm	Strength	Left	Caudate	GMH/IVH	*0.0095*
			Anterior cingulate	GA	*0.0036*
		Right	Banks of STS	GA	*0.0043*
	Local efficiency	Left	Thalamus	GMH/IVH	*0.0078*
			Putamen	GMH/IVH	*0.0089*
		Right	Parsorbitalis	GA	*0.0071*
			Postcentral	GA	*0.0097*
			Precentral region	WMI	*0.0077*
	Clustering coefficient	Right	Thalamus	GMH/IVH	*0.0020*
			Pallidum	GMH/IVH	*0.0033*
			Parsorbitalis	GA	*0.0055*

Analyses are reported at the p< 0.01 uncorrected level. GA = gestational age; WMI = white matter injury; GMH/IVH = germinal matrix/intraventricular haemorrhage.

Table B3. Regions

amygdala
hippocampus
accumbens-area
pallidum
putamen
caudate
thalamus
insula
transversetemporal
superiortemporal
bankssts
middletemporal
inferiortemporal
temporalpole
entorhinal
parahippocampal
fusiform
lingual
lateraloccipital
pericalcarine
cuneus
precuneus
inferiorparietal
superiorparietal
supramarginal
postcentral
isthmuscingulate
posteriorcingulate
caudalanteriorcingulate
rostralanteriorcingulate
paracentral
precentral
caudalmiddlefrontal
superiorfrontal
rostralmiddlefrontal
parsopercularis
parstriangularis
medialorbitofrontal
frontalpole
parsorbitalis
lateralorbitofrontal

Appendix C

Table C1. Very preterm within group analyses

Number of significant voxels								
White matter Region	**L/R**	**FA / IQ**	**ND / IQ**	**MD/ IQ**	**RD / IQ**	**IVH>no IVH**	**WMI<no WMI**	**IVH<no IVH**
Genu of corpus callosum	-	249	197	194	362	1139	-	6
Body of corpus callosum	-	492	1202	621	1085	1268	-	35
Splenium of corpus callosum	-	292	648	687	781	17	-	-
Fornix (column and body)	-	-	-	-	-	-	-	-
Corticospinal tract	R	-	92	21	22	-	-	-
	L	-	209	132	154	-	-	-
Cerebral peduncle	R	4	43	2	4	-	-	-
	L	-	163	98	170	-	-	-
Anterior limb of internal capsule	R	70	7	217	245	174	72	-
	L	-	16	52	115	39	-	-
Posterior limb of internal capsule	R	307	230	414	481	49	125	-
	L	6	193	224	244	27	-	-
Retrolenticular part of internal capsule	R	218	341	417	387	-	1	-
	L	11	548	625	628	-	-	-
Anterior corona radiata	R	414	170	257	517	870	99	-
	L	-	77	404	736	514	-	-
Superior corona radiata	R	436	731	803	808	612	544	-
	L	45	833	812	829	254	-	-
Posterior corona radiata	R	342	571	608	609	-	-	-
	L	60	555	494	570	122	-	-
Posterior thalamic radiation	R	295	324	297	379	-	-	-
	L	-	388	370	152	-	-	-
Sagittal stratum	R	116	75	105	185	-	-	-
	L	-	233	226	236	-	-	-
External capsule	R	-	-	-	-	1	-	-
	L	-	32	39	147	6	-	-
Cingulum (cingulate gyrus)	R	-	-	-	-	-	-	-
	L	-	-	-	7	-	-	-
Cingulum (hippocampus)	L	-	-	-	-	-	-	-
	R	-	-	-	-	-	-	-
Superior longitudinal fasciculus	L	329	81	135	286	76	-	-
	R	-	192	479	736	-	-	-
Superior fronto-occipital fasciculus	L	3	-	1	4	5	-	-
	R	-	11	13	15	1	-	-
Uncinate fasciculus	L	-	-	-	-	-	-	-
	R	-	1	2	20	-	-	-

Figure C1. Very preterm group with IQ: MD and RD

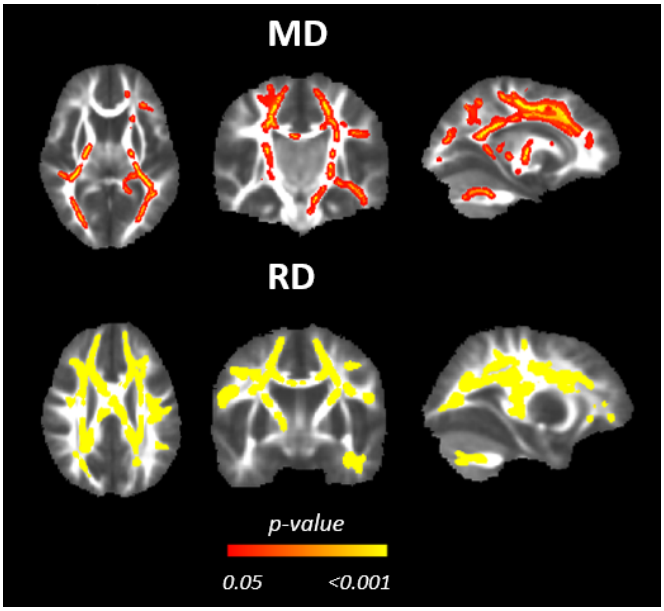

Figure C2. Full term group with IQ

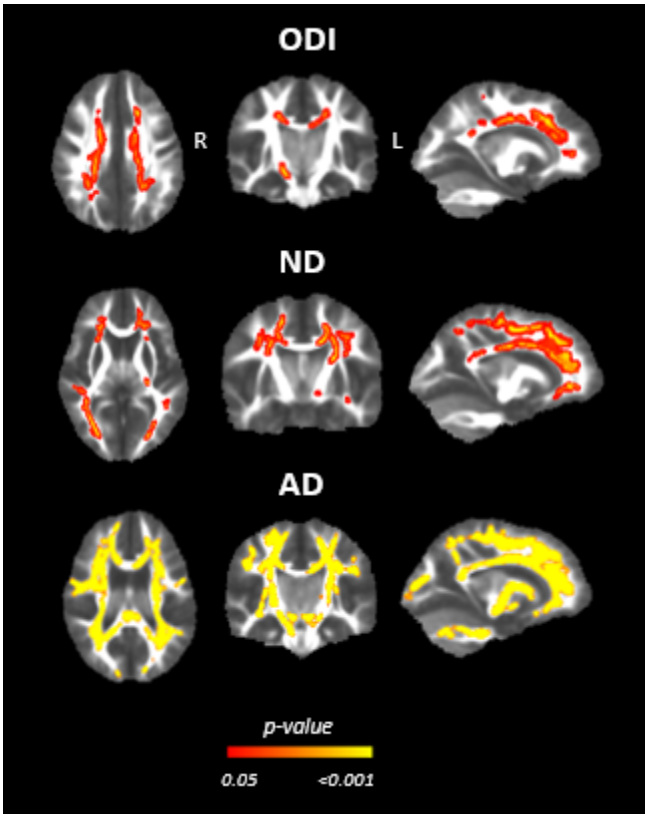

Table C2. Full term within group analyses

Number of significant voxels								
White matter Region	**L/R**	**+ND/-IQ**	**+ODI/-IQ**	**+AD/+IQ**	**+FA/-VMI**	**+ND/-VMI**	**+AD/+VMI**	**+RD/+VMI**
Genu of corpus callosum	-	263	404	780	895	705	586	1118
Body of corpus callosum	-	660	905	1454	7	1514	1582	1285
Splenium of corpus callosum	-	301	91	400	-	613	452	618
Fornix (column and body)	-	-	-	-	-	-	36	53
Corticospinal tract	R	-	-	36	-	227	256	152
	L	-	-	3	-	210	181	159
Cerebral peduncle	R	-	145	289	-	351	462	429
	L	-	13	305	100	365	353	386
Anterior limb of internal capsule	R	-	-	430	-	652	652	635
	L	16	-	458	219	489	573	556
Posterior limb of internal capsule	R	10	18	590	30	766	697	664
	L	49	1	442	361	721	493	669
Retrolenticular part of internal capsule	R	42	-	395	480	522	268	669
	L	116	1	191	385	382	142	563
Anterior corona radiata	R	1012	71	1417	375	1333	1098	1172
	L	1031	166	956	380	998	951	892
Superior corona radiata	R	884	157	1206	30	1376	1261	1017
	L	1100	177	1076	256	1278	1087	1075
Posterior corona radiata	R	720	342	774	142	709	679	545
	L	701	316	705	70	578	630	502
Posterior thalamic radiation	R	408	51	628	471	548	502	748
	L	242	27	391	285	14	36	494
Sagittal stratum	R	-	-	124	352	230	88	415
	L	1	-	34	264	131	16	311
External capsule	R	15	-	859	284	985	973	1067
	L	281	-	405	561	673	846	1140
Cingulum (cingulate gyrus)	R	-	-	-	-	4	-	-
	L	-	-	1	-	8	8	8
Cingulum (hippocampus)	L	-	-	-	-	-	-	-
	R	-	-	-	-	-	-	-
Superior longitudinal fasciculus	L	272	32	760	58	783	410	895
	R	677	155	1045	39	837	294	1144
Superior fronto-occipital fasciculus	L	-	-	3	-	5	5	5
	R	1	-	1	20	16	1	21
Uncinate fasciculus	L	-	-	51	59	60	68	69
	R	31	-	-	19	26	31	60